Md Ataul Gani

Nitrogen Retention in Different Geomorphic Units of a Large Lowland River

Propositions

1. Seasonal changes in the structure of geomorphic units lead to predictable changes in biogeochemical processes in large rivers.
   (this thesis)

2. Limiting the alteration of geomorphic units is essential for maintaining water flow path and quality in large lowland rivers.
   (this thesis)

3. Stability is a controversial concept in ecology.

4. Ethnic peoples are pioneers in promoting nature-based solutions.

5. The Bangladesh Delta Plan (2021) creates a prosperous, climate-resilient delta for society.

6. A PhD's life is unpredictable, like the Dutch weather.

Propositions belonging to the thesis, entitled

Nitrogen Retention in Different Geomorphic Units of a Large Lowland River

Md. Ataul Gani

Delft, 7 October 2024

NITROGEN RETENTION IN DIFFERENT GEOMORPHIC UNITS OF A LARGE LOWLAND RIVER

MD ATAUL GANI

Thesis committee

Promotors

Prof. Dr K.A. Irvine
Professor of Aquatic Ecosystems
IHE Delft Institute for Water Education & Wageningen University & Research

Prof. Dr M.E. McClain
Professor of Ecohydrology
IHE Delft Institute for Water Education & TU Delft

Co-promotors

Dr G.M. Gettel
Associate Professor of Aquatic Biogeochemistry
IHE Delft Institute for Water Education & Aarhus University, Denmark

Dr J. van der Kwast
Associate Professor of Open Science and Digital Innovation
IHE Delft Institute for Water Education

Other members

Prof. Dr M. van der Ploeg, Wageningen University & Research
Prof. Dr J. Griffloen, Utrecht University
Dr Md. S.N. Islam, University of Brunei Darussalam, Brunei Darussalam
Dr R. Kiese, Karlsruhe Institute of Technology, Germany

This research was conducted under the auspices of the Graduate School for Socio-Economic and Natural Sciences of the Environment (SENSE)

NITROGEN RETENTION IN DIFFERENT GEOMORPHIC UNITS OF A LARGE LOWLAND RIVER

Thesis

submitted in fulfilment of the requirements of

the Academic Board of Wageningen University and

the Academic Board of the IHE Delft Institute for Water Education

for the degree of doctor

to be defended in public

on Monday, 7 October 2024 at 14.30 hours

in Delft, the Netherlands

by Md. Ataul Gani

Born in Cumilla, Bangladesh

Published by:
IHE Delft Institute for Water Education
www.un-ihe.org

ISBN 978-90-73445-65-9 (IHE Delft)
DOI: https://doi.org/10.18174/670260

To my family

ACKNOWLEDGEMENTS

First and foremost, I would like to express my profound admiration to Almighty Allah, the most merciful and the most compassionate, for enabling me to complete this research work.

I humbly record my heartfelt gratitude and debt to my promoters, Prof. Kenneth Irvine and Prof. Michael E. McClain, and my co-promotors, Dr. Gretchen M. Gettel and Dr. Johannes van der Kwast, whose excellent supervision, constant encouragement, unfailing guidance, valuable suggestions, critical thoughts and continuous cooperation just shaped me to complete the entire thesis work.

I am very grateful to Dr. Anne van Dam for his valuable advice, support during data analysis and manuscript writing, and encouragement during my research.

I am also grateful to my colleagues and MSc students at Jagannath University, Dhaka, for assisting me during field samplings and lab analysis in Bangladesh.

I wish to express my special and warm thanks to Dr. Ruknul Ferdous, Dr. Aftab Nazeer, Dr. Shahnoor Akter, Dr. Musaed Aklan, Dr. Taha Mohammed Al-Washali, Dr. Almotasembellah Abushaban, Dr. Jeewanthi Sirisena Dickman Maheng, Maximin Djondo, Ahmed Algandour, Sebrian Baselly, Constanza Maass Morales, Mansura Akter and Saidee Hasan. Your unwavering support and assistance have made my dwelling in Delft very fruitful and have led to the success of this research so far.

I am sincerely grateful to the other people of the IHE Delft community, including professors, colleagues, and research institutions, whose influences have significantly given a remarkable structure to this research.

Finally, I would like to express my gratefulness and love toward my wife, mother, and well-wishers. Your unconditional support, continuous cooperation, and encouragement have been a persistent source of strength throughout this journey, and I deeply appreciate your role in my PhD journey.

SUMMARY

The accumulation of nitrogen on or in river beds is a dynamic process which can contribute to nitrogen retention over seasonal and annual time scales. Nitrogen retention is a valuable ecosystem service protecting the downstream aquatic ecosystem from eutrophication. Large, lowland rivers are characterised by geomorphic complexity, comprising features such as islands, bars, dry channels and river banks. Nitrogen retention of these rivers is regulated by different hydrological factors. Variations in discharge can alter the makeup and prevalence of geomorphic units, affecting the periodicity of nitrogen retention. Understanding the seasonal variation of geomorphic units and related nutrient retention of a river at a reach scale can help to predict the importance of geomorphic units on nitrogen retention. The present investigation was carried out over 50 km reach in the Padma River of Bangladesh, downstream of the confluence of Ganges and Brahmaputra rivers. The study area is highly dynamic, with diverse geomorphic units, with high rate of bank erosion, and sediment abstraction. Channelisation has occurred in different parts of the river to increase depth, which is essential for navigation, especially in the dry season.

Sentinel-2 imagery (2019-2020) was processed using NDVI values to classify geomorphic units (GUs) and map nutrient-retention/export-relevant geomorphic units (NREGUs) of the study area. Mapping NREGUs showed seasonal variations of discharge were responsible for changes in the surface area and number of GUs. The NDVI-based classification was effective in the identification of GUs at the unit level, whereas the polygon shape index was more effective in the categorisation of sub-units such as longitudinal and transverse bars.

The field measurements of potential denitrification rate (PDR) in different geomorphic units were performed to show the PDR of land use land cover (LULC) types, which are the patches of GUs. Thus, the capacity of nitrogen retention was exhibited by PDR in each geomorphic unit. To show the spatiotemporal distribution of PDR in the study reach, different linear mixed models (LMMs) were performed, including Sentinel-2 band 11 and NDVI, which were used as a proxy of soil/sediment moisture and vegetation cover, respectively. Estimated PDR through best-performed LMM showed that the number and surface area of GUs were responsible for the alteration of PDR in the study reach.

Field investigations employing the mass balance approach provide an integrated value of nitrogen retention of the study reach. To compare with mass balance measurements, nitrogen loss due to water retention (NLWR), sedimentation, potential denitrification (PDR), and nitrogen fixation (NFR) were estimated from the water column of the river. Both mass balance measurement and estimation through retention processes showed that nitrogen retention occurs throughout the year in the study reach. TN retention via NLWR accounted for the largest portion of total TN retention in every season, always exceeding 50% of total TN retention. Sedimentation was second most important in monsoon and post-monsoon seasons, while PDR in submerged GUs was second most important in dry/winter and pre-monsoon seasons. Net PDR in the water column contributed the least (1-6%) to total TN

retention in all seasons. Variations in river discharge, flooding events, and activities in GUs can impact nitrogen retention and export in the study reach.

The present research mainly focuses on seasonal dynamics of river nitrogen retention, including river geomorphology. In the study, reach variation in discharges is the main controlling factor that can influence both GUs and nitrogen retention capacity. The modelling approach showed seasonal dynamics of the nitrogen mechanism are mainly influenced by different retention processes. Alteration of GUs can regulate these retention processes, as shown by PDR. This approach can also reveal the effect of river management programmes such as river dredging to reclaim land and prevent bank erosion, thus potentially changing nitrogen retention and export scenarios.

SAMENVATTING

De accumulatie van stikstof op of in rivierbeddingen is een dynamisch proces dat kan bijdragen aan stikstofretentie op seizoens- en jaarschalen. Stikstofretentie is een waardevolle ecosysteemdienst die het stroomafwaartse aquatische ecosysteem beschermt tegen eutrofiëring. Grote laaglandrivieren worden gekenmerkt door geomorfologische complexiteit, met kenmerken zoals eilanden, zandbanken, droge beddingen en rivieroevers. De stikstofretentie van deze rivieren wordt gereguleerd door verschillende hydrologische factoren. Variaties in afvoer kunnen de samenstelling en het voorkomen van geomorfologische eenheden veranderen, wat de periodiciteit van stikstofretentie beïnvloedt. Het begrijpen van de seizoensvariatie van geomorfologische eenheden en de daarmee samenhangende nutriëntenretentie van een rivier op de schaal van een sectie kan helpen om het belang van geomorfologische eenheden voor stikstofretentie te voorspellen. Het huidige onderzoek werd uitgevoerd in een sectie van 50 km in de Padmarivier van Bangladesh, stroomafwaarts van de samenvloeiing van de Ganges- en Brahmaputrarivieren. Het onderzoeksgebied is zeer dynamisch, met diverse geomorfologische eenheden, een hoge mate van oevererosie en sedimentonttrekking. Op verschillende delen van de rivier heeft kanalisatie plaatsgevonden om de diepte te vergroten, wat essentieel is voor de navigatie, vooral in het droge seizoen.

Sentinel-2-beelden (2019-2020) werden verwerkt met behulp van NDVI-waarden om geomorfologische eenheden (GU's) te classificeren en nutriëntenretentie/export-relevante geomorfologische eenheden (NREGU's) van het onderzoeksgebied in kaart te brengen. Het in kaart brengen van NREGU's toonde aan dat seizoensvariaties in afvoer verantwoordelijk waren voor veranderingen in het oppervlak en het aantal GU's. De NDVI-gebaseerde classificatie was effectief in de identificatie van GU's op eenheidsniveau, terwijl de polygoonvormindex effectiever was in de categorisatie van subeenheden zoals longitudinale en transversale zandbanken.

Veldmetingen van de potentiële denitrificatiesnelheid (PDR) in verschillende geomorfologische eenheden werden uitgevoerd om de PDR van landgebruik- en landbekkingtypen te tonen, die de GU's vormen. Zo werd de capaciteit van stikstofretentie in verband gebracht met PDR in elke geomorfologische eenheid. Om de ruimtelijke en temporele verdeling van PDR in het onderzoeksgebied te tonen, werden verschillende Linear Mixed Models (LMM's) toegepast. Sentinel-2-band 11 en NDVI werden respectievelijk gebruikt als een proxy voor bodem/sedimentvochtigheid en vegetatiebedekking. Geschatte PDR door best presterende LMM toonde aan dat het aantal en oppervlak van GU's verantwoordelijk waren voor de verandering van PDR in het onderzoeksgebied.

Veldonderzoeken met behulp van de massabalansbenadering leveren een geïntegreerde waarde van stikstofretentie van de bestudeerde sectie. Om te vergelijken met massabalansmetingen, werd stikstofverlies door waterretentie (NLWR), sedimentatie, potentiële denitrificatie (PDR) en stikstoffixatie (NFR) geschat uit de waterkolom van de rivier. Zowel massabalansmeting als schatting door retentieprocessen toonden aan dat

stikstofretentie het hele jaar door plaatsvindt in de bestudeerde sectie. TN-retentie via NLWR was verantwoordelijk voor het grootste deel van de totale TN-retentie in elk seizoen, altijd meer dan 50% van de totale TN-retentie. Sedimentatie was het op een na belangrijkste in het moesson- en post-moessonseizoen, terwijl PDR in ondergedompelde GU's het op een na belangrijkste was in het droge/winter- en pre-moessonseizoen. Netto PDR in de waterkolom droeg het minst (1-6%) bij aan de totale TN-retentie in alle seizoenen. Variaties in rivierafvoer, overstromingen en activiteiten in GU's kunnen de stikstofretentie en -export in het de bestudeerde sectie beïnvloeden.

Het huidige onderzoek richt zich voornamelijk op de seizoensdynamiek van rivierstikstofretentie, inclusief riviergeomorfologie. In de bestudeerde sectie is variatie in afvoer de belangrijkste regulerende factor die zowel GU's als de stikstofretentiecapaciteit kan beïnvloeden. De modelbenadering toonde aan dat seizoensdynamiek van stikstof voornamelijk wordt beïnvloed door verschillende retentieprocessen. Verandering van GU's kan deze retentieprocessen reguleren, zoals getoond door PDR. Deze benadering kan ook het effect onthullen van rivierbeheerprogramma's zoals baggeren om land terug te winnen en oevererosie te voorkomen, waardoor potentieel de scenario's van stikstofretentie en -export veranderen.

TABLE OF CONTENTS

Chapter 1

INTRODUCTION

1. Background

About 2.7 billion people live near large, lowland rivers (Best, 2019), which provide essential ecosystem services, including arable land, nutrient retention, fishing, and water (Grizetti et al., 2016). However, people who live near these systems are vulnerable to flooding and riverbank erosion, which occur as a natural process of changing river geomorphology due to seasonal changes in discharge. To mitigate these vulnerabilities, rivers are often altered, channelised or dredged for e.g. navigability, flood control, or to manage lateral erosion of the floodplain (Hohensinner et al., 2018). On the other hand, alterations also increase the velocity of flow, which decreases water residence time and may affect nutrient and sediment dynamics, leading to a reduction in nitrogen retention.

Nitrogen retention is a valuable ecosystem service. At the ecosystem scale, it is used as an indicator for water purification, air quality regulation and sediment enrichment (Grizzetti et al., 2019). Besides, nitrogen plays a crucial role in freshwater ecosystem primary production and retention of this nutrient protects downstream ecosystems from eutrophication (Loken et al., 2018). Nitrogen concentrations in surface water are likely affected by the nature and complexity of the geomorphology. In a braided lowland river, geomorphic units include islands, bars, backwaters, and channels. The accumulation of nitrogen on or in the river bed is a dynamic process termed nitrogen retention and is estimated as the difference between inputs and outputs in a specified river reach. Retention processes include plant uptake, microbial decomposition and denitrification. The interface between water and sediment acts as a suitable spot for different biogeochemical processes, including denitrification. Denitrification plays a significant role in maintaining water quality by converting bioavailable nitrate and nitrite to inert N_2. Bottom anoxic sediments and the water column of suboxic river reaches are locations in which denitrification occurs (Seitzinger et al., 2006).

Geomorphic units (hereafter GUs) influence the nutrient dynamics of rivers, but there needs to be more understanding of their role, especially in large lowland tropical rivers. A GU is considered an area of the river channel where aggradation and degradation of sediments occur (Rinaldi et al., 2015). Some research, in predominately smaller streams, has focused on the role of GUs in nitrogen retention (Gucker and Boechat, 2004; Tuttle et al., 2014). With the exception of Lin et al. (2016), estimates of nitrogen retention in GUs of large rivers are lacking. Lowland tropical rivers are affected by monsoon rainfall, seasonal storms and flooding. All of these factors are responsible for altering GUs and nitrogen retention/export scenarios throughout the year. So, understanding how changes in GUs affect nitrogen retention is essential for predicting how human geomorphological alteration of large river systems affects nutrient export.

Bangladesh covers the lowest 7% of the Ganges-Brahmaputra-Meghna (GMB) river basin and consists mostly of flat deltaic land (Mirza et al., 2003). The morphological pattern of this type of river changes frequently, ranging from meandering to braided. Monsoon water flow is a vital factor in altering river morphology. Flooding events, riverbank erosion and sediment deposition usually occur during the monsoon season. For the stabilisation of the country's big rivers, the Government of Bangladesh is trying to implement appropriate management

and action plans. The capital dredging project is one of them (Khan, 2018). Under this project, the Padma River will be dredged along and across the river to prevent bank erosion and increase navigability. This will lead to the removal of GUs from the river network without knowing the impact on nitrogen retention. Due to climate change and anthropogenic stress, river nitrogen loads to the coastal areas of the country are increasing, resulting in high eutrophication potential (Sattar et al., 2014). This is favourable for the growth of harmful algal blooms (Zinia and Kroeze, 2015), which ultimately affect ecosystem services.

2. Large rivers and development context

Large rivers are extremely dynamic ecosystems and are strongly connected to the development of human civilisation, including water for drinking, domestic, agricultural and industrial uses, fish production, and areas for flood protection (Böck et al., 2019). They act as zones for pollutant discharge and transport (Grizzetti et al., 2019). Increasing human activities, including channelisation, damming, land use, and hydropower operations are shifting the functions and services of large rivers and their basin areas (Böck et al., 2018). Recently, due to climate change and anthropogenic activities, the water volume and seasonal flow of some of the world's large rivers have changed markedly (Eisner, 2017), which in turn influences sediment flux and ecological functioning (Best, 2019). Sediment load to large river systems is responsible for reshaping channel morphology (Soar et al., 2017). Changes in the landscapes of large rivers also alter nutrient removal processes and rates of sediment loads to the deltas or associated downstream water bodies. Most of the world's great rivers are polluted by nutrient enrichment leading to eutrophication; examples include the Mississippi, Danube, Rhine and Indus rivers (Best, 2019).

3. Importance of nitrogen retention and export

Large rivers are essential pathways of nitrogen transport. When they export high loads of nitrogen, downstream, reaches and especially coastal areas may become eutrophic and hypoxic (Strauss et al., 2011). Because of the complex structure of large rivers, i.e. floodplains, backwaters and deep reaches, they generally have a large capacity to retain nitrogen. Several studies have shown that nitrogen retention in large rivers is significant (Seitzinger et al., 2002; Wollheim et al., 2006; Ye et al., 2017), and they have the potential to control nitrogen flux to reduce eutrophication in coastal ecosystems (Loken et al., 2018).

A range of studies have been carried out to determine the nutrient budgets of large lowland rivers. The emphasis has been particularly given to estimating nitrogen export to the ocean through the river channel (Krishna et al., 2016). An investigation carried out on European lowland rivers by de Klein and Koelmans (2011) showed that seasonal variations of nitrogen retention must be considered when accounting for nutrient budgets. They also concluded that temperature could control nitrogen retention, especially for denitrification. Data from some of the big rivers around the world showed that flow discharge is responsible for nitrogen export flux, as in the Amazon River (Best, 2019) and in the coastal water of the Northern Indian Ocean (Krishna et al., 2016). Reach surface area to volume ratio can be a controlling factor for nitrogen retention (Alexander et al., 2000). An inverse relation between reach depth and

travel time was revealed by Seitzinger et al. (2002) after studying nitrogen retention in several catchments of North America.

4. Biogeochemical processes associated with nitrogen retention

Biogeochemical processes are important for in-stream nitrogen retention (Frederick and Basu, 2017). The anoxic condition of sediments enhances microbial activity suitable for denitrification. Denitrification is a crucial pathway producing non-bioavailable forms of nitrogen (NO, N_2O and N_2) that are volatile and vaporize into the atmosphere (Seitzinger et al., 2006). A study on Tanana River, Alaska, suggested that denitrification can play a significant role in nitrate removal in boreal forest floodplain soils, mainly at the water-sediment interface (Clilverd et al., 2008). Another biogeochemical process that can be considered a nitrogen source in the streams is N_2 fixation, which occurs by microbes in aquatic systems. Through this process, both the water column and sediments can be enriched with nitrogen. A study by Marcarelli et al. (2008) suggested that N_2 fixation can contribute higher proportions to the annual nitrogen budget in a stream when considered over daily or seasonal time scales. Thus, denitrification and N_2 fixation are vital processes in the nitrogen cycle and are associated with the overall nitrogen budget.

5. Importance of GUs on nitrogen retention

Nitrogen removal from aquatic ecosystems is connected to the hydrological and geomorphological conditions (Burt et al., 2002). Like the riparian zone, different GUs can be flooded annually and enriched with nutrients and carbon. Flooding enhances saturation, and the environment becomes anoxic, making GUs favourable for denitrification. The efficiency of denitrification in riparian areas mainly depends on the availability of carbon, nitrate and soil water content (Skiba and Smith, 2000). In the river channel, the area of GUs can be altered seasonally, and inundation during monsoon may be induced by different factors favourable for denitrification. Denitrification is the main retention process that contributes to nitrogen removal from riparian wetlands (Balestrini et al., 2006, 2011). The same condition is applicable in GUs. Gomez-Velez et al. (2015) proposed that geomorphic differences in river networks can explain the variation of denitrification efficiency between different basins of the Mississippi River network.

6. Significance of the study

There is little information on nitrogen retention in lowland tropical rivers generally, although cities and agricultural lands develop there (Balestrini et al., 2018; Tromboni et al., 2017; Johnson et al., 2015). Also, these types of rivers are subject to channel modification through development, and the effects on nitrogen retention are unknown. There is little research on the relationship between GUs and their influence on nitrogen retention in rivers, and the little there is tends to be focused on wadeable streams (Marti and Sabater, 1996; Gucker and Boechat, 2004), with one exception. Lin et al. (2016) that examined the effect of different GUs on nitrogen retention in a 6^{th}-order river in Alabama (USA). The present study focuses on the nitrogen retention of a large lowland tropical river with geomorphic complexity.

The present study has great significance for channel nitrogen retention or export to deltas. So far, there is no information available regarding nitrogen retention and export of the Padma River in Bangladesh (Sattar et al., 2014). The study reach has a channel morphology that changes frequently. The different GUs of the study area might influence nutrient retention and export. It is necessary to incorporate different GUs with nutrient retention to know the dynamics of nutrient retention/export in the study area. Very few studies are available regarding the geomorphology and channel dynamics of the Padma River in Bangladesh (CEGIS, 2004; Islam, 2016). Therefore, systematic investigation of the spatial and temporal distribution of GUs in the study area is pivotal for planning and suitable development of river restoration programs.

A number of river management activities, channelisation, dredging, and sediment extraction are going on in Bangladesh. All the activities are intended mainly to increase river depth for navigability and prevent bank erosion. These kinds of activities might play a vital role in restructuring river geomorphology, resulting in an impact on nutrient retention. Thus, nutrient retention or export will have enormous consequences on ecosystem structure and functions. From this study, it will be possible to show the impact of GUs on nitrogen retention, which might have consequences on river health and ecosystem services. In addition, without considering river health, the effect of implicating different river management projects, such as capital dredging, will be shown to some extent.

7. Research Questions

During the present investigation, the methodology will be developed to answer the following research questions:

1) How does seasonality affect the nitrogen retention capacity of each GU?
2) How do changes in GUs impact reach-scale nitrogen retention?
3) How does the retention process/es influence overall nitrogen retention in reach?

8. Research objectives

The research aims to identify the impact of GUs on nitrogen retention in a large lowland river system, the Padma River, Bangladesh. The specific objectives are to:

1) identify and map GUs that may be relevant to nitrogen retention, specifically the dynamics of the GUs in response to seasonal river discharge;
2) determine the possible contribution of denitrification to nitrogen retention by assessing potential denitrification rates in identified GUs, conducting fieldwork and laboratory analyses in the Padma River;
3) determine nitrogen retention and export of the study reach of Padma River through a mass balance approach and different retention processes.

9. Outline of the thesis

The thesis covers nitrogen retention dynamics at different spatiotemporal scales, including across different GUs. The research includes image analysis from remotely sensed data, field and laboratory analysis of water and sediments and finally, data analysis and modelling. The

thesis chapters are based on the research objectives. The first chapter (Chapter 1) includes a general introduction. The second chapter (Chapter 2) covers the identification of the GUs and their dynamics in the Padma River. The third chapter (Chapter 3) examines the measurement, prediction and spatiotemporal dynamics of the denitrification rate in identified GUs and their impact on denitrification as a retention process. The fourth chapter (Chapter 4) focuses on the overall nitrogen retention of the studied reach through the mass balance approach in the Padma River. The fifth and final chapter (Chapter 5) covers the overall synthesis and recommendation.

10. References

Alexander R. B., Smith R. A. & Shwartz G. E. (2000). Effect of stream channel size on the delivery of nitrogen to the Gulf of Mexico. Nature, 403, 758-761. https://doi.org/10.1038/35001562

Balestrini R., Arese C. & Delconte C. (2006). Nitrogen removal in a freshwater wetland: an example from Italian lowland spring. Verh. Internat. Verein. Limnol., 29. https://doi.org/10.1080/03680770.2006.11903085

Balestrini R., Arese C., Delconte C. A., Lotti A. & Slerno F. (2011). Nitrogen removal in subsurface water by narrow buffer strips in the intensive farming landscape of the Po River watershed, Italy. Ecol. Eng., 37, 148–157. https://doi.org/10.1016/j.ecoleng.2010.08.003

Balestrini R., Delconte C. A., Palumbo M. T. & Buffagni A. (2018). Biotic control of in-instream nutrient retention in nitrogen-rich springs (Po Valley, Northern Italy). Ecol. Eng., 122, 303-314. https://doi.org/10.1016/j.ecoleng.2018.08.014

Best J. (2019). Anthropogenic stresses on the world's big rivers. Nature Geoscience, 12, 7–21. https://doi.org/10.1038/s41561-018-0262-x

Böck K., Polt R. & Schülting L. (2018). Ecosystem Services in River Landscapes. Riverine Ecosystem Management, pp. 413–433. https://doi.org/10.1007/978-3-319-73250-3_21

Burt T. P., Pinay G., Matheson F. E., Haycock N. E., Butturini A., Clement J. C., Danielescu S., Dowrick D. J., Hefting M. M., Hillbricht-Ilkowska A. & Maitre V. (2002). Water table fluctuations in the riparian zone: comparative results from a pan-European experiment. J. Hydrol., 265, 129–148. https://doi.org/10.1016/S0022-1694(02)00102-6

CEGIS (2004). Identification of the different types of bank materials along the Padma River-Morphologic Study Applying Remote Sensing for the feasibility Study of Padma Bridge, Prepared for JICA Study Team in Bangladesh for the Feasibility Study of Padma Bridge, Dhaka, Bangladesh, pp.28.

Clilverd A. E., Jones Jr. J. B., Kielland K. (2008). Nitrogen retention in the hyporheic zone of a glacial river in interior Alaska. Biogeochemistry, 88, 31–46. https://doi.10.1007/s10533-008-9192-9

de Klein J. J. M. & Koelmans A. A. (2011). Quantifying seasonal export and retention of nutrients in West European lowland rivers at catchment scale. 2111, 2102–2111. https://doi.org/10.1002/hyp.7964.

Eisner S. (2017). An ensemble analysis of climate change impacts on stream flow seasonality across 11 large river basins. Clim. Change, 141, 401–417.

Fredderick C. Y., Basu N. B. (2017). Landscape Nutrient Processing. Water Resources Research, 53, 1–19. https://doi.org/10.1002/2016WR020102

Gomez-Velez J. D., Harvey J. W., Cardenas M. B. & Kiel B. (2015). Denitrification in the Mississippi River network controlled by flow through river bedforms. Nat. Geosci., 8, 941–945. https://doi.10.1038/ngeo2567

Grizzetti B., Lanzanova D., Liquete C., Reynaud A., Cardoso A. C. (2016). Assessing water ecosystem services for water resource management. Environmental Science and Policy, 61, 194–203. https://doi.org/10.1016/j.envsci.2016.04.008

Grizzetti B., Liquete C., Pistocchi A., Vigiak O., Zulian G., Bouraoui F., Roo A. D. & Cardoso A. C. (2019). Relationship between ecological condition and ecosystem services in European rivers, lakes and coastal waters. Science of the Total Environment, 671, 452–465. https://doi.org/10.1016/j.scitotenv.2019.03.155

Gücker B. & Boechat G. I. (2004). Stream morphology controls ammonium retention in tropical headwaters. Ecology, 85, 2818–2827. https://doi.org/10.1890/04-0171

Hohensinner S., Hauer C. & Muhar S. (2018). River Morphology, Channelization, and Habitat Restoration. Riverine Ecosystem Management, 41–65. https://doi.org/10.1007/978-3-319-73250-3_3

Islam A. R. M. T. (2016). Assessment of fluvial channel dynamics of Padma River in Northwestern Bangladesh. Univers. J. Geosci., 4, 41–49. https://doi.org/10.13189/ujg.2016.040204

Johnson Z. C., Warwick J. J. & Schumer R. (2015). Nitrogen retention in the main channel and two transient storage zones during nutrient addition experiments. Limnol. Oceanogr., 60, 57–77. https://doi.10.1002/lno.10006

Khan S. (2018). PM asks to go for rivers' capital dredging first. The Einancial Express (FE), published on 25/01/2018.

Krishna M. S., Prasad M. H. K., Rao D. B., Viswanadham R., Sarma V. V. S. S. & Reddy N. P. C. (2016). Export of dissolved inorganic nutrients to the northern Indian Ocean from the Indian monsoonal rivers during discharge period. Geochimica et Cosmochimica Acta, 172, 430–443. https://doi.org/10.1016/j.gca.2015.10.013

Lin L., Davis L., Cohen S., Chapman E. & Edmonds J. W. (2016). The influence of geomorphic unit spatial distribution on nitrogen retention and removal in a large river. Ecological Modelling, 336, 26–35. https://doi.org/10.1016/j.ecolmodel.2016.05.01

Loken L. C., Crawford J. T., Dornblaser M. M., Striegl R. G., Houser J. N., Turner P. A. & Stanley E. H. (2018). Limited nitrate retention capacity in the Upper Mississippi River. Environ. Res. Lett., 13(7), 074030. https://doi.org/10.1088/1748-9326/aacd51

Marcarelli A. M., Baker M. A. & Wurtsbaugh W. A. (2008). Is in-stream N_2 fixation an important N source for benthic communities and stream ecosystems ? 27, 186–211. https://doi.10.1899/07-027.1

Marti E. & Sabater F. (1996). High variability in temporal and spatial nutrient retention in mediterranean streams. Ecology, 77, 854–869. https://doi.org/10.2307/2265506

Mirza M., Warwick R. A. & Erickso N. J. (2003). The implications of climate change on floods of the Ganges, Brahmaputra and Meghna rivers in Bangladesh. Climatic Change 57:287–318. https://doi.10.1023/A: 1022825915791

Rinaldi M., Belletti B., Comiti F., Nardi L., Bussettini M., Mao L. & Gurnell A. M. (2015). The Geomorphic Units survey and classification System (GUS), Deliverable 6.2, Part 4, of REFORM (REstoring rivers FOR effective catchment Management), a Collaborative project (large-scale integrating project) funded by the European Commission within the 7th Framework Programme under Grant Agreement 282656.

Sattar M. A., Kroeze C. & Strokal M. (2014). The increasing impact of food production on nutrient export by rivers to the Bay of Bengal 1970-2050. Marine Pollution Bulletin, 80: 168–178. https://doi.org/10.1016/j.marpolbul.2014.01.017.

Seitzinger S., Harrison J. A., Böhlke J. K., Bouwman A. F., Lowrance R., Peterson B., Tobias C. & van Drecht G. (2006). Denitrification across landscapes and waterscapes: A synthesis. Ecological Applications, 16, 2064-2090. https://doi.org/10.1890/1051-0761(2006)016[2064:DALAWA]2.0.CO;2

Seitzinger S. P., Styles R. V., Boyer E. W., Alexander R. B., Billen G., Howarth R. W., Mayer B. & Breemen N. (2002). Nitrogen retention in rivers: model development and application to watersheds in the northeastern USA. In: Boyer EW, Howarth RW (eds) The Nitrogen Cycle at Regional to Global Scales. Springer, Dordrecht. https://doi.org/10.1007/978-94-017-3405-9_6

Skiba U. & Smith K. A. (2000). The control of nitrous oxide emissions from agricultural and natural soils. Chemosphere-Global Change Science, 2, 379–386. https://doi.org/10.1016/S1465-9972(00)00016-7

Soar P. J., Wallerstein N. P. & Thorne C. R. (2017). Quantifying river channel stability at the basin scale. Water (Switzerland), 9, 1–31. https://doi.org/10.3390/w9020133

Strauss E. A., Richardson W. B., Bartsch L. A. & Cavanaugh J. C. (2011). Effect of habitat type on in-stream nitrogen loss in the Mississippi River. River Syst., 9, 261–269. https://doi.org/10.1127/1868-5749/2011/019-0021

Tromboni F., Dodds W. K., Neres-Lima V., Zandona E. & Moulton T. P. (2017). Heterogeneity and scaling of photosynthesis, respiration, and nitrogen uptake in three Atlantic Rainforest streams. Ecosphere 8: e01959. https://doi.10.1002/ecs2.1959

Tuttle A. K., Mcmillan S. K., Gardner A. & Jennings G. D. (2014). Channel complexity and nitrate concentrations drive denitrification rates in urban restored and unrestored streams. Ecol. Eng., 73, 770–777. https://doi.org/10.1016/j.ecoleng.2014.09.066

Wollheim W. M., Vörösmarty C. J., Peterson B. J., Seitzinger S. P. & Hopkinson C. S. (2006). Relationship between river size and nutrient removal. Geophys. Res. Lett., 33, L06410. https://doi. 10.1029/ 2006GL025845

Ye S., Reisinger A. J., Tank J. L., Baker M. A., Hall R. O., Rosi E. J. & Sivapalan M. (2017). Scaling dissolved nutrient removal in river networks: A comparative modeling investigation. Water Resour. Res., 53, 9623–9641. https://doi.10.1002/2017WR020858

Zinia N. J. & Kroeze C. (2015). Future trends in urbanization and coastal water pollution in the Bay of Bengal: the lived experience. Environment, Development and Sustainability, 17, 531–546. https://doi.org/10.1007/s10668-014-9558-1

Chapter 2

CLASSIFICATION OF GEOMORPHIC UNITS AND THEIR RELEVANCE FOR NUTRIENT RETENTION OR EXPORT OF A LARGE LOWLAND PADMA RIVER, BANGLADESH: A NDVI BASED APPROACH

Based on

Gani M. A., van der Kwast J., McClain M. E., Gettel M. G. & Irvine K (2022). Classification of Geomorphic Units and Their Relevance for Nutrient Retention or Export of a Large Lowland Padma River, Bangladesh: A NDVI Based Approach. Remote Sens., 14, 1481. https:// doi.org/10.3390/rs14061481

Abstract

Geomorphic classification of large rivers identifies morphological patterns, as a foundation for estimating biogeochemical and ecological processes. In order to support the modelling of in-channel nutrient retention or export, the classification of geomorphic units (GUs) was done in the Padma River, Bangladesh, a large and geographically-complex lowland river. GUs were classified using the normalized difference vegetation index (NDVI) four times over a year, so as to cover the seasonal variation of water flows. GUs were categorized as primary and secondary channels (C & S); longitudinal bar (L); transverse bar (T); side bar (SB); unvegetated bank (EK); dry channel (ED); island (VI); and water depression (WD). All types of GUs were observed over the four distinct annual seasons, except ED, which was absent during the high flow, monsoon season. Seasonal variation of the surface area of GUs and discharge showed an inverse relation between discharge and exposed surface areas of VI, L, T, and SB. Nutrients mainly enter the river system through water and sediments, and during monsoon, the maximum portion of emergent GUs were submerged. Based on the assumption that nutrient retention is enhanced in the seasonally inundated portions of GUs, nutrient retention-/export-relevant geomorphic units (NREGUs) were identified. Seasonal variation in the area of NREGUs was similar to that of GUs. The mean NDVI values of the main identified NREGUs were different. The variation of NDVI values among seasons in these NREGUs resulted from changes in vegetation cover and type. The variation also occurred due to alteration of the surface area of GUs in different seasons. The changes of vegetation cover indicated by NDVI values across seasons are likely important drivers for biogeochemical and ecological processes.

Keywords: Geomorphic classification; geomorphic units; NDVI; Sentinel 2; QGIS; nutrient retention/export; large lowland river; Padma River; Bangladesh

1. Introduction

River biodiversity and ecosystem functioning depend on the geomorphology and erosional and depositional processes within geomorphic units (Fryirs and Brierley, 2013; Elosegi and Pozo, 2016). Geomorphic units, hereafter GUs, are discrete morphodynamic entities, considered building blocks of the river and defined by their position, morphology, and sediment composition. Generally, GUs are mapped at reach scale, because this scale is important for hydromorphological factors, such as water flow and sediment transport (Rinaldi et al., 2015). Different classification schemes have been proposed to delineate and map GUs at the scale of the river reach. Wyrick and Pasternack (2014) classified GUs based on hydraulic data (flow velocity and depth), whereas Wheaton et al. (2015) classified GUs based on topographic and morphological characteristics (position, attributes of sediment and vegetation). Classification of GUs has been developed to cover a wide range of river types (lowland systems, mountain systems, highly dynamic systems, etc.) and includes different sub-domains (vegetation, bed configuration, sedimentary units) and scales (macro-unit, unit, and sub-unit) (Rinaldi et al., 2015; Belletti et al., 2017).

Nutrient retention or export is influenced by seasonal discharge (Sigleo and Frick, 2007; de Klein and Koelmans, 2011) and biogeochemical processes (Jossette et al., 1999; Bernot and Dodds, 2005; Grizzetti et al., 2015). Nutrients in a river channel are both taken up by, and released from, the river bed. Data for large rivers have shown the primary importance of discharge for nutrient flux (Krishna et al., 2016; Best, 2019). Morphological changes in large rivers influence nutrient removal processes and loads to the deltas or downstream water bodies. With climate change, the water volume and seasonal flow of some of the world's biggest rivers are projected to change markedly (Eisner, 2017), changing sediment mobility and ecological functioning (Best, 2019). The sediment load to large river systems reshapes channel morphology (Soar, 2017) with consequences for biogeochemical processes and in-stream nutrient retention (Cheng et al., 2017). GUs can be inundated temporally and enriched with nutrients. This is usually observed in floodplain areas and riparian zones. Plant uptake and denitrification are biogeochemical processes that contribute to nitrogen removal from riparian wetlands (Balestrini et al., 2006, 2011). Vegetation influences these processes, by both taking up nutrients directly and influencing subsurface denitrification in their root zones (Walton et al., 2020).

A variety of satellite imagery is available for monitoring inland water quality and issues related to nutrient retention, such as water transparency, eutrophication, organic matter, biomass estimation, nutrient, and chlorophyll concentration (Masoud, 2022; Li et al., 2022; de Stefano et al., 2022; Zeng et al., 2022; Kratzer et al., 2019; Wang et al., 2018; Fay and McKinley et al., 2017; Binding et al., 2015). Recently, satellite-derived estimates of flood and vegetation cover are increasingly used in monitoring (de Grandpre et al., 2022; Wieland et al., 2019; Kwak, 2017; Ahamed and Bolte, 2017). However, this has not gone as far as estimating biogeochemical processes (Guilhen et al., 2020) or nutrient retention as a function of vegetation cover (Martinez-Espinosa et al., 2021)**,** although land use and land cover (LULC) maps are frequently generated using satellites (Faruque et al., 2022; Gameiro et al., 2022; Ge et al., 2022; Markogianni et al., 2022).

In comparison with the commonly used, and previous, SPOT and Landsat products of satellites, the new generations of freely available satellite imagery provide high-resolution multispectral imaging, with a high revisit frequency for the detection of temporal changes in LULC, including inland waters (SUHET, 2015; Drusch et al., 2012). Sentinel-2, with 13 spectral bands, can be used to derive biogeophysical indices that combine different band reflectances. This allows for calculations of the normalized difference water index (NDWI, McFeeters, 1996), which separates water cover from land surfaces (Serrano et al., 2019), and the enhanced vegetation index (EVI, Didan et al., 2015), which corrects soil background signals and atmospheric influences, to identify forest/canopy cover, enhancing estimates of the well-known normalized difference vegetation index (NDVI, Freden et al., 1974) that is often used for separating soil, water, and vegetation classes (JARS, 1993) In-channel GUs consist of water, sediment, and vegetation (Sonam et al., 2022; Fryirs et al., 2022; Han and Brierley, 2020). Nutrient retention processes in GUs are related to biophysical activities and water availability (Boz et al., 2016; Gomez-Velez et al., 2015; Tatariw et al., 2013). One of the advantages of NDVI is that it can be used to monitor the biophysical conditions related to natural water retention (Taramelli et al., 2019; Piedelobo et al., 2019 a, b) and that it is sensitive to low vegetation cover (Didan et al., 2015). However, there is a debate over EVI, regarding illumination conditions and hydroclimatic factors at decadal scales (Martin-Ortega et al., 2020; Kumari et al., 2021). Nevertheless, characteristic local features need to be considered in the estimation of biophysical indices (Xue et al., 2017).

NDVI has been used for monitoring the vegetation and ecosystem dynamics of large rivers (Marchetti et al., 2020, 2016, 2013; Luan et al., 2018; Kaplan and Avdan, 2017). Relationships between seasonal vegetation and discharge variation of large rivers can be verified by the seasonal correlation between NDVI and discharge (Xu et al., 2016). In the Parana River of South America, NDVI was used to assess fluvial dynamics, describe ecological patterns (Marchetti et al., 2020), and establish a relation between vegetation and GUs (Marchetti et al., 2013). The latter has brought an opportunity to utilize NDVI to classify GUs in large lowland rivers.

Different classification schemes of GUs have been presented, but none focus on the seasonal variation of GUs, except Marchetti et al. (2013), who used NDVI to show only the dynamics of floodplain vegetation GUs. In this paper, we set out to develop an NDVI-based geomorphic classification scheme for a large lowland river that reflects its relevance for nutrient retention and export. Therefore, the objectives of the present study are to (i) classify GUs considering the seasonal variation of a large lowland river based on remote sensing data, (ii) map areas of GUs assumed to be important for nutrient retention or export, (iii) show the seasonal dynamics of GUs, focusing on nutrient retention and export and, (iv) demonstrate the effectiveness of NDVI and shape indexes for the present classification.

2. Materials and Methods

2.1. Study Area

The study area is a part of the Padma River, downstream of the confluence of the Ganges and Brahmaputra rivers (Figure 2. 1). The morphology of the Padma River is highly variable,

ranging from straight, to meandering and braided channels (NASA Earth Observatory, 2019). The erosion and deposition patterns of the river reshape the islands and bars (locally called *chars*) (Sarker et al., 2003), which range from 1 to 36 years in age. Some are occupied by human settlements (PMBDP, 2010). Naturally, islands are a vegetated portion of the study area, but the edges are bare land that is inundated seasonally.

The study reach is about 50 km in length, demarcated as from Baruria, Manikganj to Mawa, Munsiganj, just before the Padma bridge (Figure 1). Before Mawa, an outflow called Arial Khan diverges from the main channel, but no tributaries enter the reach. The selected area is highly dynamic, with a diversified landform, ranging in width from less than 2 km to 12 km. The maximum discharge is about 75,000 m^3/s during the monsoon, and the minimum is about 5000 m^3/s during the dry/winter season (BWDB, 2021). Mean annual rainfall is about 2000 mm and mostly occurs during the monsoon (Billah, 2018). After the monsoon, in-channel emergent sediment units appear, which are used for the cultivation of a variety of crops.

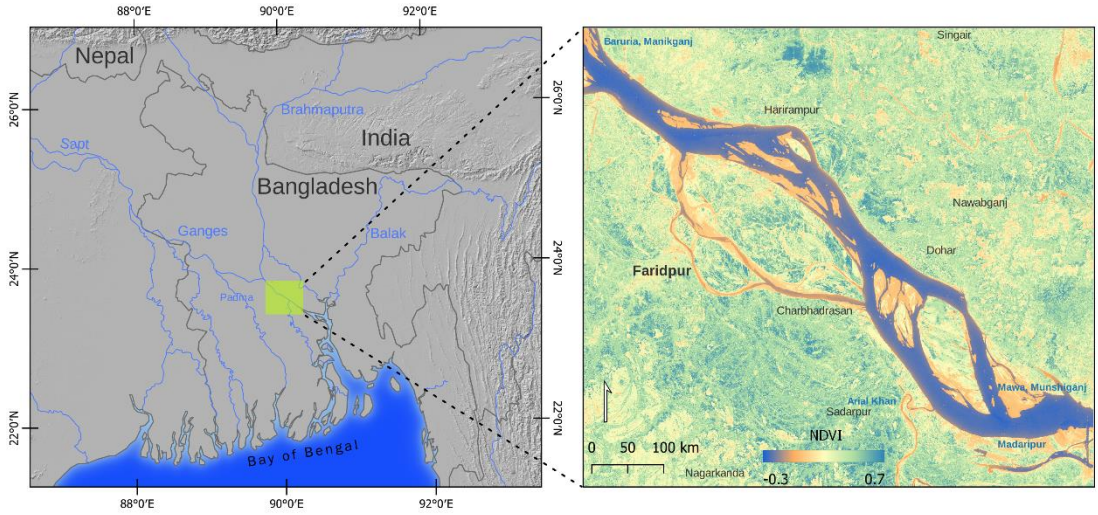

Figure 2. 1 Study area of Padma River, Bangladesh (Source: OpenStreetMap Contributors, Natural Earth, Mapzen Global Terrain).

2.2. Geomorphic Classification of GUs

Geomorphic classification of GUs followed the approach of Rinaldi et al. (2015). The spatial setting for the GU analysis was bankfull channel width, which comprises (i) 'submerged' channel units (main and secondary); (ii) 'emergent' sediment units (bars, islands, inactive channels); and (iii) in-channel vegetation units. All of these are called macro-units. Macro-units are further divided into units and sub-units. GU names and classified codes were adopted from Rinaldi et al. (2015), except water depression (WD) and sub-units (Table 2. 1).

Table 2. 1 Names and identification codes of macro-units, units, and sub-units used in the present classification.

Macro-units		Units		Sub-Units	
Name	**Code**	**Name**	**Code**	**Name**	**Code**
Submerged channel units	C S	Main channel	C	-	-
		Secondary channel	S	-	-
Emergent sediment units	E	Bank-attached bar	EA	Side bar	SB
		Mid-channel bar	EC	Longitudinal bar	L
				Transverse bar	T
		Dry channel	ED	-	-
		Unvegetated bank	EK	-	-
		Water depression	WD	-	-
In-channel vegetation units	V	Island	VI	-	-
		Water depression	WD	-	-

2.3. Seasonal Breakdown and Image Selection

Data for 2016–2020 river discharge were collected from the Bangladesh Water Development Board (BWDB) (Figure 2. 2). Based on these, four seasons of monsoon, post-monsoon, dry/winter, and pre-monsoon were identified. These were considered relevant temporal periods, for which satellite images could be used for the analysis. Additional criteria of image selection were (i) coverage of the study area, (ii) sensing date (considering seasons), (iii) mission type (Sentinel 2A/2B), (iv) product type (level 1C), and (v) percentage of cloud cover. Remotely sensed, multi-spectral satellite data (Sentinel 2) of consecutive years (2019–2020) were collected from the Copernicus Open Access Hub (https://scihub.copernicus.eu/dhus/#/home). Details of the satellite images are summarized in Table 2. 2.

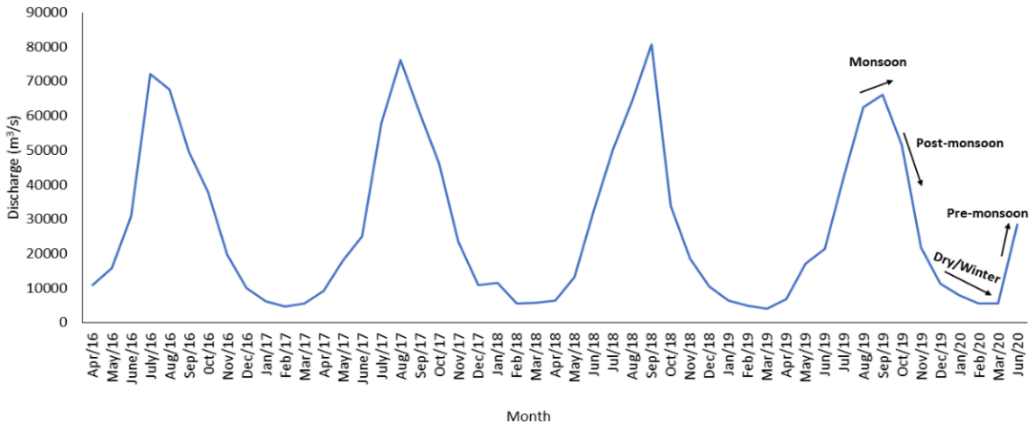

Figure 2. 2 Monthly mean discharge data from 2016 to 2020 of the study area in Padma River, Bangladesh.

Table 2. 2 Description of the Sentinel 2 level 1 product (S2MSI1C) used during the present study.

Satellite/Sensor	Acquisition Date	Season	Tile	Cloud Cover
Sentinel 2A/MSI	19 September 2019	Monsoon 2019	45QYG	2.64
Sentinel 2A/MSI	19 September 2019	Monsoon 2019	45QZG	4.56
Sentinel 2B/MSI	11 November 2019	Post-monsoon 2019	45QYG	0
Sentinel 2B/MSI	11 November 2019	Post-monsoon 2019	45QZG	0.85
Sentinel 2B/MSI	11 February 2020	Dry/Winter 2020	45QYG	0
Sentinel 2B/MSI	11 February 2020	Dry/Winter 2020	45QZG	0
Sentinel 2B/MSI	16 April 2020	Pre-monsoon 2020	45QYG	0.12
Sentinel 2B/MSI	16 April 2020	Pre-monsoon 2020	45QZG	4.17
Sentinel 2B/MSI	11 May 2020	Pre-monsoon 2020	45QYG	47.05
Sentinel 2B/MSI	11 May 2020	Pre-monsoon 2020	45QZG	52.10

2.4. Image Processing and Analysis

The Sentinel-2 Level-1C image products provide geocoded top-of-atmosphere (TOA) reflectance after computation of cloud (opaque/cirrus) and land/water masks, based on spectral criteria (SUHET, 2015). Image processing and analysis were performed in QGIS, following the steps shown in Figure 2. 3.

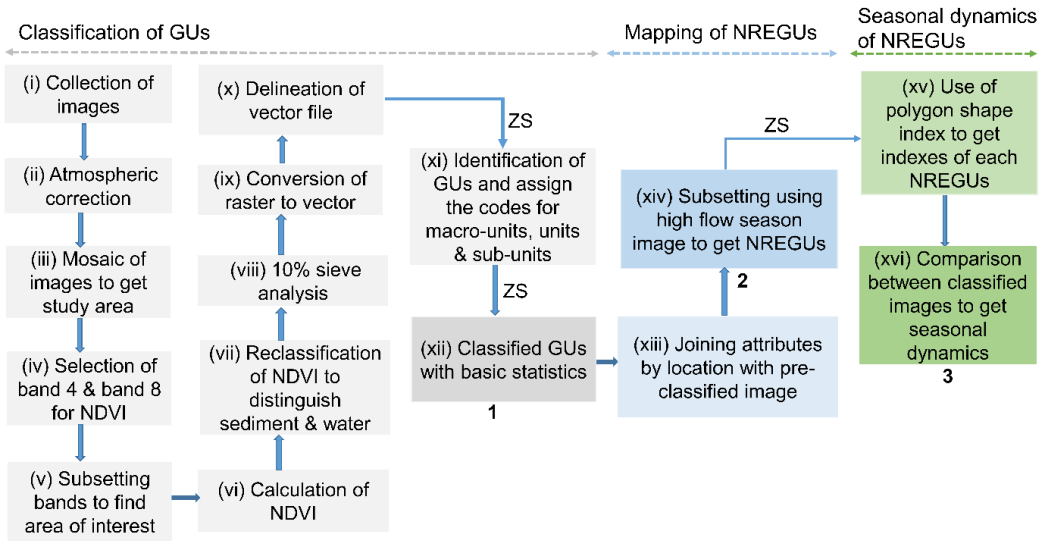

Figure 2. 3 Work flow for the identification and categorization of geomorphic units (GUs), nutrient retention, or export relevant geomorphic units (NREGUs) and their seasonal dynamics using Sentinel-2 images. The dark color of the boxes indicates different important steps of classification. ***1*** *= Completion of geomorphic units (GUs) classification;* ***2*** *= Completion of nutrient retention or export relevant GU (NREGUs) classification;* ***3*** *= Seasonal dynamics of NREGUs. ZS= Zonal statistics.*

(a) After collection, an atmospheric correction (Dark Object Subtraction, DOS1 (Moran et al., 1992) was applied to all the images, using the semi-automatic classification plugin (SCP) tool for QGIS (Congedo 2021). Mosaics of image pairs were created to cover the study area and, consequently, subsetted to the area of interest using the bands needed to calculate NDVI (Band 4—Red and Band 8—Near-Infrared). After subsetting, the study area was

devoid of cloud cover except pre-monsoon 2020. Therefore, for pre-monsoon 2020, four images were used. The first images of May 2020 were used for obtaining cloud-free areas, and after subsetting, the study area was subject to about 5% cloud cover. Using a cloud mask, two images of April 2020 were used to replace the cloud pixels (Figure 2. 3, i–v).

(b) NDVI values range from −1 to 1. Generally, the value approaching −1 represents water; the value varying from −0.1 to 0.1 corresponds to barren areas of sand, and a value greater than 0.1 corresponds to vegetated areas (JARS, 1993, Gandhi et al., 2015). Using visible red (Band 4) and near-infrared (Band 8) bands of Sentinel-2 data, NDVI was calculated and used to classify and analyze images. Based on the NDVI value, GUs were reclassified as land (emergent) and water (submerged). During the conversion from raster to vector, a 10% sieve analysis was performed to remove small polygons of 10 square meters in size from the result (Figure 2. 3, vi–viii).

(c) The study area was delineated based on the image of the dry/winter season (February 2020). Next, all the GUs were classified into units and sub-units based on position and shape, i.e., location of GUs in the main channel or secondary channel and orientation of GUs towards the flow direction. After applying zonal statistics, the end product of the analysis was classified as geomorphic units with counted pixels, mean NDVI value, surface area, perimeter, and maximum distance between two vertices of each polygon (Figure 2. 3, ix–xii).

(d) Inundated GUs or portions of GUs in high flow seasons that emerged during other seasons were termed nutrient retention- or export-relevant geomorphic units (NREGUs). Thus, classified GUs of the monsoon season (high flow) were overlapped with other seasons, to determine the nutrient retention-relevant terrestrial geomorphic units or emergent sediment units. The extraction of NREGUs was based on assumptions that (i) in large rivers, discharge is the main factor regulating nutrient retention or export (de Klein and Koelmans, 2011; Krishna et al., 2016; Best, 2019); (ii) changes in discharge are responsible for the alteration of water residence time; (iii) the surface area of the channel and water depth are considered determining factors for nutrient retention/export (Ye et al., 2017; Basu et al., 2011; Mulholland et al., 2010; Seitzinger et al., 2006; Alexander et al., 2000); (iv) like the riparian zone, GUs can be flooded annually and enriched with nutrients; and (v) nutrients enter into the system through runoff and sediment supply (Figure 2. 3, xiii–xiv).

(e) The delineation and classification of GUs were first performed for the image of the dry/winter season. Therefore, to keep the exact identification of GUs in the other images, the attributes of the GUs layer were joined by their location, resulting in corresponding GUs in other seasons. Manual cross-checking was done for each GU, other than the dry/winter seasons. Further analysis of GUs was done using zonal statistics, which provided the number of counted pixels, mean, sum, variance, maximum, and minimum value of NDVI in each GU type (emergent and submerged). The polygon shape index from SAGA (Lang and Blaschke, 2007) was used, resulting in different shape index values for each NREGU. The empirical formula of the polygon shape index is:

Polygon Shape Index = Perimeter/ [2 × Square Root (Π × Area)]

The surface area, perimeter, and polygon shape index of different NREGUs were compared among images of different seasons, to determine the seasonal dynamics (Figure 2. 3, xv–xvi).

(f) Geometric errors resulting from vectorizing raster data were corrected using the fix geometrics (FG) tool.

2.5. Field Observation and Morphometric Analysis of NREGUs

A field validation study was conducted during the dry/winter season. During the field visit, spot identification of GUs was recorded with a smartphone, using the Input app (https://inputapp.io). This app is linked with a repository of geodata (Mergin cloud service, https://public.cloudmergin.com) and can be synchronized within QGIS, avoiding further manual processing. NREGUs of the study reach of the previous year were developed prior to the field survey. The mean NDVI value of each NREGU was used to observe a seasonal variation. Besides NDVI, polygon shape index, surface area, perimeter area ratio (P/A), and maximum distance of NREGUs were used for the morphometric analysis of NREGUs. Regression analysis was performed, to determine the primary determinant of polygon shape index, which can show the suitability of the shape index to differentiate the sub-units longitudinal (L) and transverse bar (T). The analysis was performed in R v4.1.2 (Venables and Smith, 2021).

3. Results

3.1. Identification of GUs and Seasonal Dynamics

The geomorphic mapping showed that the study area consisted of three macro-units and seven sub-units. The macro-units are baseflow or submerged units (C/S), emergent sediment units (E), and in-channel vegetation (V). The units were categorized as primary and secondary channels (C & S), mid-channel bar (EC), bank-attached bar (EA), unvegetated bank (EK), dry channel (ED), island (VI), and water depression (WD). Further EC were classified into the sub-units, longitudinal bar (L) and transverse bar (T), and EA into the side bar (SB).

The identified types of GUs were observed in all four seasons, except ED in the monsoon. The surface area of C/S was maximum during monsoon and minimum during the dry/winter season (Figure 2. 4). However, the numbers of E and V were highest during pre-monsoon. An inverse relationship between discharge (m^3/s) and surface area of E and V was observed throughout the study year. The number of GUs varied with discharge. When water level increased, inundation split the bars (E) and islands (V), increasing the number, but reducing the surface area. This phenomenon was primarily observed pre-monsoon. During the dry/winter season, the surface area of E and V increased, with concomitant reductions in their number (Figure 2. 5).

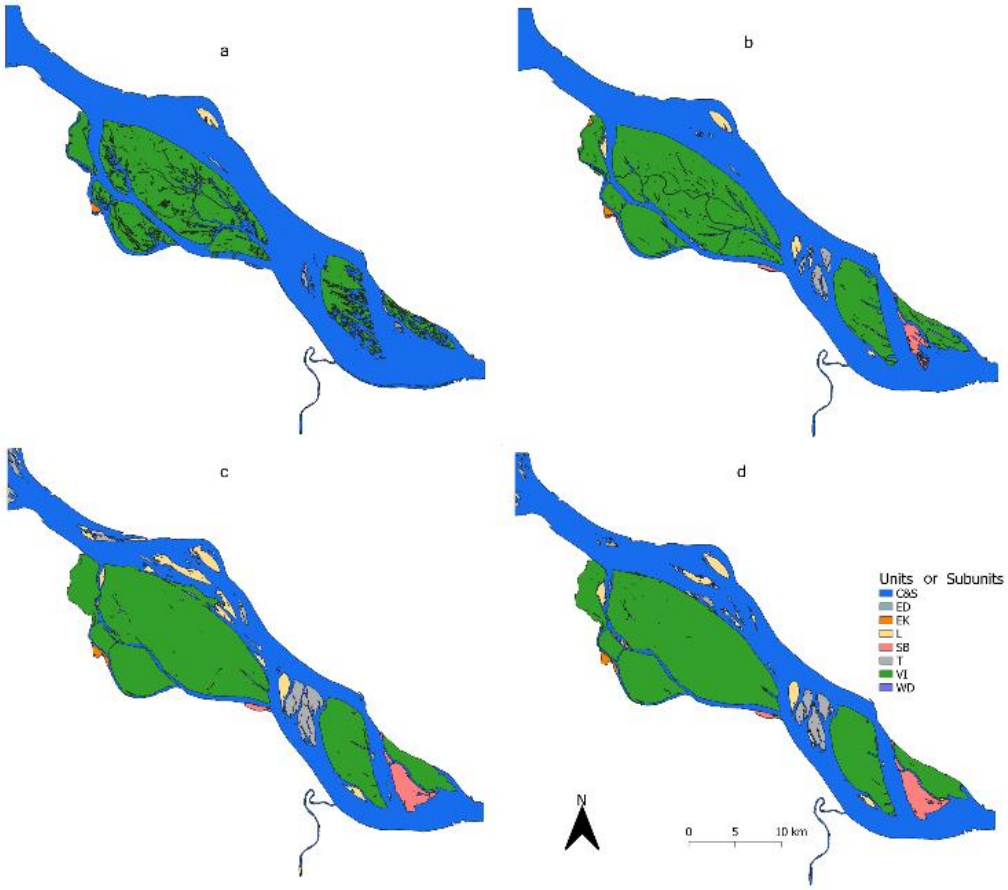

*Figure 2. 4 Geomorphic units (GUs) of the Padma River, Bangladesh during (**a**) monsoon 2019, (**b**) post-monsoon 2019, (**c**) dry/winter 2020, and (**d**) pre-monsoon 2020.*

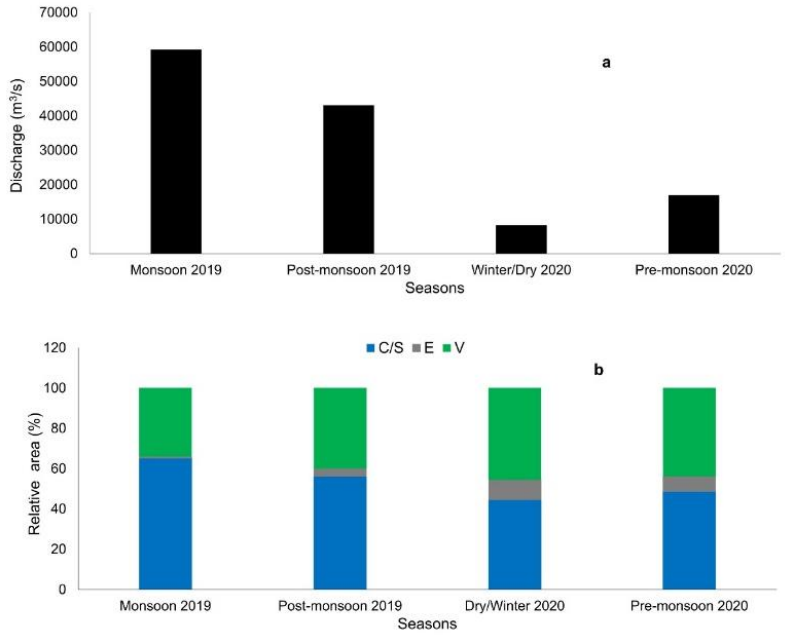

*Figure 2. 5 Seasonal changes of (**a**) discharge and (**b**) surface area of GUs (macro-unit level) of the Padma River, Bangladesh during monsoon 2019, post-monsoon 2019, dry/winter 2020, and pre-monsoon 2020.*

3.2. Seasonal Variation of NREGUs

Mapping of estimated nutrient retention or export-related GUs (NREGUs) showed that the remaining bars accounted for only 0.96% of surface area during the monsoon, and all of this was in EC. The maximum surface area of C & S was observed during the monsoon season (92.6%), followed by the post-monsoon season (87.5%), and the minimum was observed during the dry/winter season (63.5%). Among the emergent units, the surface area of VI was the maximum, followed by EC, EA, EK, and ED. The maximum surface areas of VI and EC were observed during the dry/winter season (VI = 21.9% and EC = 10.49%), and the minimum during the monsoon season (VI = 3.79% and EC = 0.96%). The surface areas of ED and EK were higher in the post-monsoon season than in the dry/winter season (Table 2. 3 and Figure 2. 6). Such a result was found because, in the dry/winter season, some of the ED and EK portions merged as islands. As with GUs, the seasonal prevalence of NREGUs was related to discharge.

Table 2. 3 The surface area of NREGUs in the Padma River, Bangladesh in km^2 and percentage.

GU	Monsoon		Post-Monsoon		Dry/Winter		Pre-Monsoon	
	km^2	%	km^2	%	km^2	%	km^2	%
C&S	362.58	92.6	315.0	87.53	250.88	63.52	274.75	77.0
EA	0.00	-	0.69	0.19	13.29	3.36	13.49	3.78
EC	3.78	0.96	13.25	3.68	41.43	10.49	24.1	6.76
ED	0.00	-	0.30	0.08	0.1	0.02	0.03	0.01
EK	0.00	-	0.94	0.26	0.57	0.14	0.53	0.15
VI	14.83	3.79	26.2	7.28	86.5	21.90	42.9	12.0
WD	10.34	2.64	3.48	0.97	2.2	0.56	0.98	0.28

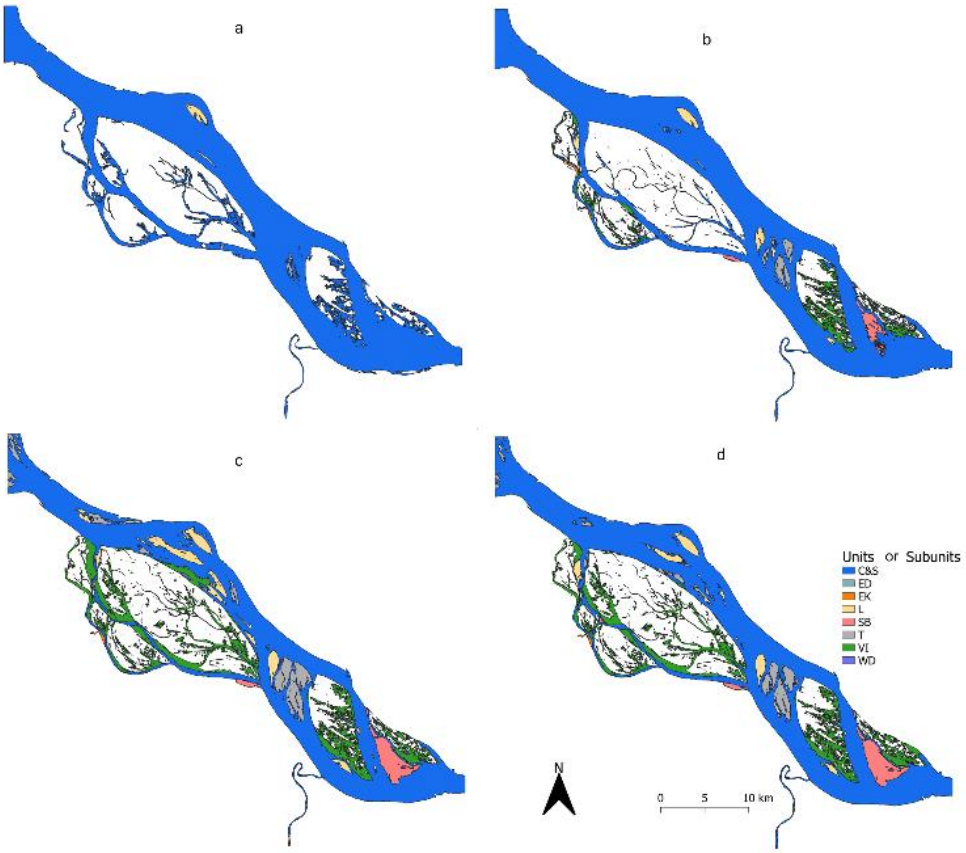

*Figure 2. 6 Nutrient retention or export-related GUs of the Padma River, Bangladesh during (**a**) monsoon 2019, (**b**) post-monsoon 2019, (**c**) dry/winter 2020, and (**d**) pre-monsoon 2020.*

3.3. Use of NDVI and Shape Indexes for Morphometric Analysis

The identification of GUs and NREGUs was mainly based on NDVI. The mean NDVI value of each NREGU showed that it explicitly differentiated channels (C & S), bars (SB, T and L), and islands (VI), and that these NREGUs represent a high proportion of the study area. The NDVI value of C & S was always less than 0, but varied across seasons. This finding demonstrated the effectiveness of the use of NDVI in the seasonal classification of NREGUs. NDVI values showed the expected results in the case of bars (0.1 < median NDVI < 0.2) and islands (median NDVI > 0.2). The bars were primarily sandy units with or without vegetation, whereas islands are the main vegetated units, showing higher NDVI than bars. The NDVI value of WD was around 0, because these were the shallow water portions inside islands or bars, represented by a relatively small surface area. The identification of NREGUs was validated by field observations during the dry/winter season. NDVI values from the field identified C & S, bars, and VI corresponding to the derived values of satellite identified NREGUs (Figure 2. 7).

Shape characterization shows the variation of spatial data. During the present study, the NDVI value was not useful to differentiate among the bar subtypes, but the polygon shape index and perimeter/area were useful. The polygon shape index distinguished longitudinal bar

(L) and transverse bar (T) during post-monsoon and dry/winter, where the median value of L was greater than 2 and T was less than 2. However, during pre-monsoon, the polygon shape index did not show satisfactory results when the median value of the polygon shape index was near 2. This happened due to the divergent nature of the bars; i.e., splitting of the bars occurred due to an increase of water volume. The perimeter area ratio (P/A) differentiated L and T during pre-monsoon, when the median values of L and T were above and below 0.1, respectively (Figure 2. 8).

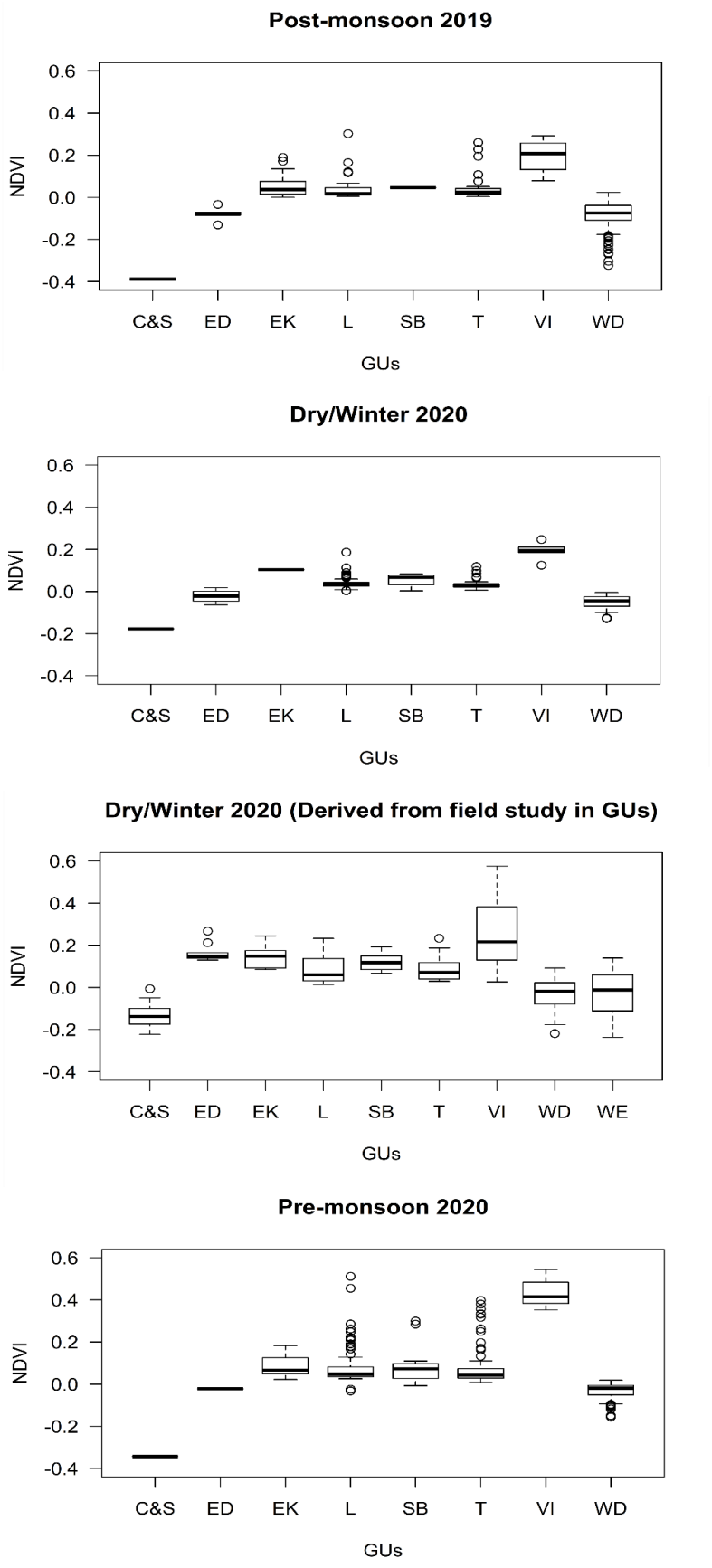

Figure 2. 7 Mean NDVI value of NREGUs during different seasons in the Padma River, Bangladesh.

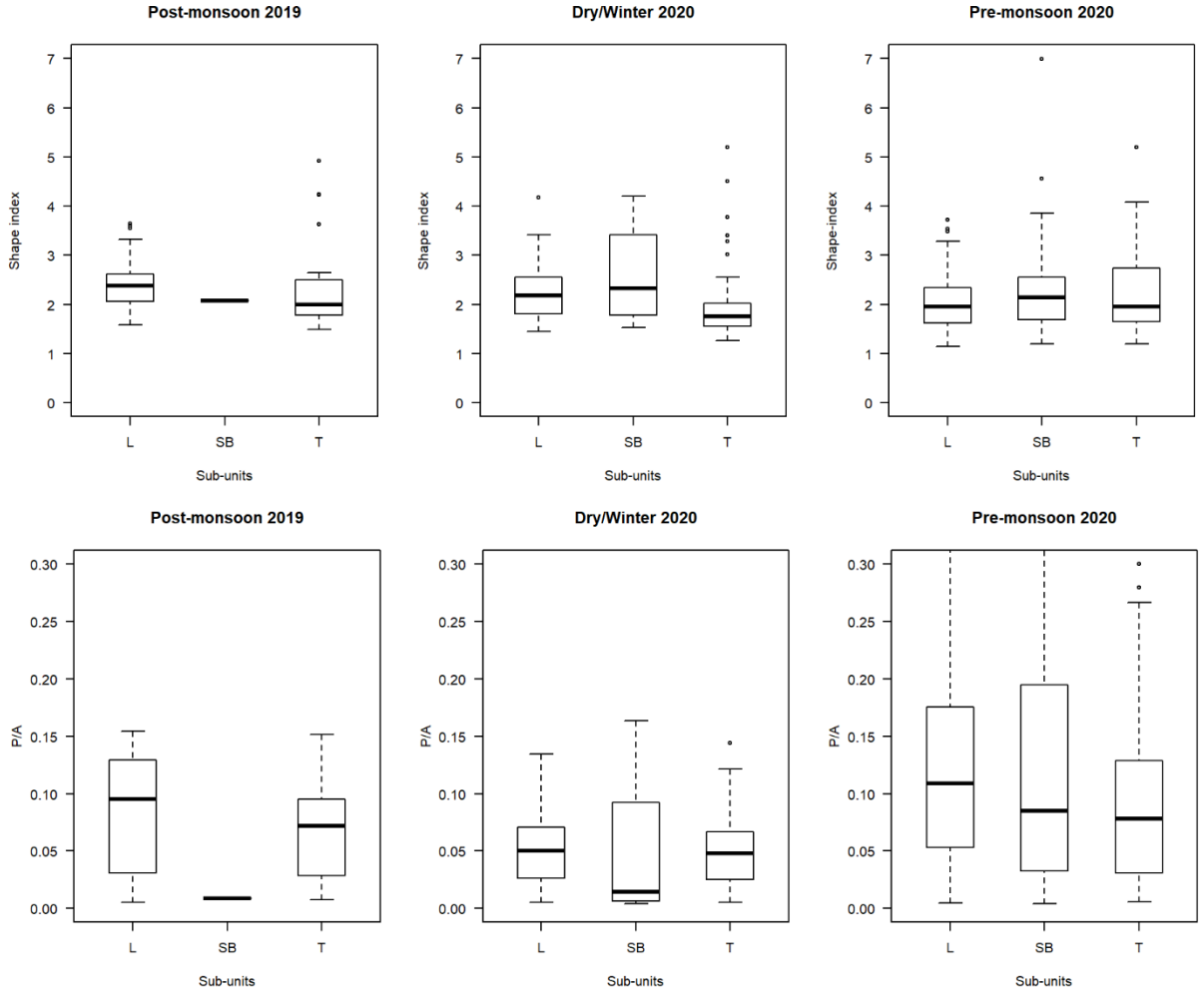

Figure 2. 8 Polygon shape index (shape index) and perimeter and area ratio (P/A) of longitudinal (L), transverse (T), and side bar (SB) in post-monsoon 2019, dry/winter 2020, and pre-monsoon 2020 in Padma River, Bangladesh.

The regression analysis between polygon shape index and different parameters (area, perimeter, and maximum distance) of the longitudinal bar (L) and transverse bar (T) in three seasons showed that the R^2 value was higher in the case of perimeter, followed by maximum distance and area (Figure 9). As such, the perimeter was the important parameter that most impacted the value of the polygon shape index. This finding mainly validated the categorization of bars. The finding even supported the results during post-monsoon and dry/winter seasons, when the shape index differentiated L and T. Thus, polygon shape index was essential for classifying the subtypes of the bar. Comparatively lower R^2 values (L = 0.541; T = 0.4742) during pre-monsoon for perimeter compared with shape index were evidence that the polygon shape index did not help differentiate between L and T, but perimeter area ratio (P/A) was effective in that case (Figures 2. 8 and 2. 9).

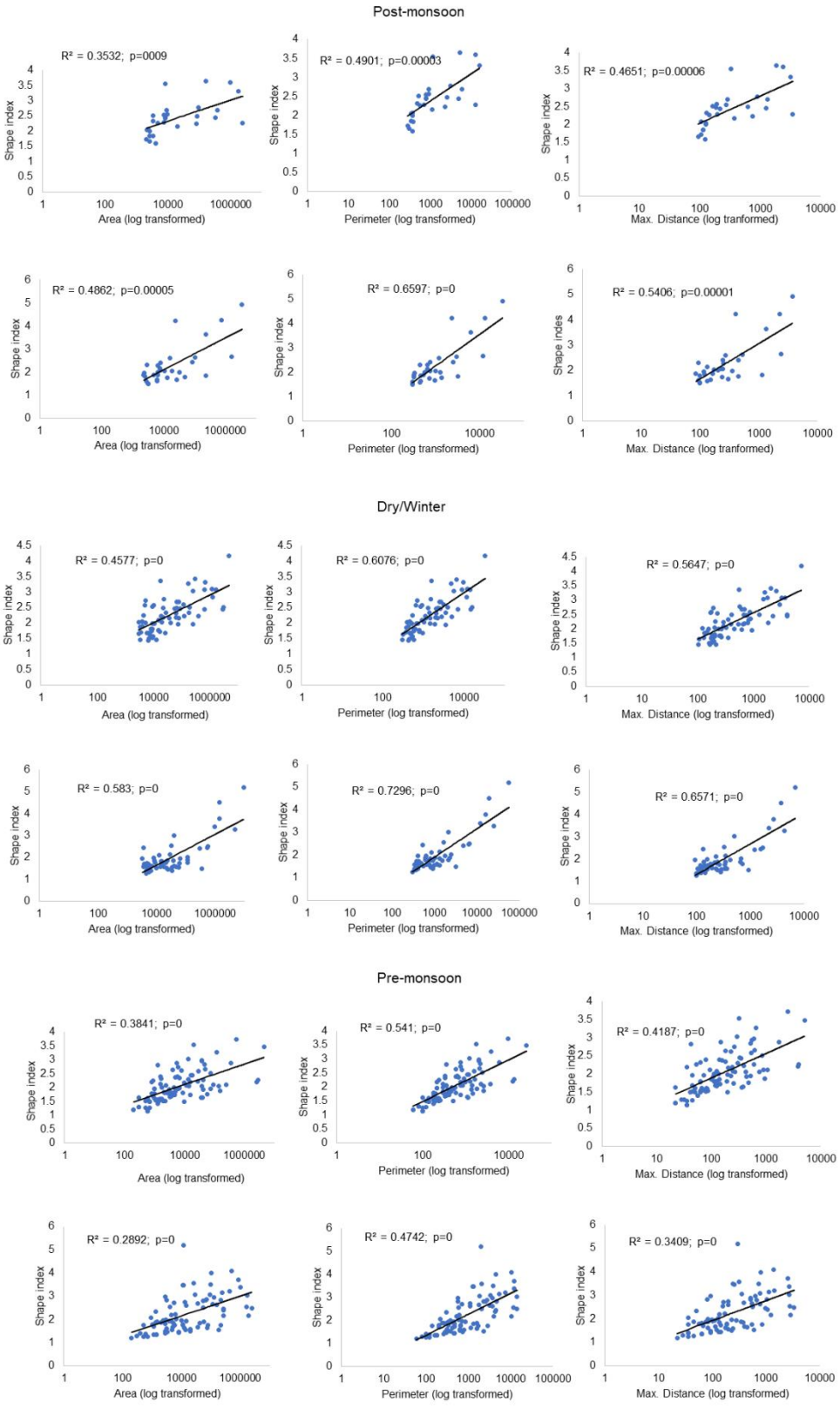

Figure 2. 9 Linear regression between shape index and surface area, perimeter, and maximum distance of longitudinal bar (L) and transverse bar (T) during post-monsoon-2019, dry/winter 2020, and pre-monsoon 2020 Padma River, Bangladesh.

4. Discussion

River hydromorphology plays a role in ecological processes, habitat structure, and water quality (del Tanago et al., 2021; Vaughan et al., 2009). Classification of GUs in rivers aids the assessment of seasonal or long-term hydromorphological alterations (Belletti et al., 2017). Previously, GUs of the upper part of the Padma River were identified and categorized as active channel, mid channel bar, lateral bar deposit, new bar deposit, old bar deposit, abandoned channel deposit, and flood plain deposit, to assess its morphological pattern over the decade using sinuosity ratio, braided index, and percentage of islands (Islam, 2016). The present classification scheme incorporates an NDVI-based seasonal approach, which can be used to establish links between hydromorphology and biogeochemical processes of the river reach.

It has been observed that erosion and deposition at GUs in large lowland rivers are related to the seasonal discharges (Liu et al., 2019) that drive hydrological and sediment dynamics (Billah, 2018; Mahmud et al., 2017). The present study illustrates the importance of seasonal discharge for the surface area and number of GUs, and how this affects NREGUs and, hence, nutrient flux in large rivers (Best, 2019; Masotti et al., 2018). In the Padma River, the area of bars (E) and islands (VI) have increased over the years (Billah, 2018; Nawfee et al., 2018; Hossain et al., 2013). This has implications for the nutrient dynamics in the river, changing flow velocity, and water residence time. The maximum exposed surface area of E and VI of the study reach was observed during the dry/winter season. Low water flows were prevalent during the winter/dry season, associated with a comparatively large portion of emergent sediment units. Nawfee et al. (2018) observed the characteristics of the river over a period from 1973 to 2014, where the erosion–deposition process of the bars was stable during the low flooding season (dry/winter season) and can be described as a geomorphologically dynamic equilibrium state (Wampler, 2012; Shields et al., 2003; Knighton, 1998). Some of the geomorphically complex large rivers consist of a significant portion of vegetated islands, due to the stable state (Islam, 2016; Pareta and Pareta, 2020; Meshkova and Carling, 2012; Latrubesse, 2008). Some portions of bars are used for cultivation and can present various LULC patterns in different seasons.

The finer resolution of Sentinel-2 was found to be useful, as it identified WD in different seasons. This also showed the applicability of NDVI over NDWI. The WD might be potentially important for nutrient retention, due to its capacity for retaining water for a longer period than other GUs, making the environment favorable for biogeochemical processes. Several studies have shown high denitrification rates in wetlands, related to temporal water retention (Palta et al., 2016; Marton et al., 2015; Pribyl et al., 2005). Unlike other studies (Wang et al., 2022; Liang et al., 2022; Fu and Burgher, 2015), the mean NDVI values of the VI in NREGUs in our study were below 0.6 in all seasons, because the study area consisted of only low growing vegetation, without trees or shrubs. Therefore, over saturation of NDVI due to dense vegetation might not be considered a hindrance for the present research and provides the effectiveness of NDVI over EVI. However, the latter is considered more suitable than NDVI in some remote sensing studies (Khare et al., 2021; Yu and Leng, 2022; Munyati, 2022).

NDVI can be used to classify land cover to some degree (Mia et al., 2019) and estimate nutrient retention (Redhead et al., 2018; Decsi etal., 2020). Classification of NREGUs based on NDVI provides the potential to categorize vegetation nutrient retention. Studies on the Parana River in Argentina showed that vegetation is closely linked with geomorphic units (Marchetti et al., 2013). Recently NDVI has been implemented for crop classification and irrigation water monitoring (Freden et al., 1974; Piedelbo et al., 2019 a; Piedelbo et al., 2018) both might be favorable for the present study, due to inundation and human-induced LULC types. In the GUs of the Padma River, both natural and human-induced vegetation were observed. Especially in the islands (VI) and bars (E), the vegetation cover and types were different. There is strong evidence that biogeochemical processes such as plant uptake and denitrification can vary according to vegetation cover and type (Yousaf et al., 2021; Ma et al., 2020; Kayima and Mayo, 2020). Thus, NDVI-based LULC mapping might be useful to predict the spatial and temporal variation of nutrient retention processes of the study reach and other similar river systems.

Shape characterization is important for mapping and delineating in-channel GUs and describing spatiotemporal changes of GUs (Wheaton et al., 2015; Wyrick et al., 2014). The position and geometry of the bars change over time in the Padma River (Islam, 2016). A significant association was observed during the present study between polygon shape index and perimeter from post-monsoon to dry/winter seasons, when water depth and discharge decreased. This finding could be associated with other seasonal measurements of nutrient retention processes, to determine the impact of the shape of the bars. Alternatively, the spatial variation of nutrient retention of a geomorphically complex river can be linked, by determining the geometry of the bars, i.e., shape characterization, because discharge plays a vital role in both cases.

5. Conclusions

The NDVI based GU classification scheme provides a new approach for assessing GUs in large geomorphically complex lowland rivers. The use of NDVI brings the opportunity to incorporate vegetation and LULC. Thus, LULC types in GUs can be considered patches that might be useful to link with the biogeochemical and ecological processes of river systems. Mean NDVI distinguished, not only primary and secondary channels (C & S), islands (VI), and bars (EC), but also changes across seasons. This finding indicates the effectiveness of NDVI-based classification. The study confirmed that seasonal discharge could significantly change the surface area of water and sediment portions of the river channel. The present study also showed that morphometric parameters, i.e., polygon shape index, help categorize the types of bar, such as longitudinal (L) and transverse (T), where NDVI was ineffective. The perimeter of the bars (L and T) is the primary determiner of the polygon shape index. This provides the potential for using shape index to estimate the spatiotemporal variation of nutrient retention processes among in-channel emergent sediment units, which can be further tested with field research. The approach we presented here should also be tested with complementary direct and indirect techniques using other satellite data.

6. References

Ahamed A. & Bolten J. D. A. (2017). MODIS-Based Automated Flood Monitoring System for Southeast Asia. Int. J. Appl. Earth Obs. Geoinf, 61, 104–117. https://doi.org/10.1016/J.JAG.2017.05.006.

Alexander R. B., Smith R. A. & Schwarz G. E. (2000). Effect of Stream Channel Size on the Delivery of Nitrogen to the Gulf of Mexico. Nature, 403, 758–761. https://doi.org/10.1038/35001562.

Balestrini R., Arese C. & Delconte C. (2006). Nitrogen Removal in a Freshwater Riparian Wetland: An Example from an Italian Lowland Spring. Internationale Vereinigung für Theoretische und Angewandte Limnologie Verhandlungen 29, 2217–2220. https://doi.org/10.1080/03680770.2006.11903085.

Balestrini R., Arese C., Delconte C. A., Lotti A. & Salerno F. (2011). Nitrogen Removal in Subsurface Water by Narrow Buffer Strips in the Intensive Farming Landscape of the Po River Watershed, Italy. Ecol. Eng., 37, 148–157. https://doi.org/10.1016/j.ecoleng.2010.08.003.

Basu N. B., Rao P. S. C., Thompson S. E., Loukinova N. V., Donner S. D., Ye S. & Sivapalan M. (2011) Spatiotemporal Averaging of In-Stream Solute Removal Dynamics. Water Resour. Res., 47, W00J06, ~~1–13~~. https://doi.org/10.1029/2010WR010196.

Belletti B., Rinaldi M., Bussettini M., Comiti F., Gurnell A. M., Mao L., Nardi L. & Vezza P. (2017). Geomorphology Characterising Physical Habitats and Fl Uvial Hydromorphology: A New System for the Survey and Classi Fi Cation of River Geomorphic Units. Geomorphology, 283, 143–157. https://doi.org/10.1016/j.geomorph.2017.01.032.

Bernot M. J. & Dodds W. K. (2005). Nitrogen Retention, Removal, and Saturation in Lotic Ecosystems. Ecosystems, 8, 442–453. https://doi.org/10.1007/s10021-003-0143-y.

Best J. (2019). Anthropogenic Stresses on the World's Big Rivers. Nat. Geosci., 12, 7–21. https://doi.org/10.1038/s41561-018-0262-x.

Billah M. M. (2018). Mapping and Monitoring Erosion-Accretion in an Alluvial River Using Satellite Imagery-The River Bank Changes of The Padma River in Bangladesh. Quaestiones Geographicae, 37, 87–95.

Binding C. E., Greenberg T. A., Watson S. B., Rastin, S. & Gould J. (2015). Long Term Water Clarity Changes in North America's Great Lakes from Multi-Sensor Satellite Observations. Limnol. Oceanogr., 60, 1976–1995. https://doi.org/10.1002/lno.10146.

Boz B. & Gumiero B. (2016). Nitrogen Removal in an Afforested Riparian Zone: The Contribution of Denitrification Processes. Hydrobiologia, 774, 167–182. https://doi.org/10.1007/s10750-015-2609-2.

BWDB (Bangladesh Water Development Board) (2021). Available online: http://www.hydrology.bwdb.gov.bd/index.php?pagetitle=discharge_data_view&sub2=139&_subid=132&id=134 (accessed on 20 March 2021).

Cheng F. Y. & Basu N. B. (2017). Biogeochemical Hotspots: Role of Small Water Bodies in Landscape Nutrient Processing. Water Resour. Res., 53, 5038–5056. https://doi.org/10.1002/2016WR020102.

Congedo L. (2021). Semi-Automatic Classification Plugin: A Python tool for the download and processing of remote sensing images in QGIS. J. Open Source Softw. **2021,** 6, 3172. https://doi.org/10.21105/joss. 03172.

de Grandpré A., Kinnard C. & Bertolo A. (2022). Open-Source Analysis of Submerged Aquatic Vegetation Cover in Complex Waters Using High-Resolution Satellite Remote Sensing: An Adaptable Framework. Remote Sens., 14, 267. https://doi.org/10.3390/rs14020267.

de Klein J. J. M. & Koelmans A. A. (2011). Quantifying Seasonal Export and Retention of Nutrients in West European Lowland Rivers at Catchment Scale. Hydrol. Processes, 25, 2102–2111. https://doi.org/10.1002/hyp.7964.

de Stefano L. G., Valdivia A. S., Gianello D., Gerea M., Reissig M., García P. E., García R. D., Cárdenas C. S., Diéguez M. C., Queimaliños C. P., et al. (2022). Using CDOM Spectral Shape Information to Improve the Estimation of DOC Concentration in Inland Waters: A Case Study of Andean Patagonian Lakes. Sci. Total Environ., 824, 153752. https://doi.org/10.1016/J.SCITOTENV.2022.153752.

Decsi B., Vári Á. & Kozma Z (2020). The Effect of Future Land Use Changes on Hydrologic Ecosystem Services: A Case Study from the Zala Catchment, Hungary. Biologia Futura, 71, 405–418. https://doi.org/10.1007/s42977-020-00032-6.

del Tánago G. M., Martínez-Fernández V., Aguiar F. C., Bertoldi W., Dufour S., García de Jalón D., Garófano-Gómez V., Mandzukovski D. & Rodríguez-González P. M. (2021). Improving River Hydromorphological Assessment through Better Integration of Riparian Vegetation: Scientific Evidence and Guidelines. J. Environ. Manag., 292, 112730.

Didan K., Munoz B. A., Solano R. & Huete A. (2015). MODIS Vegetation Index User's Guide (MOD13 Series); University of Arizona: Tucson, AZ, US.

Drusch M., del Bello U., Carlier S., Colin O., Fernandez V., Gascon F., Hoersch B., Isola C., Laberinti P., Martimort P., et al. (2012). Sentinel-2: ESA's Optical High-Resolution Mission for GMES Operational Services. Remote Sens. Environ., 120, 25–36. https://doi.org/10.1016/J.RSE.2011.11.026.

Eisner S., Flörke M., Chamorro A., Daggupati P. (2017). An Ensemble Analysis of Climate Change Impacts on Streamflow Seasonality across 11 Large River Basins. Clim. Change, 141, 401–417. https://doi.org/10.1007/s10584-016-1844-5.

Elosegi A. & Pozo J. (2016). Altered Organic Matter Dynamics in Rivers and Streams: Ecological Consequences and Management Implications. Limnetica, 35, 303–322. https://doi.org/10.23818/limn.35.25.

Faruque M. J., Vekerdy Z., Hasan M. Y., Islam K. Z., Young B., Ahmed M. T., Monir M. U., Shovon S. M., Kakon J. F. & Kundu P. (2022). Monitoring of Land Use and Land Cover Changes by Using Remote Sensing and GIS Techniques at Human-Induced Mangrove Forests Areas in Bangladesh. Remote Sens. Appl. Soc. Environ., 25, 100699. https://doi.org/10.1016/J.RSASE.2022.100699.

Fay A. R. & McKinley G. A. (2017). Correlations of Surface Ocean PCO2 to Satellite Chlorophyll on Monthly to Interannual Timescales. Glob. Biogeochem. Cycles, 31, 436–455. https://doi.org/10.1002/2016GB005563.

Freden S. C., Mercanti E. P. & Becker M. A. (1974.). Third Earth Resources Technology Satellite-1 Symposium—Volume 1: Technical Presentations; NASA: Washington, DC, USA (Eds), pp. 309–317.

Fryirs K. & Brierley G. (2022). Assemblages of Geomorphic Units: A Building Block Approach to Analysis and Interpretation of River Character, Behaviour, Condition and Recovery. Earth Surf. Processes Landf, 47, 92–108. https://doi.org/10.1002/esp.5264.

Fryirs K. A. & Brierley G. J. (2013). Geomorphic Analysis of River Systems: An Approach to Reading the Landscape; John Wiley & Sons, Ltd.: Hoboken, NJ, USA, ISBN 9781741382983.

Fu B. & Burgher I. (2015). Riparian Vegetation NDVI Dynamics and Its Relationship with Climate, Surface Water and Groundwater. J. Arid Environ., 113, 59–68. https://doi.org/10.1016/J.JARIDENV.2014.09.010.

Gameiro S., Nascimento V., Facco D., Sfredo G. & Ometto J. (2022). Multitemporal Spatial Analysis of Land Use and Land Cover Changes in the Lower Jaguaribe Hydrographic Sub-Basin, Ceará, Northeast Brazil. Land, 11, 103. https://doi.org/10.3390/land11010103.

Gandhi G. M., Parthiban S., Thummalu N. & Christy A. (2015). Ndvi: Vegetation Change Detection Using Remote Sensing and Gis—A Case Study of Vellore District. Procedia Comput. Sci., 57, 1199–1210.

Ge G., Zhang J., Chen X., Liu X., Hao Y., Yang X. & Kwon S. M. (2022). Effects of Land Use and Land Cover Change on Ecosystem Services in an Arid Desert-Oasis Ecotone along the Yellow River of China. Ecol. Eng., 176, 106512. https://doi.org/10.1016/J.ECOLENG.2021.106512.

Gomez-Velez J. D., Harvey J. W., Cardenas M. B. & Kiel B. (2015). Denitrification in the Mississippi River Network Controlled by Flow through River Bedforms. Nat. Geosci., 8, 941–945. https://doi.org/10.1038/ngeo2567.

Grizzetti B., Passy P., Billen G., Bouraoui F., Garnier J. & Lassaletta L. (2015). The Role of Water Nitrogen Retention in Integrated Nutrient Management: Assessment in a Large Basin Using Different Modelling Approaches. Environ. Res. Lett., 10, 065008. https://doi.org/10.1088/1748-9326/10/6/065008.

Guilhen J., al Bitar A., Sauvage S., Parrens M., Martinez J. M., Abril G., Moreira-Turcq P. & Sánchez-Pérez J. M. (2020). Denitrification and Associated Nitrous Oxide and Carbon Dioxide Emissions from the Amazonian Wetlands. Biogeosciences, 17, 4297–4311. https://doi.org/10.5194/bg-17-4297-2020.

Han M., Brierley G. (2020). Channel Geomorphology and Riparian Vegetation Interactions along Four Anabranching Reaches of the Upper Yellow River. Prog. Phys. Geogr. Earth Environ., 44, 898–922. https://doi.org/10.1177/0309133320938768.

Hossain M. A., Gan T. Y. & Baki A. B. M. (2013). Assessing Morphological Changes of the Ganges River Using Satellite Images. Quat. Int., 304, 142–155. https://doi.org/10.1016/j.quaint.2013.03.028.

Islam A. B. M. T. (2016). Assessment of Fluvial Channel Dynamics of Padma River in Northwestern Bangladesh. Univers. J. Geosci., 4, 41–49. https://doi.org/10.13189/ujg.2016.040204.

JARS (Japan Association on Remote Sensing) (1993). Remote Sensing Note; Nihon Printing Co. Ltd.: Tokyo, Japan.

Jossette G., Leporcq B. & Sanchez N. (1999). Philippon Biogeochemical Mass-Balances (C, N, P, Si) in Three Large Reservoirs of the Seine Basin (France). Biogeochemistry, 47, 119–146.

Kaplan G. & Avdan U. (2017). Mapping and Monitoring Wetlands Using Sentinel-2 Satellite Imagery. ISPRS Annals of the Photogrammetry, Remote Sensing and Spatial Information Sciences, Volume IV-4/W4, 4th International GeoAdvances Workshop, Safranbolu, Turkey, 14–15 October 2017; pp. 271–277.

Kayima J. K. & Mayo A. W. (2020). Nitrogen Removal Buffer Capacity of the Lubigi Wetland in Uganda. Phys. Chem. Earth Parts A/B/C, 117, 102883. https://doi.org/10.1016/J.PCE.2020.102883.

Khare S., Deslauriers A., Morin H., Latifi H. & Rossi S. (2021). Comparing Time-Lapse PhenoCams with Satellite Observations across the Boreal Forest of Quebec, Canada. Remote Sens., 14, 100. https://doi.org/10.3390/rs14010100.

Knighton A. D. (1998). Fluvial Forms and Processes: A New Perspective; Edward Arnold Publishers: London, UK, 383p., ISBN 0 340 66313 8. https://doi.org/10.7202/004839ar.

Kratzer S., Kyryliuk D., Edman M., Philipson P. & Lyon S. (2019). Synergy of Satellite, In Situ and Modelled Data for Addressing the Scarcity of Water Quality Information for Eutrophication Assessment and Monitoring of Swedish Coastal Waters. Remote Sens., 11, 2051. https://doi.org/10.3390/rs11172051.

Krishna M. S., Prasad M. H. K., Rao D. B., Viswanadham R., Sarma V V. S. S. & Reddy N. P. C. (2016). ScienceDirect Export of Dissolved Inorganic Nutrients to the Northern Indian Ocean from the Indian Monsoonal Rivers during Discharge Period. Geochim. Cosmochim. Acta, 172, 430–443. https://doi.org/10.1016/j.gca.2015.10.013.

Kumari N., Srivastava A. & Dumka U. C. (2021). A Long-Term Spatiotemporal Analysis of Vegetation Greenness over the Himalayan Region Using Google Earth Engine. Climate, 9, 109. https://doi.org/10.3390/cli9070109.

Kwak Y. (2017). Nationwide Flood Monitoring for Disaster Risk Reduction Using Multiple Satellite Data. ISPRS Int. J. Geo-Inf., 6, 203. https://doi.org/10.3390/ijgi6070203.

Lang S. & Blaschke T. (2007). Landschaftsanalyse Mit GIS; utb GmbH: Stuttgart, Germany; ISBN 9783838583471.

Latrubesse E. M. (2008). Patterns of Anabranching Channels: The Ultimate End-Member Adjustment of Mega Rivers. Geomorphology, 101, 130–145. https://doi.org/10.1016/j.geomorph.2008.05.035.

Li S., Chen F., Song K., Liu G., Tao H., Xu S., Wang X., Wang Q. & Mu G. (2022). Mapping the Trophic State Index of Eastern Lakes in China Using an Empirical Model and Sentinel-2 Imagery Data. J. Hydrol., 608, 127613. https://doi.org/10.1016/J.JHYDROL.2022.127613.

Liang S., Gong Z., Wang Y., Zhao J. & Zhao W. (2022). Accurate Monitoring of Submerged Aquatic Vegetation in a Macrophytic Lake Using Time-Series Sentinel-2 Images. Remote Sens., 14, 640. https://doi.org/10.3390/rs14030640.

Liu X., Shi C., Zhou Y., Gu, Z. & Li H. (2019). Response of Erosion and Deposition of Channel Bed, Banks and Floodplains Towater and Sediment Changes in the Lower Yellow River, China. Water, 11, 357. https://doi.org/10.3390/w11020357.

Luan J., Liu D., Zhang L., Huang Q., Feng J., Lin M. & Li G. (2018). Analysis of the Spatial-Temporal Change of the Vegetation Index in the Upper Reach of Han River Basin in 2000–2016. Proc. Proc. Int. Assoc. Hydrol. Sci., 379, 287–292.

Ma L., Xiong Z., Yao L., Liu G., Zhang Q. & Liu W. (2020). Soil Properties Alter Plant and Microbial Communities to Modulate Denitrification Rates in Subtropical Riparian Wetlands. Land Degrad. Dev., 31, 1792–1802. https://doi.org/10.1002/ldr.3569.

Mahmud I. H., Pal P. K., Rahman A. & Yunus A. (2017). A Study on Seasonal Variation of Hydrodynamic Parameters of Padma River. J. Mod. Sci. Technol., 5, 1–10.

Marchetti Z. Y., Latrubesse E. M., Pereira M. S. & Ramonell C. G. (2013). Vegetation and Its Relationship with Geomorphologic Units in the Parana River floodplain, Argentina. J. South Am. Earth Sci., 46, 122–136. https://doi.org/10.1016/j.jsames.2013.03.010.

Marchetti Z. Y., Minotti P. G., Ramonell C. G., Schivo F., Kandus P. (2016). NDVI Patterns as Indicator of Morphodynamic Activity in the Middle Paraná River Floodplain. Geomorphology, 253, 146–158. https://doi.org/10.1016/j.geomorph.2015.10.003.

Marchetti Z. Y., Ramonell C. G., Brumnich F., Alberdi R. & Kandus P. (2020). Vegetation and Hydrogeomorphic Features of a Large Lowland River: NDVI Patterns Summarizing Fluvial Dynamics and Supporting Interpretations of Ecological Patterns. Earth Surf. Processes Landf, 45, 694–706. https://doi.org/10.1002/esp.4766.

Markogianni V., Kalivas D., Petropoulos G. P., Dimitriou E. (2022). Modelling of Greek Lakes Water Quality Using Earth Observation in the Framework of the Water Framework Directive (WFD). Remote Sens., 14, 739. https://doi.org/10.3390/rs14030739.

Martínez-Espinosa C., Sauvage S., al Bitar A., Green P. A., Vörösmarty C. J., Sánchez-Pérez J. M. (2021). Denitrification in Wetlands: A Review towards a Quantification at Global Scale. Sci. Total Environ., 754, 142398. https://doi.org/10.1016/J.SCITOTENV.2020.142398.

Martín-Ortega P., García-Montero L. G. & Sibelet N. (2020). Temporal Patterns in Illumination Conditions and Its Effect on Vegetation Indices Using Landsat on Google Earth Engine. Remote Sens., 12, 211. https://doi.org/10.3390/rs12020211.

Marton J. M., Creed I. F., Lewis D. B., Lane C. R., Basu N. B., Cohen M. J. & Craft C. B. (2015). Geographically Isolated Wetlands Are Important Biogeochemical Reactors on the Landscape. BioScience, 65, 408–418. https://doi.org/10.1093/biosci/biv009.

Masotti I., Aparicio-Rizzo P., Yevenes M. A., Garreaud R., Belmar L. & Farías L. (2018). The Influence of River Discharge on Nutrient Export and Phytoplankton Biomass off the Central Chile Coast (33°–37°S): Seasonal Cycle and Interannual Variability. Front. Mar. Sci., 5, 423. https://doi.org/10.3389/fmars.2018.00423.

Masoud A. A. (2022). On the Retrieval of the Water Quality Parameters from Sentinel-3/2 and Landsat-8 OLI in the Nile Delta's Coastal and Inland Waters. Water, 14, 593. https://doi.org/10.3390/w14040593.

McFeeters S. K. (1996). The Use of the Normalized Difference Water Index (NDWI) in the Delineation of Open Water Features. Int. J. Remote Sens., 17, 1425–1432. https://doi.org/10.1080/01431169608948714.

Meshkova L. V. & Carling P. A. (2012). The Geomorphological Characteristics of the Mekong River in Northern Cambodia: A Mixed Bedrock–Alluvial Multi-Channel Network. Geomorphology, 147–148, 2–17. https://doi.org/10.1016/J.GEOMORPH.2011.06.041.

Mia M. B., Hasan T., Akhter S. H. (2019). Change Detection of Landuse-Landcover in and around Cox's Bazar-Teknaf Coastal Area of Bangladesh Using Satellite Images. Dhaka Univ. J. Earth Environ. Sci., 8, 1–9.

Moran M. S., Jackson R. D., Slater P. N. & Teillet P. M. (1992). Evaluation of Simplified Procedures for Retrieval of Land Surface Reflectance Factors from Satellite Sensor Output. Remote Sens. Environ., 41, 169–184. https://doi.org/10.1016/0034-4257(92)90076-V.

Mulholland P. J. & Webster J. R. (2010). Nutrient Dynamics in Streams and the Role of J-NABS Nutrient Dynamics in Streams and the Role of J-NABS. J. North Am. Benthol. Soc., 29, 100–117. https://doi.org/10.1899/08-035.1.

Munyati C. (2022). Detecting the Distribution of Grass Aboveground Biomass on a Rangeland Using Sentinel-2 MSI Vegetation Indices. Adv. Space Res., 69, 1130–1145. https://doi.org/10.1016/J.ASR.2021.10.048.

NASA Earth Observatory (2019). Available online: https://earthobservatory.nasa.gov/world-of-change/PadmaRiver (accessed on 27 March 2019).

Nawfee S. M., Dewan A. & Rashid T. (2018). Integrating Subsurface Stratigraphic Records with Satellite Images to Investigate Channel Change and Bar Evolution: A Case Study of the Padma River, Bangladesh. Environ. Earth Sci., 77, 89. https://doi.org/10.1007/s12665-018-7264-2.

Palta M. M., Ehrenfeld J. G., Giménez D., Groffman P. M. & Subroy V. (2016). Soil Texture and Water Retention as Spatial Predictors of Denitrification in Urban Wetlands. Soil Biol. Biochem., 101, 237–250. https://doi.org/10.1016/J.SOILBIO.2016.06.011.

Pareta K. & Pareta U. (2020). Geomorphic Classification and Mapping of Rapti River System Using Satellite Remote Sensing Data. Am. J. Geophys. Geochem. Geosystems, 6, 1–15.

Piedelobo L., Taramelli A., Schiavon E., Valentini E., Molina J. L., Nguyen X. A., González-Aguilera D. (2019a) Assessment of Green Infrastructure in Riparian Zones Using Copernicus Programme. Remote Sens., 11, 2967. https://doi.org/10.3390/rs11242967.

Piedelobo L., Hernández-López D., Ballesteros R., Chakhar A., del Pozo S., González-Aguilera D. & Moreno M. A. (2019b). Scalable Pixel-Based Crop Classification Combining Sentinel-2 and Landsat-8 Data Time Series: Case Study of the Duero River Basin. Agric. Syst., 171, 36–50. https://doi.org/10.1016/J.AGSY.2019.01.005.

Piedelobo L., Ortega-Terol D., del Pozo S., Hernández-López D., Ballesteros R., Moreno M., Molina J. L. & González-Aguilera D. (2018). HidroMap: A New Tool for Irrigation Monitoring and Management Using Free Satellite Imagery. ISPRS Int. J. Geo-Inf., 7, 220. https://doi.org/10.3390/ijgi7060220.

PMBDP (Padma Multipurpose Bridge Design Project) (2010). Updated Scheme Design Report for River Training Works; AECOM New Zealand Limited, Ed.; Bangladesh Bridge Authority: Dhaka, Bangladesh; Volume 1.

Pribyl A. L., Mccutchan J. H., Lewis W. M., Saunders J. F. (2005). Whole-System Estimation of Denitrification in a Plains River: A Comparison of Two Methods. Biogeochemistry, 73, 439–455. https://doi.org/10.1007/s10533-004-0565-4.

Redhead J. W., May L., Oliver T. H., Hamel P., Sharp R., Bullock J. M. (2018). National Scale Evaluation of the InVEST Nutrient Retention Model in the United Kingdom. Sci. Total Environ., 610–611, 666–677. https://doi.org/10.1016/j.scitotenv.2017.08.092.

Rinaldi M., Belletti B., Comiti F., Nardi L., Bussettini M., Mao L. & Gurnel A. M. (2015). The Geomorphic Units Survey and Classification System (GUS), Deliverable 6.2, Part 4, of REFORM (REstoring Rivers FOR Effective Catchment Management), a Collaborative Project (Large-Scale Integrating Project) Funded by the European Commission within the 7th Framework Programme under Grant Agreement 282656.

Sarker M. H., Koudstaal R. & Alam M. (2003). Rivers, Chars and Char Dwellers of Bangladesh. Int. J. River Basin Manag., 1, 61–80. https://doi.org/10.1080/15715124.2003.9635193.

Seitzinger S., Harrison J. A., Böhlke J. K., Bouwman A. F., Lowrance R., Peterson B., Tobias C., van Drecht G. (2006). Denitrification across Landscapes and Waterscapes: A Synthesis. Ecol. Appl., 16, 2064–2090. https://doi.org/10.1890/1051-0761(2006)016[2064:DALAWA]2.0.CO;2.

Serrano J., Shahidian S. & da Silva M. J. (2019). Evaluation of Normalized Difference Water Index as a Tool for Monitoring Pasture Seasonal and Inter-Annual Variability in a Mediterranean Agro-Silvo-Pastoral System. Water, 11, 62. https://doi.org/10.3390/w11010062.

Shields F. D., Copeland R. R., Klingeman P. C., Doyle M. W. & Simon A. (2003). Design for Stream Restoration. J. Hydraul. Eng., 129, 575–584. https://doi.org/10.1061/(asce)0733-9429(2003)129:8(575).

Sigleo A. C. & Frick W. E. (2007). Seasonal Variations in River Discharge and Nutrient Export to a Northeastern Pacific Estuary. Estuar. Coast. Shelf Sci., 73, 368–378. https://doi.org/10.1016/j.ecss.2007.01.015.

Soar P. J., Wallerstein N. P. & Thorne C. R. (2017). Quantifying River Channel Stability at the Basin Scale. Water, 9, 133. https://doi.org/10.3390/w9020133.

Sonam J. V., Fryirs K. & Brierley G. (2022). Geomorphic Characterization of a Seasonal River Network in Semi-Arid Western India Using the River Styles Framework. J. Asian Earth Sci. X , 7, 100077. https://doi.org/10.1016/J.JAESX.2021.100077.

SUHET (2015). Sentinel-2 User Handbook; European Space Agency: Paris, France, pp. 1–64.

Taramelli A., Lissoni M., Piedelobo L., Schiavon E., Valentini E., Xuan A. N. & González-Aguilera D. (2019). Monitoring Green Infrastructure for Natural Water Retention Using Copernicus Global Land Products. Remote Sens., 11, 1583. https://doi.org/10.3390/rs11131583.

Tatariw C., Chapman E. L., Sponseller R. A., Mortazavi B. & Edmonds J. W. (2013). Denitrification in a Large River: Consideration of Geomorphic Controls on Microbial Activity and Community Structure. Ecology, 94, 2249–2262.

Vaughan I. P., Diamond M., Gurnell A. M., Hall K. A., Jenkins A., Milner N. J., Naylor L. A., Sear D. A., Woodward G. & Ormerod S. J. (2009). Integrating Ecology with Hydromorphology: A Priority for River Science and Management. Aquat. Conserv. Mar. Freshw. Ecosyst. 2009, 19, 113–125.

Venables W. N. & Smith D. M. (2021). R Development Core Team. An Introduction to R; Notes on R: A Programming Environment for Data Analysis and Graphics; R Development Core Team: Vienna, Austria.

Walton C. R., Zak D., Audet J., Petersen R. J., Lange J., Oehmke C., Wichtmann W., Kreyling J., Grygoruk M., Jabłońska E., et al. (2020). Wetland Buffer Zones for Nitrogen and Phosphorus Retention: Impacts of Soil Type, Hydrology and Vegetation. Sci. Total Environ., 727, 138709. https://doi.org/10.1016/j.scitotenv.2020.138709.

Wampler P. J. (2012). Rivers and Streams-Water and Sediment in Motion. Nat. Educ. Knowl., 3, 18.

Wang S., Li J., Zhang B., Spyrakos E., Tyler A. N., Shen Q., Zhang F., Kuster T., Lehmann M. K., Wu Y., et al. (2018). Trophic State Assessment of Global Inland Waters Using a MODIS-Derived Forel-Ule Index. Remote Sens. Environ., 217, 444–460. https://doi.org/10.1016/J.RSE.2018.08.026.

Wang W., Hu P., Yang Z., Wang J., Zhao J., Zeng Q., Liu H. & Yang Q. (2022). Prediction of NDVI Dynamics under Different Ecological Water Supplementation Scenarios Based on a Long Short-Term Memory Network in the Zhalong Wetland, China. J. Hydrol., 608, 127626. https://doi.org/10.1016/J.JHYDROL.2022.127626.

Wheaton J. M., Fryirs K. A., Brierley G., Bangen S. G., Bouwes N. & O'Brien G. (2015). Geomorphic Mapping and Taxonomy of Fluvial Landforms. Geomorphology, 248, 273–295. https://doi.org/10.1016/j.geomorph.2015.07.010.

Wieland M., Martinis S. A (2019). Modular Processing Chain for Automated Flood Monitoring from Multi-Spectral Satellite Data. Remote Sens., 11, 2330. https://doi.org/10.3390/rs11192330.

Wyrick J. R. & Pasternack G. B. (2014). Geospatial Organization of Fluvial Landforms in a Gravel-Cobble River: Beyond the Riffle-Pool Couplet. Geomorphology, 213, 48–65. https://doi.org/10.1016/j.geomorph.2013.12.040.

Wyrick J. R., Senter A. E. & Pasternack G. B. (2014). Revealing the Natural Complexity of Fluvial Morphology through 2D Hydrodynamic Delineation of River Landforms. Geomorphology, 210, 14–22. https://doi.org/10.1016/j.geomorph.2013.12.013.

Xu W., Yang D., Li Y. & Xiao R. (2016). Correlation Analysis of Mackenzie River Discharge and NDVI Relationship. Can. J. Remote Sens., 42, 292–306. https://doi.org/10.1080/07038992.2016.1171135.

Xue J. & Su B. (2017). Significant Remote Sensing Vegetation Indices: A Review of Developments and Applications. J. Sens., 2017, 1353691.

Ye S., Reisinger A. J., Tank J. L., Baker M. A., Hall R. O. Jr., Rosi E. J. & Sivapalan M. (2017). Scaling Dissolved Nutrient Removal in River Networks: A Comparative Modeling Investigation. Water Resour. Res., 53, 9623–9641. https://doi.org/10.1002/2017WR020858.

Yousaf A., Khalid N., Aqeel M., Noman A., Naeem N., Sarfraz W., Ejaz U., Qaiser Z. & Khalid A. (2021). Nitrogen Dynamics in Wetland Systems and Its Impact on Biodiversity. Nitrogen, 2, 13. https://doi.org/10.3390/nitrogen2020013.

Yu L. & Leng G. (2022). Identifying the Paths and Contributions of Climate Impacts on the Variation in Land Surface Albedo over the Arctic. Agric. For. Meteorol., 313, 108772. https://doi.org/10.1016/J.AGRFORMET.2021.108772.

Zeng S., Du C., Li Y, Lyu H., Dong X., Lei S., Li J. & Wang H. (2022). Monitoring the Particulate Phosphorus Concentration of Inland Waters on the Yangtze Plain and Understanding Its Relationship with Driving Factors Based on OLCI Data. Sci. Total Environ., 809, 151992. https://doi.org/10.1016/J.SCITOTENV.2021.151992

Chapter 3

ESTIMATION OF POTENTIAL DENITRIFICATION AND ITS SPATIOTEMPORAL DYNAMICS IN SEASONALLY INUNDATED GEOMORPHIC UNITS OF A LARGE TROPICAL RIVER USING SATELLITE DATA

Abstract

Denitrification in large tropical river systems is likely important for nitrogen retention estimates but is limited by the need for measurements and the ability to scale these estimates to relate seasonal changes in river geomorphology and discharge. Geomorphic units (GUs), which are classifications of features of a river system based on their inundation frequency and vegetation cover, may be useful to characterise features in river systems that influence denitrification rates. In this study, we tested the hypothesis that measurements of potential denitrification rate (PDR) using the denitrification enzyme assays from different GUs could be used first to relate PDR to soil, vegetation and different land use and land-cover (LULC) types as controlling factors and second that these characteristics could be assessed using remote sensing data to model PDR over a large spatial scale (along a 50 km reach) for the Padma River (Bangladesh). Specifically, 240 PDR measurements were made from the four LULC types within eight GUs during the dry/winter season 2020. Linear regression using a mixed-modelling approach showed that PDR was highly related to vegetation cover and soil moisture across all GUs. Sentinel-2 data were then used to develop relationships between NDVI and vegetation cover and between band 11 and soil moisture, which also reasonably described PDR rates. We then used this satellite data to estimate reach-scale PDR in post-monsoon, dry/winter and pre-monsoon seasons. The satellite-based model showed that PDR increased from post-monsoon 2019 to pre-monsoon 2020 in GUs. The vegetation islands and the bars were the most important GUs in all seasons for denitrification. The satellite-assisted approach developed in this study can be applied to the GUs in large lowland rivers where inundation occurs frequently.

Keywords: Sentinel-2, NDVI, soil moisture, LULC, linear mixed models (LMMs), Padma River, Bangladesh.

1. Introduction

Large rivers are geomorphologically diverse and dynamic with variations in flow that influence nitrogen transport to coastal areas. Water and sediment transport rates alter these systems continuously, creating a variety of recognisable geomorphic units (GUs) (Gupta, 2007; Syvitski et al., 2014) considered as building blocks of river morphology (Rinaldi et al., 2015). Seasonally inundated GUs of a lowland river can act like floodplains or riparian zones, making them either sinks or sources for nutrients (Alexander et al., 2000; Tank et al., 2008; Strauss et al., 2011; Ritz et al., 2018;). These potential nutrient retention/export areas can be mapped based on seasonal changes in area exposed (Gani et al., 2022). Among nutrients, nitrogen is of special importance for regulating river productivity (Nanus et al., 2008), but excess levels of nitrogen may cause adverse effects downstream like coastal eutrophication and hypoxia (van Wijk et al., 2020; Ritz and Fischer 2019; Lin et al., 2020). or contributing to poor health. Nitrogen in river systems can be conserved through retention, reducing export to the downstream part of the river.

Denitrification is one of the main biogeochemical processes that result in nitrogen loss from natural ecosystems, as nitrate is converted to N_2O and N_2 gases (Davidson and Seitzinger, 2006; Beaulieu et al., 2011; Yao et al., 2016). In rivers, denitrification varies with geomorphology, water residence time, nutrient content and biotic factors (Pina-Ochoa and Alvarez-Cobelas, 2006; Seitzinger et al., 2006; Solomon et al., 2009; Xiong et al., 2017; Korol et al., 2019), particularly oxygen availability and concentrations of nitrate and organic carbon (Boyer et al., 2006; Liu et al., 2016; Shrestha et al., 2012; Groffman et al., 1991; Sogouridis and Ullah, 2014). The soil/sediment's water content amplifies the rate of denitrification (Ding et al., 2019, Garnier et al., 2010; Ullah and Faulkner, 2006; Bai et al., 2005). A high moisture percentage restricts oxygen diffusion, creating favourable conditions for denitrification. Microorganism communities interact in the plant rhizosphere, so the presence or absence of vegetation drives the changes in land use and land cover (LULC), which influence the nitrogen budget in the sediment and thus the denitrification process (Audet et al., 2021; Nilsson et al., 2020). Seasonally inundated areas of GUs are characterized by soil/sediment moisture regimes, sediment characteristics, and vegetation dynamics that are important for denitrification.

The spatial variation of LULC types, representing different conditions of oxygen, nitrate and carbon, can be used as indirect predictors of denitrification (Kreilling et al., 2019; Xiong et al., 2015; Han et al., 2017). On a larger scale, LULC can be used as a proxy of vegetation dynamics (Guo et al., 2020) and soil moisture (Zucco et al., 2014; Yang et al., 2017). Recent research has shown that temporal variation of inundation should be considered to upscale potential denitrification because this controls nutrient and water supply to the floodplain ecosystems (Kaden et al., 2021). Therefore, many characteristics of the river channel can control denitrification directly or indirectly; methodological constraints make it difficult to link the spatial dynamics of the river channels to estimates of denitrification.

A number of techniques are available to estimate denitrification rates in soils/sediments (Tuttle et al., 2014; Tatariw et al., 2013; Opdyke et al., 2006). The acetylene inhibition

method (Sørensen, 1978) is mostly used because it is relatively simple to apply and allows for analysing large numbers of samples in space and time (Hansen, 2016; Groffman, 2006). Other methods such as mass balance approaches (Seitzinger et al., 2002), isotope analyses (Sebilo et al., 2017; Böhlke et al., 2004), membrane inlet mass spectrometry (Laursen and Seitzinger, 2002; Pribyl et al., 2005) and modelling (Sun et al., 2017; Hoang et al., 2017; Maavara et al., 2019) have been used based on the conditions of the study sites. For these, however, it is difficult to determine the spatial variability of denitrification across river reaches due to their applicability, complexity and data demand to scale up at the desired level. It is even more complicated when the study area comprises different geomorphic units and is subject to seasonal flood dynamics and LULC changes.

Data derived from remote sensing creates opportunities to quantify biogeochemical processes like denitrification over larger areas; thus, satellite data are used as input data together with process-based measurements. Such an approach was applied in the Amazonian basin to quantify denitrification rates using available carbon and nitrate from *in situ* data and surface water extent from satellite data (Guilhen *et al*., 2020). Other researchers suggested that soil moisture might be one of the most relevant factors for scaling up denitrification at an appropriate spatial scale (Martínez-Espinosa et al., 2022, 2021; Robertson et al., 1993).

The Normalised Difference Vegetation Index (NDVI) is a widely used biogeophysical index to estimate vegetation cover (Yi et al., 2022; Dai et al., 2022; Yuan et al., 2013). NDVI is sensitive to inundation, varying according to water depth (Cho et al., 2008; Szabó et al., 2020). Different satellite products are available to estimate soil moisture that can be implemented from very local to large scales (Peng et al., 2021). Sentinel -2 band 11 is a shortwave infrared (1610 nm) (SWIR) band which can be used to discriminate moisture content in soil and vegetation (Holzman et al., 2021). One of the advantages of using Sentinel-2 products is that it can provide high spatial resolution data, i.e. 10 m for its visible and near-infrared bands (VNIR) and 20 m for band 11.

The present study aimed to assess the spatiotemporal distribution of PDR and develop a predictive model based on field-based and satellite data. The specific objectives of the research are to: (i) show the influence of LULC in field-based PDR measurement; (ii) determine whether satellite products can be related to soil moisture, vegetation cover, and LULC to model PDR at the reach scale; (iii) use the best model to predict reach-scale estimates of denitrification in the GU's and compare with seasons; and iv) show the impact of GUs on reach-scale denitrification.

2. Material and methods

2.2 Study Design and Site Description

The study area is a roughly 50 km reach of the Padma River below the confluence of the Brahmaputra and Ganges rivers (Figure 3. 1). Seasonal inundation and the erosion and deposition of sediment in the study reach lead to the formation of seasonally inundated GUs, which are classified as primary and secondary channels (C & S), longitudinal bars (L), transverse bars (T), side bars (SB), unvegetated banks (EK), dry channels (ED), vegetated

islands (VI) and water depressions (WD) (Gani et al. 2022). Each of these GUs is composed of patches of LULC types that change in area and vegetation cover through the year. During the field observation, five types of LULC were identified and included cropland (CL), natural vegetation (NV), land with water (LW), dry, bare land (DBL) and water bodies (WB). Water depressions (WD) in bars and islands, river edges and any wet portions of the terrestrial GUs were considered in the LW category. In some of the LW land cover types, algal mats were observed. Variations in the area of emergent GUs occur over four seasons. March-May is considered pre-monsoon, June-September is monsoon, October-November is considered post-monsoon, and December to February is considered dry/winter (Gani et al., 2022). The seasonally emergent GUs identified in this study are fully inundated during the monsoon. In the present research, field samples and analyses of denitrification rates were done for GUs in post-monsoon 2019, dry/winter 2020 and pre-monsoon 2020.

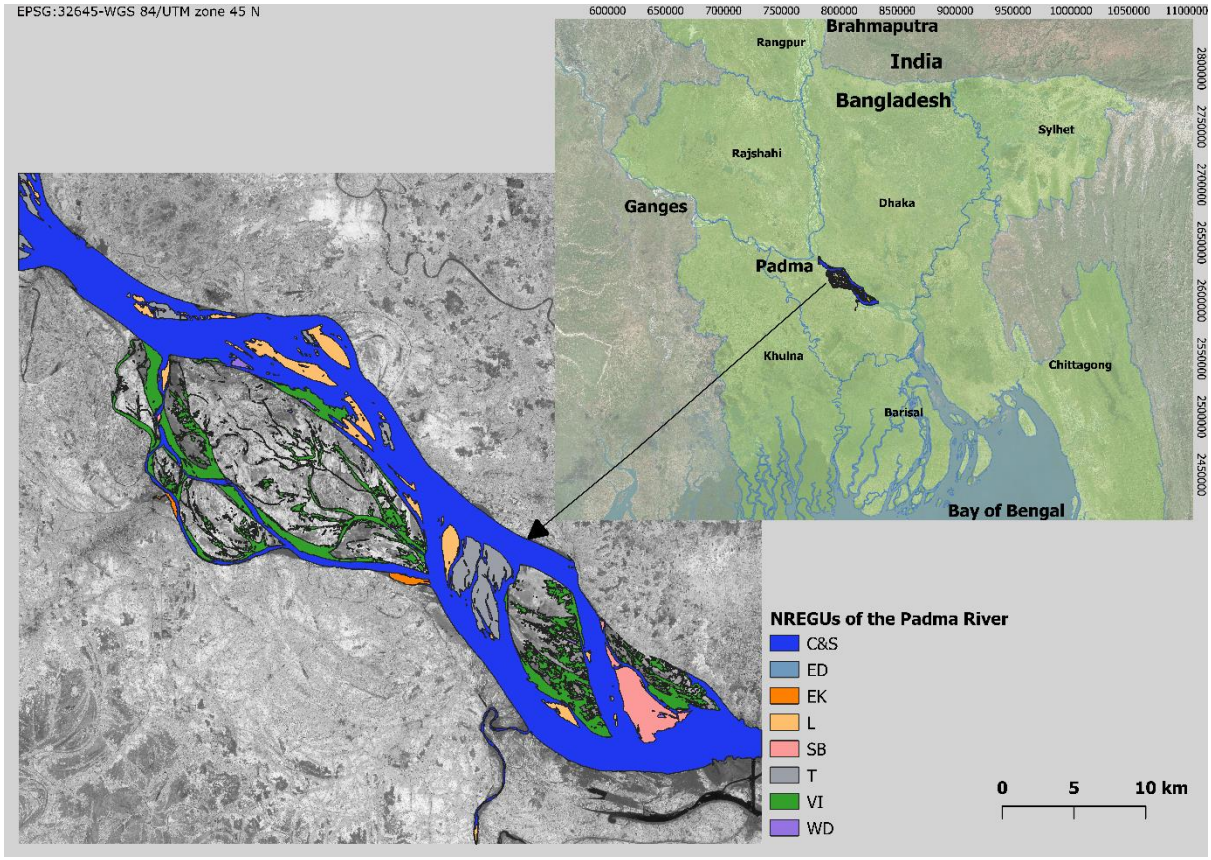

Figure 3. 1 Study area of Padma River, Bangladesh, showing the classified nutrient retention or export relevant geomorphic units (NREGUs) (C&S=Primary and secondary channels, ED= Dry channel, EK= Unvegetated bank, L= Longitudinal bar, SB= Side bar, T=Transverse bar, VI= Vegetation Island, WD= Water Depression).

2.2. Overall approach

To meet the research objectives, we performed field observation and samplings, laboratory analysis, classification of LULC, and data analysis sequentially, as shown in Figure 3. 2. In data analysis, the estimation of PDR by depth and LULC, and the development of linear mixed models (LMMs) were done separately. After developing the LMMs, raster data were prepared for model application, and finally, the model was applied in the GUs to determine spatiotemporal dynamics of PDR (Figure 3. 2).

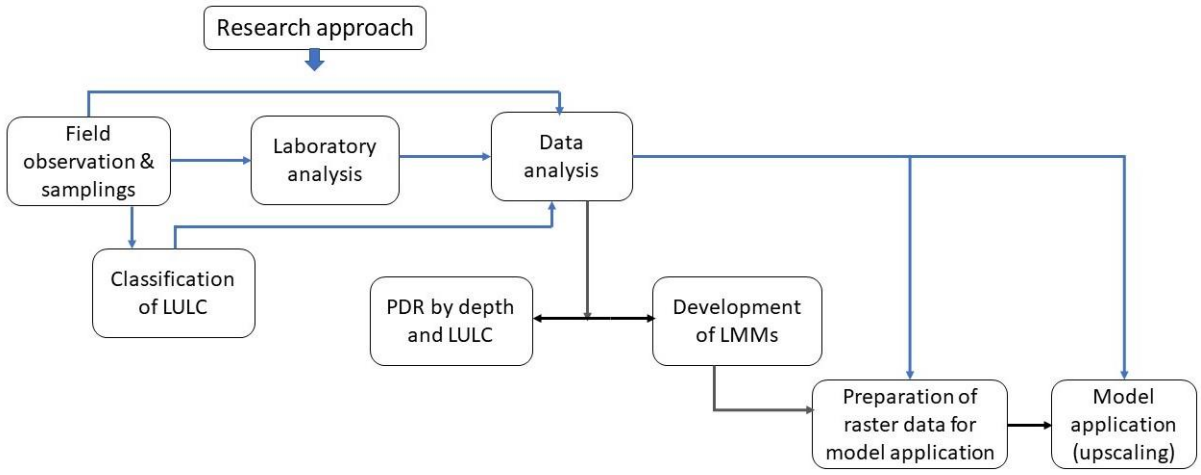

Figure 3. 2 Overall approach to meet the research objectives.

2.2.1. Field observation and samplings

During the field visit, spot identification of LULC types in different GUs (identified using sentinel-2 data) was done, and coordinates were recorded using the Input app (https://inputapp.io, accessed on 25 January 2022) in a smartphone. This app was linked with a geodata repository (Mergin cloud service, https://public.cloudmergin.com, accessed on 25 January 2022) and synchronised within QGIS. In QGIS, the sample points were buffered at a 10-meter distance to convert sampling points into polygons because homogeneous LULCs were found for at least 10 m distances during field observations.

Field sampling was carried out during the dry/low flow season (February 2020). Coordinates and % vegetation cover were also estimated at each sampling point within the GUs and recorded to reassess vegetation, if necessary. Simultaneous sediment samples were collected from the sampling points, covering all types of LULC (Fig. 2). Two sets of samples were taken from the top 5 cm (2 times 190 samples) and 5 – 10 cm (2 times 55 samples) of soil with a 10 cm-diameter PVC ring. All samples were kept separately in Ziplock bags stored in an icebox for the duration of the field campaign (1 or 2 days) and then transported to the research laboratory in the Department of Botany, Jagannath University, Dhaka, Bangladesh.

2.2.2 Laboratory analysis

In the laboratory, the samples were divided so that one set was used to estimate soil moisture and bulk density and the other denitrification. Samples were processed within 24 hours after reaching the laboratory. PDR was estimated by denitrification enzyme activity (DEA) as a

part of the acetylene block method as the accumulation of N_2O in the presence of acetylene (Groffman et al., 1999). In the laboratory, sediment samples were placed in gas-tight flasks with a septum port with the addition of media composed of NO_3 (100 mg N kg^{-1}), dextrose (40 mg kg^{-1}) and chloramphenicol (10 mg kg^{-1}). Anaerobic conditions were established by evacuating and flushing the headspace of flasks with nitrogen three times for 30 sec. Then, purified acetylene (98 to 99.5%) was added, and flasks were placed on a rotary shaker at 125 rpm for half an hour. Gas accumulated in the flask was extracted using a syringe and then injected into evacuated gas vials (15 mL) at three times every 30 mins. After processing, the resulting gas vials were transported to IHE Delft Institute for Water Education, the Netherlands. In Delft, N_2O was measured by gas chromatography (Scion 456-GC) using ambient air and standard N_2O concentration with the electron capture detector (ECD) at 250 ^oC (Groffman et al., 1999).

Potential denitrification rate (PDR)

Potential denitrification rate (PDR) was calculated as the slope of N_2O produced in the jars over the incubation time. The solubility of N_2O was accounted for using the Bunsen coefficeint at 0 ^oC. Mass-specific denitrification rates were converted to areal rates by using the bulk density. Specifically, PDR was calculated according to the following equations:

$$PDR = k \times M_r \times \left[\frac{\sum_{i=0}^{n}(C-\check{C})(T-\check{T})}{\sum_{i=0}^{n}(T-\check{T})} / S_w\right] \times \rho \times D$$

C and T are the known values of C (C0, C1, C2) and T (T0, T1 and T2), whereas $\check{\mathbf{C}}$ is the mean value of C0, C1, C2, and $\check{\mathbf{T}}$ is the mean value of T0, T1 and T2.

C0, C1 and C2 were calculated as µg N_2O= µg N_2O/mL× [vol. of gas in mL + (vol. of water in mL× Bunsen Coefficient)]

PDR is the rate of potential denitrification (mg N_2O-N m^{-2} h^{-1}), C0 is the N_2O mass at 30 mins (µg N_2O-N), C1 is the N_2O mass at 60 mins (µg N_2O-N), and C2 is the N_2O mass at 90 mins (µg N_2O-N). k is the conversion factor (µg cm^{-2} to mg m^{-2}) =10, M_r is the mass ratio of N_2 to N_2O (0.64), Sw is sample weight (g), ρ is bulk density (g/cm^3), D is the depth of collected sediment samples (5 cm) and T0, T1, and T2 are the durations of incubation (h).

2.3. Classification of LULC and Accuracy Assessment

Two segments of Sentinel 2B images during the dry period (11 February 2020) were downloaded (https://scihub.copernicus.eu/) and used to map LULC types. The image processing and analysis were performed using the semi-automatic classification plugin (SCP) tool in QGIS (Congedo, 2021). After collecting Sentinel-2 Level 1C products, an atmospheric correction was applied (Dark Object Subtraction, DOS1; Moran et al., 1992). To create a training set for the LULC classification, field-based observed LULC types were used. About 70% of the polygons were used as training data and the remainder as test data for the accuracy assessment. The training data were corrected by observing the NDVI value during post-monsoon and pre-monsoon. Next, the random forest classification algorithm (Breiman, 2001) was applied, using the ESA SNAP tool (SNAP version 8, http://step.esa.int). The

accuracy of the LULC classification was assessed based on the confusion matrix, user's accuracy, producer's accuracy, overall accuracy and kappa hat coefficient values.

2.4. Data Analysis

2.4.1. Differences in PDR by depth and LULC

A paired t-test was performed to compare the measured PDR from 0 – 5 cm depth and 5 – 10 cm depth. As there was no significant difference between the depths, data of 0 – 5 cm depth were used for the rest of the analysis. A Kruskal-Wallis rank test was applied to compare the PDR among the LULC types, with a post-hoc Dunn test with Bonferroni correction (R package "dunn.test"). All analyses were performed in R version 4.1.2 (R core Team, 2021).

2.4.2. Development of linear mixed models (LMMs)

In order to develop an effective model for predicting PDR from satellite data, we first developed best-fit multivariate models using field data that relied on soil moisture and vegetation parameters. These models (defined in this paper as models F) were then modified by substituting satellite data products for field data, either partly (models FS) or completely (models S). The resulting models predicted PDR for the entire study reach.

All models were linear mixed models (LMMs) developed following the procedure described by Zuur et al. (2007, 2009). This procedure includes a series of steps starting with a conventional regression model with the best possible fit, and extending this model with random effects and variance structures to further improve the fit of the model. The best fit model is selected based on the Akaike Information Criterion (AIC) and log-likelihood (logLik) (Sakamoto et al., 1986).

LMMs based on field observation (Model F)

First, a linear covariance model was developed with PDR (10 log-transformed) as the dependent variable and LULC, soil moisture, vegetation cover or bulk density or elevation as independent variables (Model F-0) (Appendix 1). Variables to retain in the model were selected based on the amount of variance explained by the R^2 and the significance of intercept and slope in the model estimation. To avoid multicollinearity, Pearson correlation coefficients were calculated including correlated variables in the model (Appendix 2), and a variance inflation factor ("vif") test was conducted between the predictor variables.

Next, the model F-0 was re-analysed with a generalised least-squares model fitted by the restricted maximum likelihood method (REML) using the same independent variables (Model F-1). This model was extended with LULC as random effect (Model F-2, random intercept model) or a variance term allowing separate variances for each LULC type (Model F-3, VarIdent model). The fourth (Model F-4) combined the random intercept and the variance structure (Appendix 1). The functions "gls" and "lme" (nlme package; Pinheiro et al., 2021) were used to run all the models.

Replacing field variables with Satellite data (Model FS)
For the selection of satellite-based variables, we calculated correlation between 12 Sentinel 2-derived bands and 35 indices and the best-fit field-based variables derived from the model F (Appendix 3 a, b). The Sentinel-2 band 11 and NDVI were correlated most strongly to SM and VC, respectively and were used as fixed variables in the models, resulting in models FS-1, FS-2, FS-3 and FS-4 (Appendix 1). Field-observed LULC was retained as a random variable in the FS models.

LMMs with solely satellite data (Model S)
The third model type was developed solely with satellite data. Satellite-derived LULC was used as a random variable instead of field-based LULC, and the models termed S-1, S-2, S-3 and S-4 (Appendix 1). The same satellite-derived indices used in the S models were used as fixed variables.

Effects plots and model comparison
To visualise the effect of the predictor variables, effect plots were produced for all models (F, FS, S) using the R package "effects". Effect plots show the change in PDR caused by one predictor variable while assuming the average value for the other predictors. The Model II regression (method OLS) was performed between models F-4 and FS-4/S-4 using the "lmodel2" package in R to evaluate modelling results (Jansen, 1986).

2.4.3 Preparation of raster data for model application
The resulting LULC raster data were clipped to the pre-classified NREGUs vector data to get the LULC relevant for nitrogen retention/export. After that, using Sentinel-2 bands 4 and 8, NDVI was calculated and clipped with LULC raster data. Sentinel-2 band 11 was also clipped to get the desired area of interest.

2.4.4 Model application (upscaling)
The best-fit LMM (Model C4) was applied to each pixel of the NREGUs of the study area. The pixel size was 10 × 10 m, and the obtained pixels for the NREGUs in post-monsoon, dry/winter and pre-monsoon were 3665373, 3832900 and 3822060, respectively. To perform model simulation across all pixels, all the raster data were converted into spatRaster using the function "Rast" in the "terra" package in R. Then, raster data were converted to spatVector format and model computation was performed according to LULC types using the "ifelse" function in R. After that, the "rasterise" function predicted the denitrification rate converted into a raster file. Mapping and further analysis were done in QGIS and R, respectively.

3. Results

3.1. Classification of LULC types
The LULC types of the study area were categorized as cropland (CL), natural vegetation (NV), land with water (LW), dry, bare land (DBL) and water body (WB) in all seasons except post-monsoon (Figure 3. 3). The land portion starts appearing in pre-monsoon, so the study area is devoid of CL. In all seasons, the area was dominated by water bodies, including

primary and secondary channels, covering an area of 305, 197 and 270 km^2 during post-monsoon, dry/winter and pre-monsoon, respectively. LW, where inundation occurs for a short time, mainly comprises river edges and water depressions inside the land portion covered by about 25% of the study area. Other LULC types, CL, NV, and DBL, covered an area of 5%, 9% and 12%, respectively (Table 3. 1).

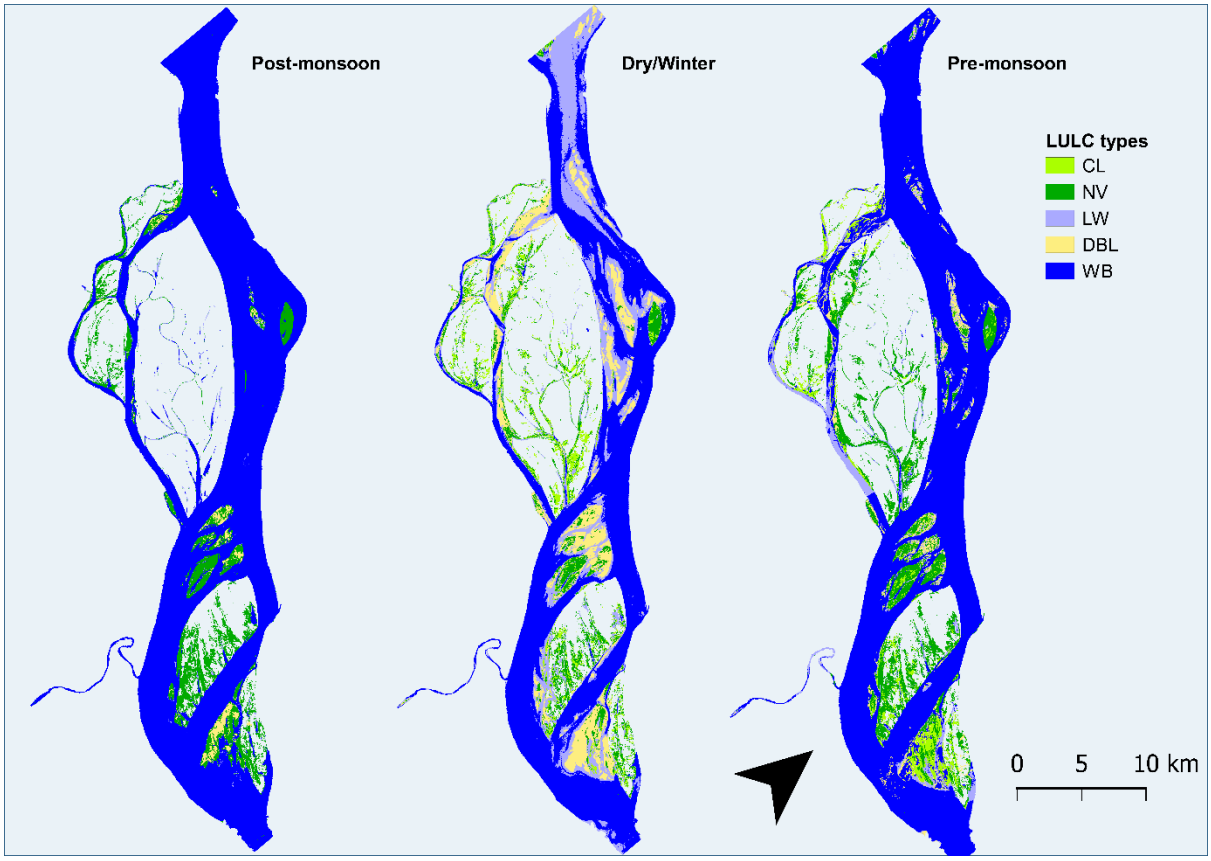

Figure 3. 3 LULC types of the study area of the Padma River, Bangladesh, during post-monsoon 2019, dry/winter 2020 and pre-monsoon 2020 (CL=Cropland, NV= Natural vegetation, LW=Land with water, DBL=Dry bare land and WB=Water bodies).

Table 3. 1 The total estimated area of LULC types of the study area of Padma River during different seasons.

Class	Area (km^2)			Percentage (%)		
	Post-monsoon	Dry/Winter	Pre-monsoon	Post-monsoon	Dry/Winter	Pre-monsoon
CL	-	20.4	19.7	-	5.32	5.16
NV	48.1	33.6	53.5	13.1	8.77	14.0
LW	6.2	86.1	24.9	1.69	22.5	6.51
DBL	6.8	46.0	13.6	1.85	12.0	3.57
WB	305	197	270	83.3	51.5	70.8

The LULC classification had a total accuracy value of 82.4%, 87.4% and 91.7% and a kappa hat coefficient of 0.57, 0.7 and 0.69 during post-monsoon, dry/winter and pre-monsoon, respectively (Appendix 4a, 4b and 4c).

3.2. Potential denitrification rate (PDR) in different LULC types

The measured PDR at sample sites during the dry/winter season varied from 0.41 to 643 mg N_2O-N m^{-2} d^{-1} in CL, 0.11-523 mg N_2O-N m^{-2} d^{-1} in NV, 0.11– 250 mg N_2O-N m^{-2} d^{-1} in LW and 0.07– 37.72 mg N_2O-N m^{-2} d^{-1} in DBL. The highest mean value of PDR (56 mg N_2O-N m^{-2} d^{-1}) was found in CL, and the lowest mean value was in DBL (4.27 mg N_2O-N m^{-2} d^{-1}). In the case of LW and NV, the mean value of PDR was about 20 mg N_2O-N m^{-2} d^{-1} (Fig. 4). The Kruskal-Wallis test showed a significant difference of PDR among LULC types (chi-squared=39.8, df=3, p-value=1.17e-8). The post-hoc Dunn's test showed that PDR in CL (group a) and DBL (group b) were significantly different from the others (Figure 3. 4).

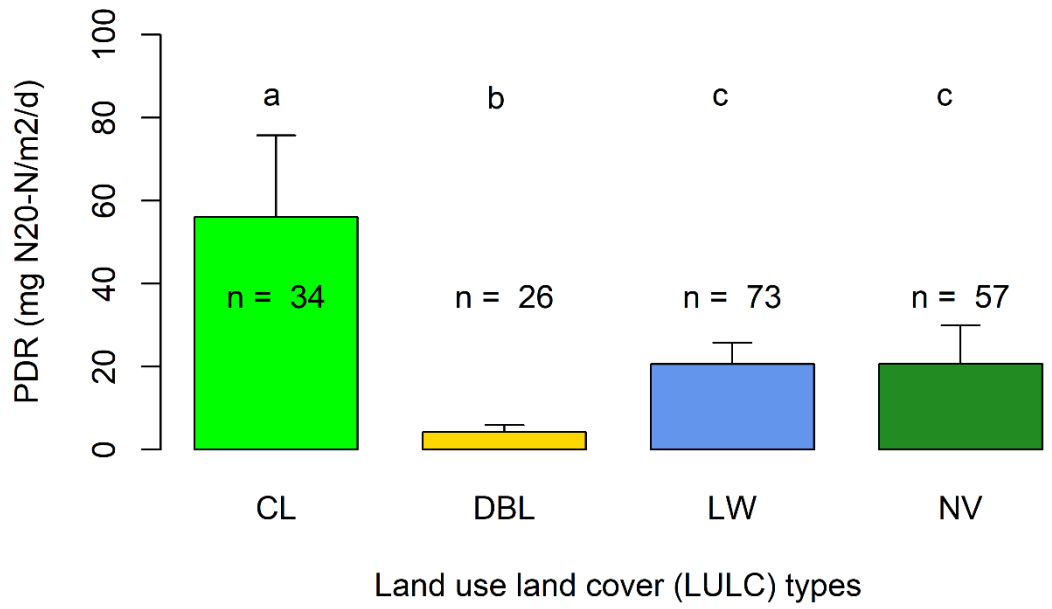

Figure 3. 4 Mean potential denitrification rate (PDR) in different LULC types (CL=Cropland, DBL=Dry bare land, LW=Land with water and NV=Natural vegetation) with standard error of the mean and number of samples in the study area of Padma River (Groups sharing a same letter not were significantly different (p<0.01) according to Kruskal-Wallis test with a post-hoc Dunn test.

3.3. Model results

The linear model with vegetation cover (VC), soil moisture (SM) and LULC had an R^2 of 0.31. In this model, the intercept, explanatory variables VC and SM, and categorical variables LULC types were significant ($p<0.001$ or $P<0.05$) except marginally significant for LW. The

developed LMMs showed better results for models F-1 to F-4. There was a significant difference between models F-3 and F-4 and the lowest AIC, and the log-likelihood value indicates that model F-4 was the best for predicting PDR in the present study. Replacing VC and SM with NDVI and band11 with field-based/satellite-based LULC types showed similar results (Model FS-1 to FS-4 and model S-1 to S-4). In all cases, the random intercept models with variance structure (Models F-4, FS-4 and S-4) showed the lowest AIC and log-likelihood values (Table 3. 2). The explanatory variables (VC and SM) and fixed intercept were significant, and there were random effects of LULC types. The random effects showed that the highest PDR was estimated in CL, followed by LW, NV and DBL (Table 3. 3).

Table 3. 2 Comparison of different LMMs. The best-fit models with the lowest AIC and Log-likelihood values are marked in bold.

Model	Model type	Explanatory	LULC data	AIC	Log-
A1	Generalised least-square	Field	Field	424.49	-205.25
A2	Random intercept	Field	Field	423.06	-206.53
A3	Generalised least-square with	Field	Field	425.63	-205.82
A4	Random intercept with variance	Field	Field	**416.31**	**-200.15**
B1	Generalised least-square	Satellite	Field	421.45	-203.73
B2	Random intercept	Satellite	Field	422.22	-206.11
B3	Generalised least-square with	Satellite	Field	444.49	-215.24
B4	Random intercept with variance	Satellite	Field	**418.45**	**-201.23**
C1	Generalised least-square	Satellite	Satellite	432.18	-209.09
C2	Random intercept	Satellite	Satellite	431.84	-210.92
C3	Generalised least-square with	Satellite	Satellite	444.28	-215.14
C4	Random intercept with variance	Satellite	Satellite	**428.52**	**-206.26**

*Table 3. 3 Results of LMMs (Models F-4, FS-4 and S-4) showing fixed effects and random effects of different factors on predicting PDR. The significance of intercepts and slopes are indicated with ** (p<0.01) and *** (p<0.001). The total number of observations was 190. (F = model with field-based data, FS = model with satellite and field-based data and S = model with satellite-based data)*

	Model estimates					
	Model F-4		Model FS-4		Model S-4	
Fixed effects						
Intercept	-2.378	***	-1.457	***	-1.357	***
Slopes						
Veg. Cover (%)	0.0072	***				
Soil Moisture (%)	0.0348	***				
NDVI			1.356	***	1.264	**
Sentinel-2 band 11			-1.981	**	-2.271	***
Random effects						
Intercepts						
CL	0.2783		0.4564		0.3983	
DBL	-0.1773		-0.3966		-0.2820	
LW	0.0790		0.1239		0.0437	
NV	-0.1799		-0.1838		-0.1599	
Intercept stdev	0.2449		0.3873		0.3171	
Residual stdev	0.4167		0.4771		0.4794	

For all type models (F-4, FS-4, S-4), the effect plots showed the impact of fixed variables on PDR estimation, but the magnitude of the effect differed based on LULC type (Figure 3. 5). CL showed an effect of higher magnitude than the other LULC types in PDR estimation, whereas DBL showed the minimum. The differences in PDR effects between NV and DBL were observed in models FS-4 and S-4, whereas in model F-4, the effects were the same (Figure 3. 5).

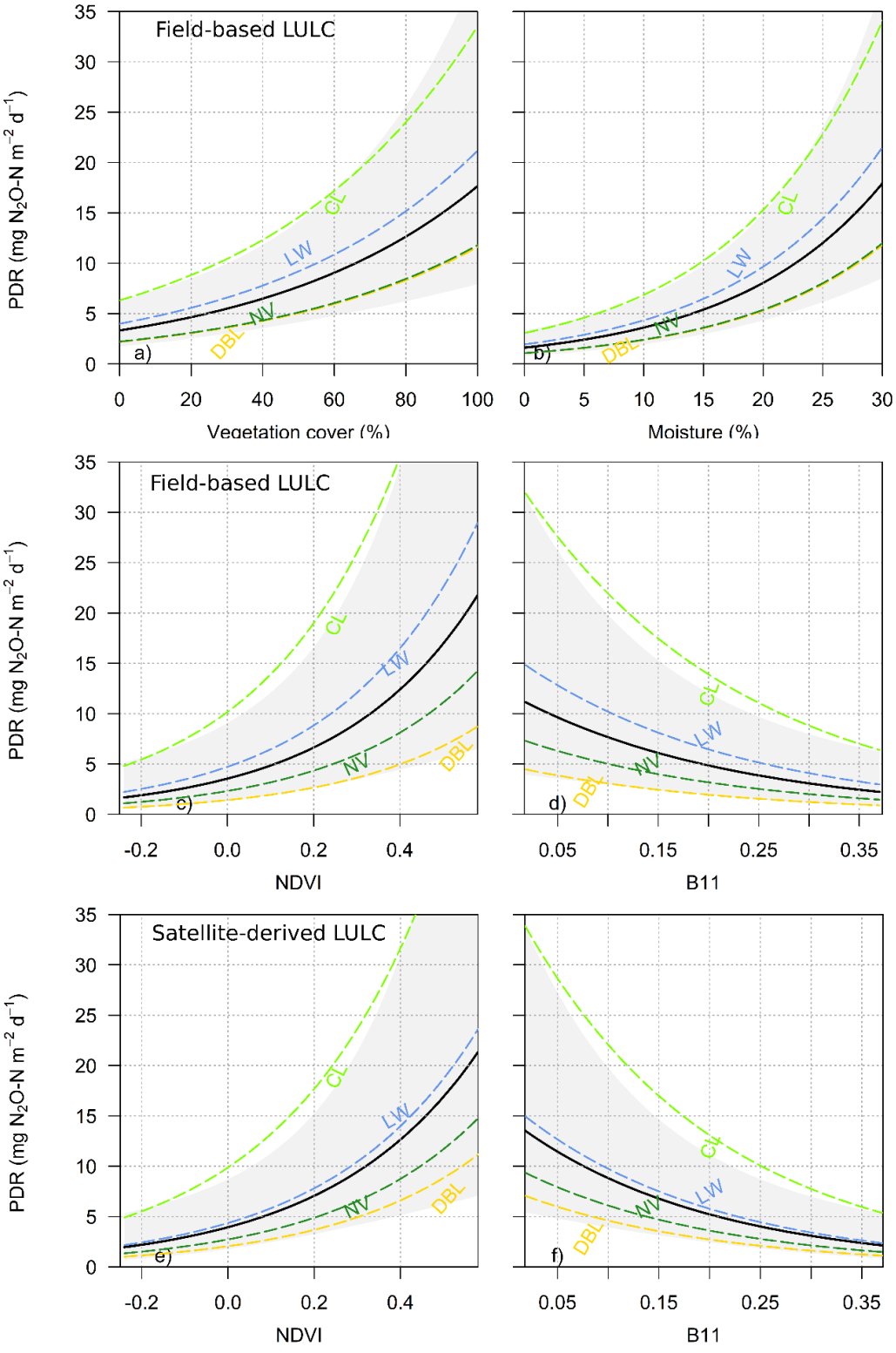

Figure 3. 5 Plots showing the effects of different parameters using LULC types in estimating PDR for models F-4, FS-4 and S-4. a, b) effect of vegetation cover and soil moisture; c, d) effect of NDVI and B11 (band 11) using field observed LULC, and e, f) same as (c, d) but with satellite-derived LULC. The bold line in the plot indicates the fixed effect of the models, and the dashed lines with different colours indicate the LULC type-specific effect of the models. The shaded area indicates the 95% confidence interval for the mean effect value.

3.4. Comparison between satellite and field-based measurements

Satellite data estimated denitrification rate was plotted against field data-measured denitrification rate (Fig. 6). Both regression lines were not significantly different from the y = x line based on the 95% confidence interval of the slopes and intercepts (Figure 3. 6, Table 3. 4). The coefficient of determination (R^2 = 0.66) indicates a good correspondence between the two datasets (i.e. field compared with satellite). This provides evidence that NDVI and band11 can be used as a proxy for vegetation cover and soil moisture. However, when satellite-derived LULC was used, the R^2 was 0.49 (Figure 3. 6). This was logical because satellite-derived LULC is not as precise as field-observed LULC types.

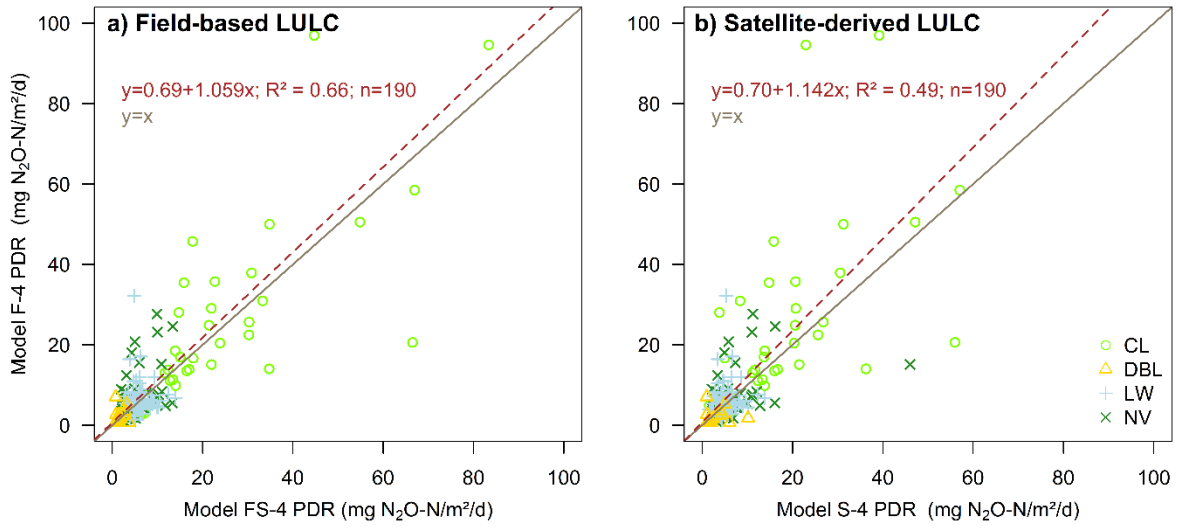

Figure 3. 6 Field-based (VC and SM) vs satellite-based (NDVI and band 11) estimation of PDR using field-based and satellite-derived LULC types. The dashed lines indicate the model performed estimates. The solid black line indicates the y = x line. Coloured symbols in the data represent LULC types (Cropland = light green, Natural vegetation = dark green, Land with water = blue, Dry bare land = gold).

Table 3. 4 Confidence intervals of the Model II regressions (Model FS-4 vs Model F-4 and Model S-4 vs Model F-4).

Regression Models	2.5 % intercept	97.5% intercept	2.5 % slope	97.5% slope
Model FS-4 vs Model F-4	-0.919	2.291	0.949	1.171
Model S-4 vs Model F-4	-1.364	2.764	0.974	1.309

3.5. Spatio-temporal distribution of PDR

3.5.1 Mapping of the model estimated PDR

The model estimation (model S-4) showed that PDR ranged from 0 − 35 mg N_2O-N m^{-2} d^{-1} during post-monsoon, 0 − 82.8 mg N_2O-N m^{-2} d^{-1} during dry/winter, and 0 − 120 mg N_2O-N m^{-2} d^{-1} during post-monsoon (Fig. 7). An increase of modelled PDR was observed from post-monsoon 2019 to pre-monsoon, 2020. The lowest value of modelled PDR was observed in

DBL during all three seasons. The higher PDR was found in the VI, where CL and NV were the dominant LULC types (Figures 3. 3 and 3. 7).

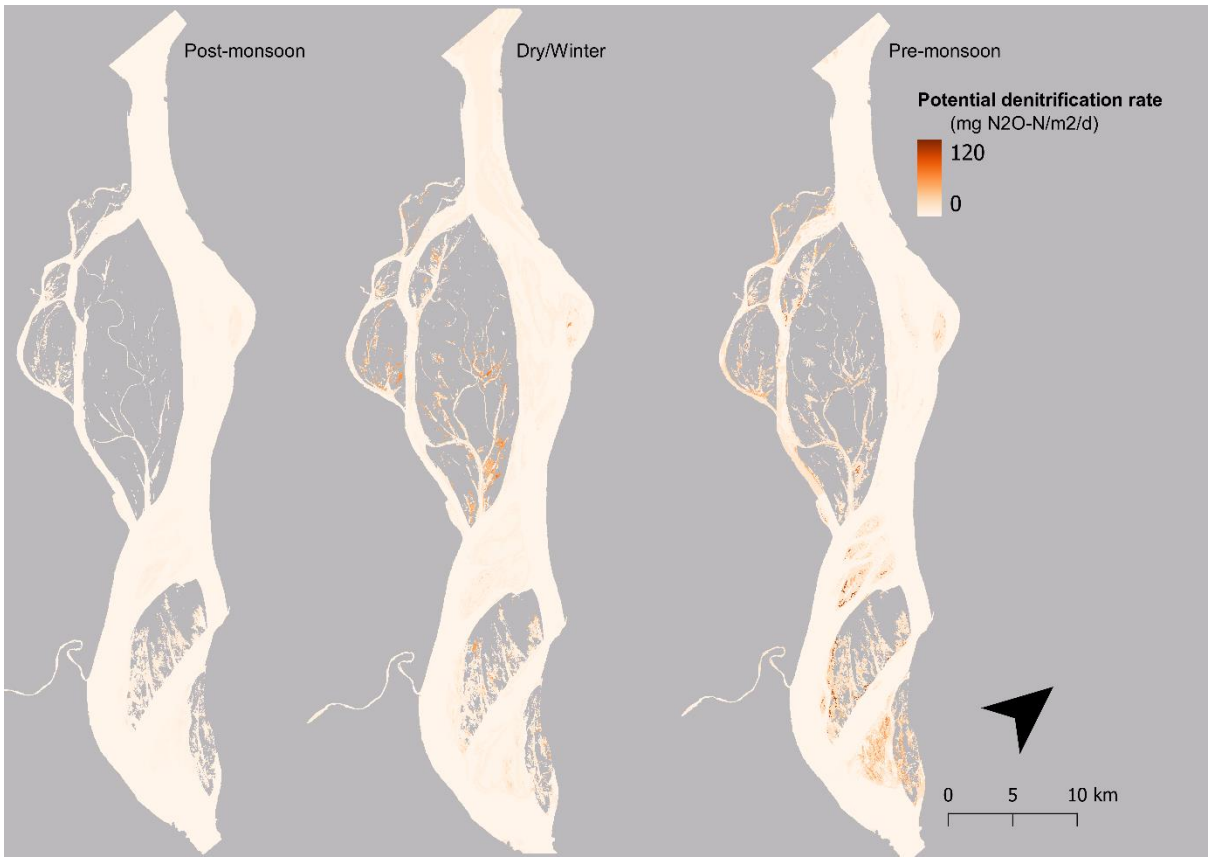

Figure 3. 7 Estimated PDR (potential denitrification rate) in the study area of Padma River during the post-monsoon 2019, dry/winter 2020 and pre-monsoon 2020 (WB was excluded in the estimation) based on model S-4 which relies on NDVI, band 11 and LULC. See text for further information.

3.5.2. Comparison of estimated PDR in different NREGUs

The mean estimated PDR (Model S-4) ranged from 0 − 10, 0 − 15 and 0 − 20 mg N_2O-N m^{-2} d^{-1} in post-monsoon, dry/winter and post-monsoon, respectively. The median value of PDR was increased from post-monsoon 2019 to pre-monsoon 2020 in all GUs except EK, in post-monsoon. In all three seasons, the highest median value was found in VI, mainly due to CL or NV, and the lowest median PDR was found in the unvegetated bank (EK) post-monsoon as the GUs started emerging then. In WD, the median value of PDR was higher than the bars in the river (L, T and SB) except in the pre-monsoon. In this season, PDR was higher in EK and occurred due to the start of inundation (Figure 3. 8). An increase in the water content of EK mainly increases PDR.

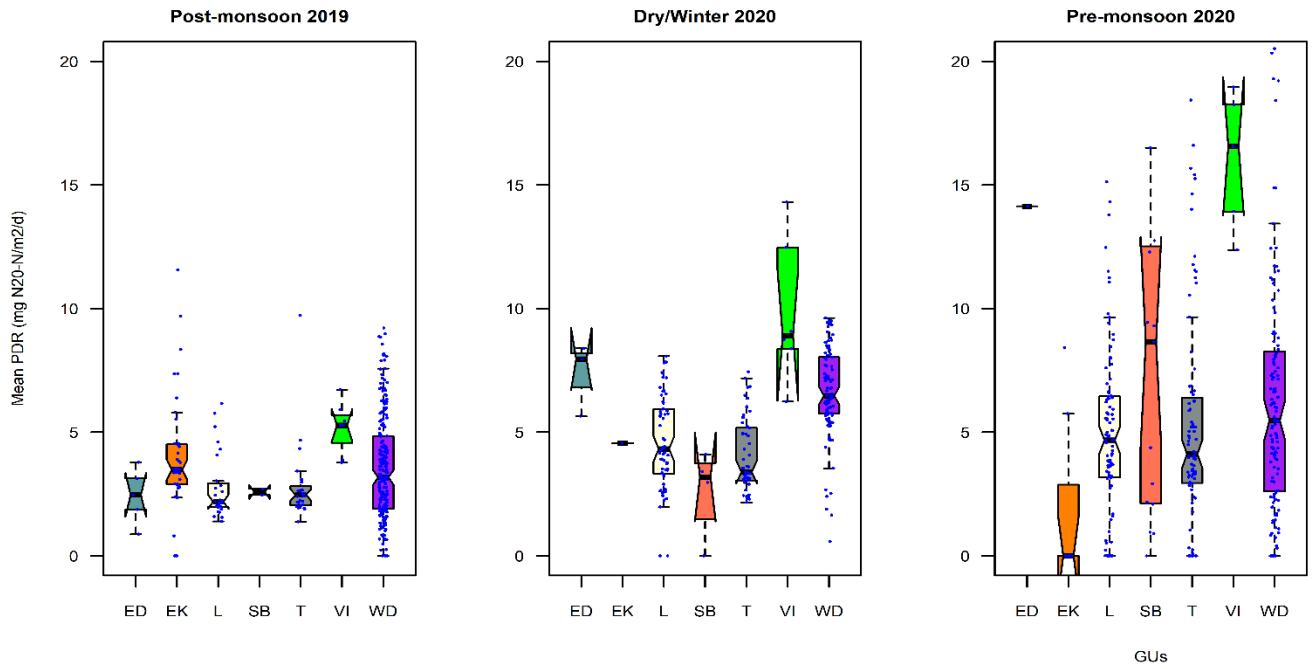

Figure 3. 8 Model estimated mean denitrification rate in different GUs during post-monsoon 2019, dry/winter 2020 and pre-monsoon 2020 (ED=Dry channel, EK = Unvegetated bank, L= Longitudinal bar, SB = Side bar, T = Transverse bar, VI = Vegetation Island, WD = Water depression).

5.3. Impact of GUs on PDR estimation

Estimated nitrogen lost from the study area through denitrification was 191, 1087 and 972 kg N_2O-N d^{-1} during post-monsoon, dry/winter and pre-monsoon, respectively. The total PDR count in the vegetation island (VI) showed that the estimated PDR increased from post-monsoon 2019 to dry/winter 2020 and decreased in pre-monsoon 2020, associated with the increased surface area from post-monsoon to dry/winter. After that, it tended to decrease. Again, in mid bars (L and T) the surface area and the number of NREGUs increased from post-monsoon to pre-monsoon, accelerating the increasing tendency of PDR from post-monsoon to pre-monsoon, but in case of the side bar (SB), the PDR was maximum during pre-monsoon due to increase of the number of NREGUs. In the case of EK, ED and WD, the maximum surface area and the highest number were observed post-monsoon, which corresponded to the highest total estimated PDR in these NREGUs (Figure 3. 9).

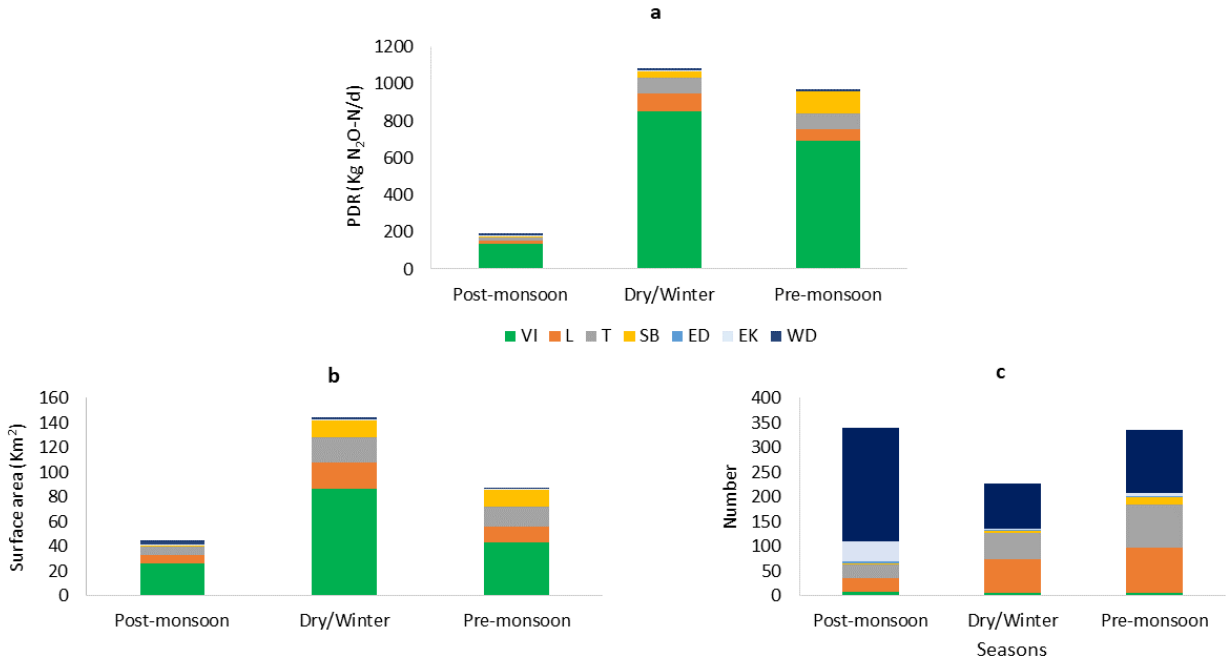

Figure 3. 9 Estimated PDR (a), the total surface area of GUs (b) and the number of GUs (c) during different seasons in the study area of Padma River, Bangladesh (ED=Dry channel, EK= Unvegetated bank, L= Longitudinal bar, SB= Side bar, T=Transverse bar, VI= Vegetation Island, WD= Water Depression).

4. Discussion

LMMs developed during this study were able to predict PDR reasonably well using independent variables of vegetation cover, soil moisture and LULC. These factors have been shown previously to have a regulating role for PDR (Xiong et al., 2017; Orr et al., 2014; Chen et al., 2009), although PDR can vary with changes in LULC types in river systems (Korol et al., 2019; Jung et al., 2014). Satellite-derived remote sensing data enables scaling up of PDR across river reaches. The remote sensing derived NDVI provided a robust proxy for vegetation dynamics, as we found a significant correlation between vegetation cover and NDVI. NDVI mostly correlated with Sentinel-2-derived indexes used to determine soil moisture, but Sentinel -2 band 11 did not correlate significantly with NDVI. In the LMM model, a combination of these two showed better results in the model estimation than the other Sentinel-2 bands and indexes. In the dataset, LULC played a significant role in model PDR estimation providing random effects as intercepts based on LULC. The highest PDR estimated in CL due to application of fertiliser to get the maximum production level for some crops, (Ahmmed, 2018) or the presence of legumes. PDR is commonly higher in river catchments dominated by agriculture compared with forests and natural vegetation (Welsh et al., 2017; Han et al., 2017; Liu et al., 2016).

As seasonal discharge affects the surface area of NREGUs in the study area (Gani et al., 2022), it is likely also influential for altering PDR from post-monsoon 2019 to pre-monsoon

2020, supplying nitrogen through infiltrating river water and deposited river sediment that supported vegetation growth. The nature of the NREGUs was also responsible for PDR. During pre-monsoon, both in CL and NV vegetation were in a seasonally mature stage, so the highest mean PDR was observed in that period due to the higher value of NDVI. On the other hand, the lowest mean PDR occurred post-monsoon because the plants just started growing as the islands and bars began appearing. In addition, the cultivation of CL throughout the year, except for post-monsoon, impacted the spatiotemporal distribution of PDR.

The present study area is comparable to floodplain areas or riparian zones where inundation occurs temporally, accelerating the enrichment of nitrogen in NREGUs (Xiong et al., 2017; Koschorreck and Darwich, 2003). The nitrate concentration of inundating waters is one of the factors that control denitrification (Ma et al., 2020; Orr et al., 2014). The study area also acts as a buffer zone for nitrate concentration, especially when water interacted with the edges of NREGUs. During the present study, we found the total maximum PDR during dry/winter due to surface area, but the mean value of PDR was the highest in all NREGUs during pre-monsoon. During this time, river discharge tends to increase, so the edge of all NREGUs becomes saturated with water, creating anoxic condition that are needed for denitrification (Seitzinger et al., 2006). It was not possible to show the influence of nitrogen inputs via river water and deposited sediments during the present study in the case of individual NREGUs separately, but the impact of the number of bars (SB) and dry channels (ED) and unvegetated banks (EK) on PDR estimation during post-monsoon and pre-monsoon showed that increasing tendency of water connectivity, i.e. inundation frequency with the bars increases microbial activity (Fischer et al., 2005). Hence, PDR increased in pre-monsoon and post-monsoon for these types of NREGUs. Such a phenomenon was observed in case of N_2O emissions (indicative of PDR) in the White River vegetation (Jacinthe et al., 2012) and in the Congo river basin (Borges et al., 2019), where flood frequency or wetland connectivity increased the denitrification rate. There might be other factors responsible for accelerating PDR during pre-monsoon. Recent studies showed that high temperatures could influence denitrification in lowland rivers (Gervasio et al., 2022; Ding et al., 2019). During pre-monsoon, the area experienced higher temperatures than the other seasons, which likely contributed to a higher mean value of PDR.

The measurement of PDR is based on the denitrification enzyme activity (DEA), which estimates the denitrifier population in soils that is reflective of long-term in situ denitrification rates (Tiedje et al., 1982). So, the present model estimated PDR as a proxy for actual denitrification. Measuring the actual denitrification rate for large rivers with high discharge is challenging, where access to sampling sites is difficult (Boyer et al., 2006; Goffman et al., 2006). Even though possible, applying the small-scale field measurements to the riverscape scale is more challenging due to the considerable variability of environmental factors and spatial distribution (Orr et al., 2014; Martínez-Espinosa et al., 2021). Considering this, the modelling we used provides an alternative approach for estimating the denitrification rate and scaling up to the larger reach of basin scales.

Denitrification is one of the key retention processes in large rivers, but due to methodological difficulties, its quantification has been largely limited to point locations. Previous studies have been unable to realistically and representatively map the spatiotemporal distribution of denitrification. At reach or even larger scales, denitrification is mainly controlled by nitrogen flux and water residence time, which is influenced by river discharge and GUs. Considering this interaction between hydrology and geomorphology in large tropical rivers, the current approach is more effective. The model can estimate denitrification from very local to large-scale because PDR is calculated in the model pixel to pixel and reported per day. Moreover, the use of Sentinel-2 data provides the opportunity to predict PDR on finer time scales (the global revisit time of Sentinel 2 is five days) with higher resolution (20 m). Therefore, the present modelling is a parsimonious tool that can provide a more precise temporal estimation.

We expect this satellite-based model is applicable to any river system with temporary inundation. But to apply this model, a potential area of nutrient retention must be identified, as described by Gani et al. (2022), and LULC types should be classified more precisely. There are other limitations of the model. We validated the model with field data for only one season. Due to the highly dynamic and flooding nature of the river, it was not possible to collect samples in other seasons. This constraint can be overcome by validating this model in other river systems. Due to the cloud cover of the study area, we were only able to show the PDR estimation on a seasonal basis, but this can be done monthly based on the availability of satellite products.

5. Conclusion

In the present study, the importance of soil moisture, vegetation, and LULC as the drivers of PDR was determined by the use of LMMs. The developed model showed the spatiotemporal distribution of PDR using Sentinel-2 data at reach scale and could explain reasonably well the role of NREGUs in PDR on spatial and seasonal scales in the study area. The vegetation islands and the bars were the most important GUs in all seasons for denitrification. Together with the surface area, the number of NREGUs, LULC and river discharge was also responsible for the spatiotemporal distribution of PDR. The present research is a novel approach that uses satellite products to estimate PDR and can be applied to the GUs in large lowland rivers where inundation occurs frequently.

6. References

Ahmmed S., Jahiruddin M., Razia S., Begum R. S., Biswas J. S., Rahman A. S. M. M., Ali M. M., Islam K. M. S., Hossain M. M., Gani M. N., Hossain G. M. A. & Sultan M. A. (2018). Fertilizer Recomendation Guide- 2018. In Bangladesh Agricultural Research Council (BARC), Farmgate, Dhaka 1215.

Alexander R. B., Smith R. A. & Schwarz G. E. (2000). Effect of stream channel size on the delivery of nitrogen to the Gulf of Mexico. Nature, 403(6771), 758–761. https://doi.org/10.1038/35001562

Audet J., Olsen T. M., Elsborg T., Baattrup-Pedersen A. & Riis T. (2021). Influence of plant habitats on denitrification in lowland agricultural streams. Journal of Environmental Management, 286. https://doi.org/10.1016/j.jenvman.2021.112193

Bai J., Ouyang H., Deng W., Zhu Y., Zhang X. & Wang Q. (2005). Spatial distribution characteristics of organic matter and total nitrogen of marsh soils in river marginal wetlands. Geoderma, 124(1–2), 181–192. https://doi.org/10.1016/j.geoderma.2004.04.012

Beaulieu J. J., Tank J. L., Hamilton S. K., Wollheim W. M., Hall R. O., Mulholland P. J., Peterson B. J., Ashkenas L. R., Cooper L. W., Dahm C. N., Dodds W. K., Grimm N. B., Johnson S. L., McDowell W. H., Poole G. C., Maurice Valett H., Arango C. P., Bernot M. J., Burgin A. J., …… & Thomas S. M. (2011). Nitrous oxide emission from denitrification in stream and river networks. Proceedings of the National Academy of Sciences of the United States of America, 108(1), 214–219. https://doi.org/10.1073/pnas.1011464108

Böhlke J. K., Harvey J. W. & Voytek M. A. (2004). Reach-scale isotope tracer experiment to quantify denitrification and related processes in a nitrate-rich stream, midcontinent United States. Limnology and Oceanography, 49(3), 821–838. https://doi.org/10.4319/lo.2004.49.3.0821

Borges A. V., Darchambeau F., Lambert T., Morana C., Allen G. H., Tambwe E., Toengaho Sembaito A., Mambo T., Wabakhangazi J. N., Descy J. P., Teodoru C. R. & Bouillon S. (2019). Variations in dissolved greenhouse gases (CO2, CH4, N2O) in the Congo River network overwhelmingly driven by fluvial-wetland connectivity. Biogeosciences, 16(19), 3801–3834. https://doi.org/10.5194/bg-16-3801-2019

Boyer E. W., Alexander R. B., Parton W. J., Li C., Butterbach-Bahl K., Donner S. D., Skaggs R. W. & Del Grosso S. J. (2006). Modeling denitrification in terrestrial and aquatic ecosystems at regional scales. Ecological Applications, 16(6), 2123–2142. https://doi.org/10.1890/1051-0761(2006)016[2123:MDITAA]2.0.CO;2

Breiman L. (2001). Random Forests. Machine Learning **45**, 5–32. https://doi.org/10.1023/A:1010933404324

Chen F., Jia G. & Chen J. (2009). Nitrate sources and watershed denitrification inferred from nitrate dual isotopes in the Beijiang River, south China. Biogeochemistry, 94(2), 163–174. https://doi.org/10.1007/s10533-009-9316-x

Cho H. J., Kirui P. & Natarajan H (2008). Test of Multi-spectral Vegetation Index for Floating and Canopy-forming Submerged Vegetation. Int. J. Environ. Res. Public Health, 5(5), 477-483.

Congedo L. (2021). Semi-Automatic Classification Plugin: A Python tool for the download and processing of remote sensing images in QGIS. Journal of Open Source Software, 6(64), 3172. https://doi.org/10.21105/joss.03172

Dai Q., Cui C. F & Wang S. (2022). Spatiotemporal variation and sustainability of NDVI in the Yellow River basin. Irrigation and Drainage, 1–15. https://doi.org/10.1002/ird.2740

Davidson E. A. & Seitzinger S. (2006). The enigma of progress in denitrification research. Ecological Applications, 16(6), 2057–2063. https://doi.org/10.1890/1051-0761(2006)016[2057:TEOPID]2.0.CO;2

Ding J., Xi B., Xu Q., Meng H., Shen Y. & Cheng H. (2019). Isotopic evidence of nitrate sources and its transformations in a human-impacted watershed. Environmental Science: Processes and Impacts, 21(3), 575–583. https://doi.org/10.1039/c8em00424b

Fischer H., Kloep F., Wilzcek S. & Pusch M. T. (2005). A river's liver - Microbial processes within the hyporheic zone of a large lowland river. Biogeochemistry, 76(2), 349–371. https://doi.org/10.1007/s10533-005-6896-y

Gani M. A., van der Kwast J., McClain M. E., Gettel G. & Irvine K. (2022). Classification of Geomorphic Units and Their Relevance for Nutrient Retention or Export of a Large Lowland Padma River, Bangladesh: A NDVI Based Approach. Remote Sensing, 14(6). https://doi.org/10.3390/rs14061481

Garnier J. A., Mounier E. M., Laverman A. M. & Billen G. F. (2010). Potential Denitrification and Nitrous Oxide Production in the Sediments of the Seine River Drainage Network (France). Journal of Environmental Quality, 39(2), 449–459. https://doi.org/10.2134/jeq2009.0299

Gervasio M. P., Soana E., Granata T., Colombo D. & Castaldelli G. (2022). An unexpected negative feedback between climate change and eutrophication: higher temperatures increase denitrification and buffer nitrogen loads in the Po River (Northern Italy). Environmental Research Letters, 17(8). https://doi.org/10.1088/1748-9326/ac8497

Groffman P. M., Holland E. A., Myrold D. D., Robertson G. P. (1999). Denitrification. In S. P. Robertson G. P., Coleman D C., Bledose C S (Ed.), Standard soil methods for long-term ecological research, pp. 272–288. Oxford University Press.

Groffman P. M., Altabet M. A., Böhlke J. K., Butterbach-Bahl K., David M. B., Firestone M. K., Giblin A. E., Kana T. M., Nielsen L. P. & Voytek M. A. (2006). Methods for measuring denitrification: Diverse approaches to a difficult problem. Ecological Applications, 16(6), 2091–2122. https://doi.org/10.1890/1051-0761(2006)016[2091:MFMDDA]2.0.CO;2

Groffman P. M., Axelrod E. A., Lemunyon J. L. & Sullivan W. M. (1991). Denitrification in Grass and Forest Vegetated Filter Strips. Journal of Environmental Quality, 20(3), 671–674. https://doi.org/10.2134/jeq1991.00472425002000030027x

Guilhen J., Al Bitar A., Sauvage S., Parrens M., Martinez J. M., Abril G., Moreira-Turcq P. & Sanchez-Perez J. M. (2020). Denitrification and associated nitrous oxide and carbon dioxide emissions from the Amazonian wetlands. Biogeosciences, 17(16), 4297–4311. https://doi.org/10.5194/bg-17-4297-2020

Guo X., Fu Q., Hang Y., Lu H., Gao F. & Si J. (2020). Spatial Variability of Soil Moisture in Relation to Land Use Types and Topographic Features on Hillslopes in the Black Soil (Mollisols) Area of Northeast China. Sustainability, 12(9), 3552. https://doi.org/10.3390/su12093552

Gupta A. (2007). Greatest Floods and Largest Rivers. In Large Rivers: Geomorphology and Management. https://doi.org/10.1002/9780470723722

Han L., Huang W., Yuan X., Zhao Y., Ma Z. & Qin J. (2017). Denitrification Potential and Influencing Factors of the Riparian Zone Soils in Different Watersheds,Taihu Basin. Water, Air, and Soil Pollution, 228(3). https://doi.org/10.1007/s11270-017-3287-7

Hansen A. T., Dolph C. L. & Finlay J. C. (2016). Do wetlands enhance downstream denitrification in agricultural landscapes? Ecosphere, 7(10), e01516. https://doi.org/10.1002/ecs2.1516

Hoang L., van Griensven A. & Mynett A. (2017). Enhancing the SWAT model for simulating denitrification in riparian zones at the river basin scale. Environmental Modelling and Software, 93, 163–179. https://doi.org/10.1016/j.envsoft.2017.03.017

Holzman M. E., Rivas R. E. & Bayala M. I. (2021). Relationship between tir and nir-swir as indicator of vegetation water availability. Remote Sensing, 13(17). https://doi.org/10.3390/rs13173371

Jacinthe P. A., Bills J. S., Tedesco L. P. & Barr R. C. (2012). Nitrous Oxide Emission from Riparian Buffers in Relation to Vegetation and Flood Frequency. Journal of Environmental Quality, 41(1), 95–105. https://doi.org/10.2134/jeq2011.0308

Jensen A. L. (1986). Functions Regression and Correlation Ana. Canadian Journal of Fisheries and Aquatic Sciences, 43, 6–9.

Jung S. P., Kim Y. J. & Kang H. (2014). Denitrification rates and their controlling factors in streams of the Han River basin with different land-use patterns. Pedosphere, 24(4), 516–528. https://doi.org/10.1016/S1002-0160(14)60038-2

Kaden U. S., Fuchs E., Geyer S., Hein T., Horchler P., Rupp H., Scholz M., Schulz-Zunkel C. & Weigelhofer G. (2021). Soil Characteristics and Hydromorphological Patterns Control Denitrification at the Floodplain Scale. Frontiers in Earth Science, 9. https://doi.org/10.3389/feart.2021.708707

Korol A. R., Noe G. B. & Ahn C. (2019). Controls of the spatial variability of denitrification potential in nontidal floodplains of the Chesapeake Bay watershed, USA. Geoderma, 338, 14–29. https://doi.org/10.1016/j.geoderma.2018.11.015

Koschorreck M. & Darwich A. (2003). Nitrogen dynamics in seasonally flooded soils in the Amazon floodplain. Wetlands Ecology and Management, 11(5), 317–330. https://doi.org/10.1023/B:WETL.0000005536.39074.72

Kreiling R. M., Richardson W. B., Bartsch L. A., Thoms M. C. & Christensen V. G. (2019). Denitrification in the river network of a mixed land use watershed: unpacking the complexities. Biogeochemistry, 143(3), 327–346. https://doi.org/10.1007/s10533-019-00565-6

Laursen A. E. & Seitzinger S. P. (2002). Measurement of denitrification in rivers: An integrated, whole reach approach. Hydrobiologia, 485, 67–81. https://doi.org/10.1023/A:1021398431995

Lin J., Chen N., Wang F., Huang Z., Zhang, X. & Liu, L. (2020). Urbanization increased river nitrogen export to western Taiwan Strait despite increased retention by nitrification and denitrification. Ecological Indicators, 109, 105756. https://doi.org/10.1016/j.ecolind.2019.105756

Liu W., Xiong Z., Liu H., Zhang Q. & Liu G. (2016). Catchment agriculture and local environment affecting the soil denitrification potential and nitrous oxide production of riparian zones in the Han River Basin, China. Agriculture, Ecosystems and Environment, 216, 147–154. https://doi.org/10.1016/j.agee.2015.10.002

Ma L., Xiong Z., Yao L., Liu G., Zhang Q. & Liu, W. (2020). Soil properties alter plant and microbial communities to modulate denitrification rates in subtropical riparian wetlands.

Land Degradation and Development, 31(14), 1792–1802. https://doi.org/10.1002/ldr.3569

Maavara T., Lauerwald R., Laruelle G. G., Akbarzadeh Z., Bouskill N. J., Van Cappellen P. & Regnier, P. (2019). Nitrous oxide emissions from inland waters: Are IPCC estimates too high? Global Change Biology, 25(2), 473–488. https://doi.org/10.1111/gcb.14504

Martínez-Espinosa C., Sauvage S., Al Bitar A., Green P. A., Vörösmarty C. J. & Sánchez-Pérez J. M. (2021). Denitrification in wetlands: A review towards a quantification at global scale. Science of the Total Environment, 754, 142398. https://doi.org/10.1016/j.scitotenv.2020.142398

Martínez-Espinosa C., Sauvage S., Al Bitar A. & Sánchez Pérez J. M. (2022). A dynamic model for assessing soil denitrification in large-scale natural wetlands driven by Earth Observations. Environmental Modelling & Software, 158, 105557. https://doi.org/10.1016/J.ENVSOFT.2022.105557

Moran M. S., Jackson R. D., Slater P. N. & Teillet P. M. (1992). Evaluation of simplified procedures for retrieval of land surface reflectance factors from satellite sensor output. Remote Sensing of Environment, 41(2–3), 169–184. https://doi.org/10.1016/0034-4257(92)90076-V

Nanus L., Williams M. W., Campbell D. H., Elliott E. M. & Kendall C. (2008). Evaluating regional patterns in nitrate sources to watersheds in national parks of the rocky mountains using nitrate isotopes. Environmental Science and Technology, 42(17), 6487–6493. https://doi.org/10.1021/es800739e

Nilsson J. E., Liess A., Ehde P. M. & Weisner S. E. B. (2020). Mature wetland ecosystems remove nitrogen equally well regardless of initial planting. Science of the Total Environment, 716, 137002. https://doi.org/10.1016/j.scitotenv.2020.137002

Opdyke M. R., David M. B. & Rhoads B. L. (2006). Influence of Geomorphological Variability in Channel Characteristics on Sediment Denitrification in Agricultural Streams. Journal of Environmental Quality, 35(6), 2103–2112. https://doi.org/10.2134/jeq2006.0072

Orr C. H., Predick K. I., Stanley E. H. & Rogers K. L. (2014). Spatial autocorrelation of denitrification in a restored and a natural floodplain. Wetlands, 34(1), 89–100. https://doi.org/10.1007/s13157-013-0488-8

Peng J., Albergel C., Balenzano A., Brocca L., Cartus O., Cosh M. H., Crow W. T., Dabrowska-Zielinska K., Dadson S., Davidson M. W. J., de Rosnay P., Dorigo W., Gruber A., Hagemann S., Hirschi M., Kerr Y. H., Lovergine F., Mahecha M. D., Marzahn P., ….. & Loew A. (2021). A roadmap for high-resolution satellite soil moisture applications – confronting product characteristics with user requirements. Remote Sensing of Environment, 252, 112162. https://doi.org/10.1016/j.rse.2020.112162

Piña-Ochoa E. & Álvarez-Cobelas M. (2006). Denitrification in aquatic environments: A cross-system analysis. Biogeochemistry, 81(1), 111–130. https://doi.org/10.1007/s10533-006-9033-7

Pinheiro J., Bates D., DebRoy S., Sarkar D. & R. C. Team (2021). nlme: Linear and Nonlinear Mixed Effects Models (3.1-152). https://doi.org/https://CRAN.R-project.org/package=nlme

Pribyl A. L., McCutchan J. H., Lewis W. M. & Saunders J. F. (2005). Whole-system estimation of denitrification in a plains river: A comparison of two methods. Biogeochemistry, 73(3), 439–455. https://doi.org/10.1007/s10533-004-0565-4

R Core Team (2021). R: A Language and Environment for Statistical Computing (4.1.2). R Foundation for Statistical Computing. https://www.r-project.org/

Rinaldi M., Belletti B., Comiti F., Nardi L., Bussettini M., Mao L. & Gurnel A. M. (2015). Deliverable 2.1, Part 1, of REFORM (REstoring rivers FOR effective catchment Management), a Collaborative project (large-scale integrating project) funded by the European Commission within the 7th Framework Programme under Grant Agreement 282656.

Ritz S., Dähnke K., & Fischer H. (2018). Open-channel measurement of denitrification in a large lowland river. Aquatic Sciences, 80(1), 1–13. https://doi.org/10.1007/s00027-017-0560-1

Ritz S. & Fischer H. (2019). A Mass Balance of Nitrogen in a Large Lowland River (Elbe, Germany). Water, 11(11), 2383. https://doi.org/10.3390/w11112383

Robertson K., Klemedtsson L., Axelsson S. & Rosswall, T. (1993). Estimates of denitrification in soil by remote sensing of thermal infrared emission at different moisture levels. Biology and Fertility of Soils, 16(3), 193–197. https://doi.org/10.1007/BF00361407

Sakamoto Y., Ishiguro M. and Kitagawa G. (1986). Akaike Information Criterion Statistics. D. Reidel Publishing Company.

Sebilo M., Billen G., Grably M. & Mariotti A. (2017). Isotopic Composition of Nitrate-Nitrogen as a Marker of Riparian and Benthic Denitrification at the Scale of the Whole Seine River System. Biogeochemistry, 63(1), 35–51.

Seitzinger S. P., Styles R. V., Boyer E. W., Alexander R. B, Billen G., Howarth R. W., Bernhard M. & Bremeen N. V. (2002). Nitrogen retention in rivers: model development and application to watersheds in the northeastern U.S.A. In E. W. Boyer & R. W. Howarth (Eds.), The Nitrogen Cycle at Regional to Global Scales (pp. 199–237). Springer Netherlands. https://doi.org/10.1007/978-94-017-3405-9

Seitzinger S., Harrison J. A., Böhlke J. K., Bouwman A. F., Lowrance R., Peterson B., Tobias C. & van Drecht G. (2006). Denitrification across landscapes and waterscapes: A synthesis. Ecological Applications, 16(6), 2064–2090. https://doi.org/10.1890/1051-0761(2006)016[2064:DALAWA]2.0.CO;2

Sgouridis F. & Ullah S. (2014). Denitrification potential of organic, forest and grassland soils in the Ribble-Wyre and Conwy River catchments, UK. Environmental Sciences: Processes and Impacts, 16(7), 1551–1562. https://Zhangdoi.org/10.1039/c3em00693j

Shrestha J., Niklaus P. A., Frossard E., Samaritani E., Huber B., Barnard R. L., Schleppi P., Tockner K., & Luster J. (2012). Soil Nitrogen Dynamics in a River Floodplain Mosaic. Journal of Environmental Quality, 41(6), 2033–2045. https://doi.org/10.2134/jeq2012.0059

Solomon C. T., Hotchkiss E. R., Moslemi J. M., Ulseth A. J., Stanley E. H., Hall R. O. & Flecker A. S. (2009). Sediment size and nutrients regulate denitrification in a tropical stream. Journal of the North American Benthological Society, 28(2), 480–490. https://doi.org/10.1899/07-157.1

Sørensen J. (1978). Denitrification Rates in a Marine Sediment as Measured by the Acetylene Inhibition Technique. Applied and Environmental Microbiology, 36(1), 139–143. https://doi.org/10.1128/aem.36.1.139-143.1978

Strauss E. A., Richardson W. B., Bartsch L. A. & Cavanaugh J. C. (2011). Effect of habitat type on in-stream nitrogen loss in the Mississippi River. River Syst., 19, 261–269, https://doi.org/10.1127/1868-5749/2011/019-0021.

Sun X., Bernard-Jannin L., Sauvage S., Garneau C., Arnold J. G., Srinivasan R. & Sánchez-Pérez J. M. (2017). Assessment of the denitrification process in alluvial wetlands at floodplain scale using the SWAT model. Ecological Engineering, 103, 344–358. https://doi.org/10.1016/j.ecoleng.2016.06.098

Syvitski J. P. M., Cohen S., Kettner A. J. & Brakenridge G. R. (2014). How important and different are tropical rivers? - An overview. Geomorphology, 227, 5–17. https://doi.org/10.1016/j.geomorph.2014.02.029

Szabó L., Deák B., Bíró T., Dyke G. J. & Szabó S. (2020). NDVI as a proxy for estimating sedimentation and vegetation spread in artificial lakes-monitoring of spatial and temporal changes by using satellite images overarching three decades. Remote Sensing, 12(9). https://doi.org/10.3390/RS12091468

Tank J. L., Rosi-Marshall E. J., Baker M. A., & Hall R. O. (2008). Are rivers just big streams? A pulse method to quantify nitrogen demand in a large river. Ecology, 89(10), 2935–2945. https://doi.org/10.1890/07-1315.1

Tatariw C., Chapman E. L., Sponseller R. A., Mortazavi B. & Edmonds J. W. (2013). Denitrification in a large river: Consideration of geomorphic controls on microbial activity and community structure. Ecology, 94(10), 2249–2262. https://doi.org/10.1890/12-1765.1

Tiedje J. M., Sexstone A. J., Myrold D. D. & Robinson J. A. (1982). Denitrification: ecological niches, competition and survival. Antonie van Leeuwenhoek, 48(6), 569–583. https://doi.org/10.1007/BF00399542

Tuttle A. K., McMillan S. K., Gardner, A. & Jennings G. D. (2014). Channel complexity and nitrate concentrations drive denitrification rates in urban restored and unrestored streams. Ecological Engineering, 73, 770–777. https://doi.org/10.1016/j.ecoleng.2014.09.066

Ullah S. & Faulkner S. P. (2006). Denitrification potential of different land-use types in an agricultural watershed, lower Mississippi valley. Ecological Engineering, 28(2), 131–140. https://doi.org/10.1016/j.ecoleng.2006.05.007

van Wijk D, Teurlincx S, Brederveld R. J., de Klein J. J. M., Janssen A. B. G., Kramer L, van Gerven L. P. A., Kroeze C & Mooij W. M. (2022). Smart Nutrient Retention Networks: a novel approach for nutrient conservation through water quality management, Inland Waters, 12:1, 138-153, DOI: 10.1080/20442041.2020.1870852

Welsh M. K., McMillan S. K. & Vidon P. G. (2017). Denitrification along the Stream-Riparian Continuum in Restored and Unrestored Agricultural Streams. Journal of Environmental Quality, 46(5), 1010–1019. https://doi.org/10.2134/jeq2017.01.0006

Xiong Z., Guo L., Zhang Q., Liu G. & Liu W. (2017). Edaphic Conditions Regulate Denitrification Directly and Indirectly by Altering Denitrifier Abundance in Wetlands

along the Han River, China. Environmental Science and Technology, 51(10), 5483–5491. https://doi.org/10.1021/acs.est.6b06521

Xiong Z., Li S., Yao L., Liu G., Zhang Q. & Liu W. (2015). Topography and land use effects on spatial variability of soil denitrification and related soil properties in riparian wetlands. Ecological Engineering, 83, 437–443. https://doi.org/10.1016/J.ECOLENG.2015.04.094

Yang Y., Dou Y., Liu D. & An S. (2017). Spatial pattern and heterogeneity of soil moisture along a transect in a small catchment on the Loess Plateau. Journal of Hydrology, 550, 466–477. https://doi.org/10.1016/J.JHYDROL.2017.05.026

Yao X., Zhang L., Zhang Y., Xu H., & Jiang X. (2016). Denitrification occurring on suspended sediment in a large, shallow, subtropical lake (Poyang Lake, China). Environmental Pollution, 219, 501–511. https://doi.org/10.1016/j.envpol.2016.05.073

Yi L., Sun Y., Ouyang X. & Yin S. (2022). Identifying the Impacts of Climate Change and Human Activities on Vegetation Cover Changes: A Case Study of the Yangtze River Basin, China. International Journal of Environmental Research and Public Health, 19(10), 6239. https://doi.org/10.3390/ijerph19106239

Yuan L. H., Jiang W. G., Shen W. M., Liu Y. H., Wang W. J., Tao L. L., Zheng H. & Liu X. F. (2013). The spatio-temporal variations of vegetation cover in the Yellow River Basin from 2000 to 2010. Shengtai Xuebao/ Acta Ecologica Sinica, 33(24), 7798–7806. https://doi.org/10.5846/stxb201305281212

Zucco G., Brocca L., Moramarco T. & Morbidelli R. (2014). Influence of land use on soil moisture spatial–temporal variability and monitoring. Journal of Hydrology, 516, 193–199. https://doi.org/10.1016/J.JHYDROL.2014.01.043

Zuur A.F., Ieno E.N., Walker N. J., Saveliev A. A. & Smith G. M. (2009). Mixed Effects Models and Extensions in Ecology with R. In W. W. M. Gail, K. Krickeberg, J.M. Samet, A. Tsiatis (Ed.), Statistics for Biology and Health. Springer Science and Business Media. https://doi.org/10.4324/9780429201271-2

Zuur A. F., Ieno E. N. & Smith G. M. (2007). Analysing Ecological Data. In W. W. M. Gail, K. Krickeberg, J.M. Samet, A. Tsiatis (Ed.), Springer. Springer New York. https://doi.org/https://doi.org/10.1007/978-0-387-45972-1

Chapter 4

NITROGEN RETENTION OF A LARGE TROPICAL FLOODPLAIN RIVER

Abstract

Large tropical rivers act as important pathways of nitrogen transport from land to the sea, and the final river reaches where nitrogen can be retained. In the present study, a mass balance approach was used to evaluate nitrogen retention over a two-year period from a 50 km reach of the Padma River in Bangladesh, approximately 150 km upstream of where the river discharges into the Bay of Bengal. The relationship between concentration and discharge was estimated from 58 nitrogen concentration and discharge measurements. Nitrogen flux was then calculated daily from the inflow and outflows of the reach, and total nitrogen (TN) retention was estimated based on the flux difference of TN inflows and outflows. To compare with mass balance estimates, nitrogen loss due to water retention (NLWR), sedimentation, potential denitrification (PDR), and nitrogen fixation (NFR) were estimated from the water column of the river. NLWR and sedimentation were estimated from the nitrogen concentration and discharge. PDR and NFR were measured using the acetylene inhibition method and upscaled using outflow discharge and water travel time. Up-scaled PDR and NFR were compared with hydrologic retention and sedimentation to assess the relative contributions of these processes to retention. Monthly mass-balance measurements showed a substantial seasonal variation in nitrogen retention. Estimated maximum retention values (tonnes per month) of NLWR, sedimentation, PDR, and NFR were all associated with the monsoons. However, the percentage contribution of PDR and NFR to TN retention was higher in non-monsoon months (post-monsoon, dry/winter and pre-monsoon), suggesting nitrogen retention mechanisms varied seasonally. TN retention via NLWR accounted for the largest portion of total TN retention in every season, always exceeding 50% of total TN retention. Sedimentation was second most important in monsoon and post-monsoon seasons, while PDR in submerged GUs was second most important in dry/winter and pre-monsoon seasons. Net PDR in the water column contributed the least (1-6%) to total TN retention in all seasons.

Keywords: Retention processes, seasonal variation, water retention, sedimentation, denitrification, N_2 fixation, Padma River.

1. Introduction

Large tropical rivers are important for supporting the ecological, cultural, and economic development of human civilisation. They also provide drinking water for humans and livestock and transport nutrients from land to sea (e.g. Nicole, 2003; Subramanian, 2008; Campbell, 2009; Davidson et al., 2012). Many large rivers in the tropics are under development pressures due to anthropogenic activities, including the construction of dams and hydropower stations, reclamation linked to mining, deforestation, and channelisation (Winemiller et al., 2016, Böck et al., 2018; Best, 2019). Climate change has disrupted the hydrological regimes of discharge and floodplain inundation, exerting an impact on the ecological structure, river functioning, and seasonality (Hamilton, 2010; Eisner et al., 2017).
Large rivers have more potential to retain nitrogen than small ones because of notably high discharge (Wang et al., 2020), sediment transport (Wang et al., 2022), flow path modification increasing transport distances (Tanaka et al., 2021, Seitzinger et al., 2002; Wollheim et al., 2006; Mulholland and Webster 2010). The river water column acts as a zone where removal processes of nitrogen (N), such as denitrification and sedimentation, occur. However, retention also occurs at the interface between the water column and sediment (Grizzetti et al., 2015). Most tropical rivers have extensive floodplains and deltas, which can potentially deliver sediments and nutrients to the oceans (Cotrim et al., 2007). In addition, they exhibit dynamic channel form (geomorphic units), changing their pattern from single- to multi-channel systems (Latrubesse et al., 2005). This can amplify the magnitude of the interaction between sediment and water column, regulating nitrogen retention and export.

Seasonal variation is a distinctive feature of most tropical rivers. This seasonality is observed in the changes in flow, precipitation, and temperature (Hamilton et al., 2010). In the Ganges and Brahmaputra Rivers, high temperatures during the monsoon amplify snow or ice melt in the Himalayas, resulting in an enormous discharge of water (Islam, 2016). Concurrent high rainfall and storm events accelerate discharge and sediment load (Syvitski et al. 2014).

Most nitrogen retention estimations have been limited to temperate regions, with few studies in large rivers (e.g., Loken et al., 2018; Ritz and Fischer, 2019; Wang et al., 2020). Available studies show that the measurement of upstream compared with downstream nitrogen fluxes (mass balance) is used as an empirical approach for estimating nitrogen retention in large rivers (McKee et al., 2000; Chen et al., 2009; Bukaveckas and Isenberg, 2013; Ritz and Fischer, 2019). However, retention estimates usually do not provide information on specific internal physical and biogeochemical processes (Buckavecks and Isenberg, 2013). In large tropical rivers, water loss to floodplains and aquifers, sedimentation, and denitrification can contribute to in-channel nitrogen retention. So, understanding different retention mechanisms is important to unravel the estimates of the nitrogen budget.

The Ganges and Brahmaputra are the largest basin areas of Bangladesh and also drain a large area of India, all of Nepal and Bhutan, and a relatively small area of China. Land use activities and the construction of dams and barrages in the upper parts of these rivers affect the water and sediment supply downstream, resulting in the alteration of riverine ecosystems (Bouwman et al., 2013; Weigelhofer et al., 2018; Hauer et al., 2018). Increased nitrogen loads are of concern in the lower river system and the Bay of Bengal, which is subject to

harmful algal blooms (Sattar et al., 2014; Zenia and Kroeze, 2015; Shaika et al., 2022). A better understanding of the nitrogen retention mechanism of these rivers is of high importance for implementing river management and restoration programs. Key research areas are identifying and quantifying N retention, the processes involved, and how these are affected by river discharge and geomorphology. The present study focuses on a large tropical floodplain, Padma River, one of the world's largest and most populated downstream river basins (Metcalfe, 2003). The overall research objective was to determine how variations in discharge, water retention, and biogeochemical processes (sedimentation and denitrification) influence nitrogen retention in a large tropical floodplain river. Specific research objectives were to:

- estimate the nitrogen retention of a 50 km reach of the Padma River, Bangladesh, including monsoon, post-monsoon, dry/winter, and post-monsoon seasons;
- show the contribution of water losses to floodplains and aquifers, sedimentation, and potential denitrification rate (PDR) to the nitrogen retention estimation; and
- determine how discharge, water retention, and denitrification control the nitrogen retention capacity of the reach.

2. Materials and Methods

2.1. Description of the study reach

The study reach, of about 50 km in length with a maximum width of 20 km, is downstream of the confluence of the Ganges and the Brahmaputra rivers, termed the Padma River in Bangladesh. Extensive in-channel geomorphic units and high discharge and sediment loads make the study reach very hydrologically dynamic for sediment transport (Nasa Earth Observatory, 2019) and, thus, nitrogen transport.

The mean annual discharge is 30,000 m^3/s, and the mean annual sediment load is 900 (Mt/year) (Sarker and Throne, 2008). Seasonal variation can, be considerable based on the hydrograph, March − May is considered pre-monsoon, June − September is monsoon, October − November is post-monsoon, and December − February is dry/winter (Gani et al., 2022). River bank erosion, aggradation, and degradation of bars and islands are frequent features of the reach.

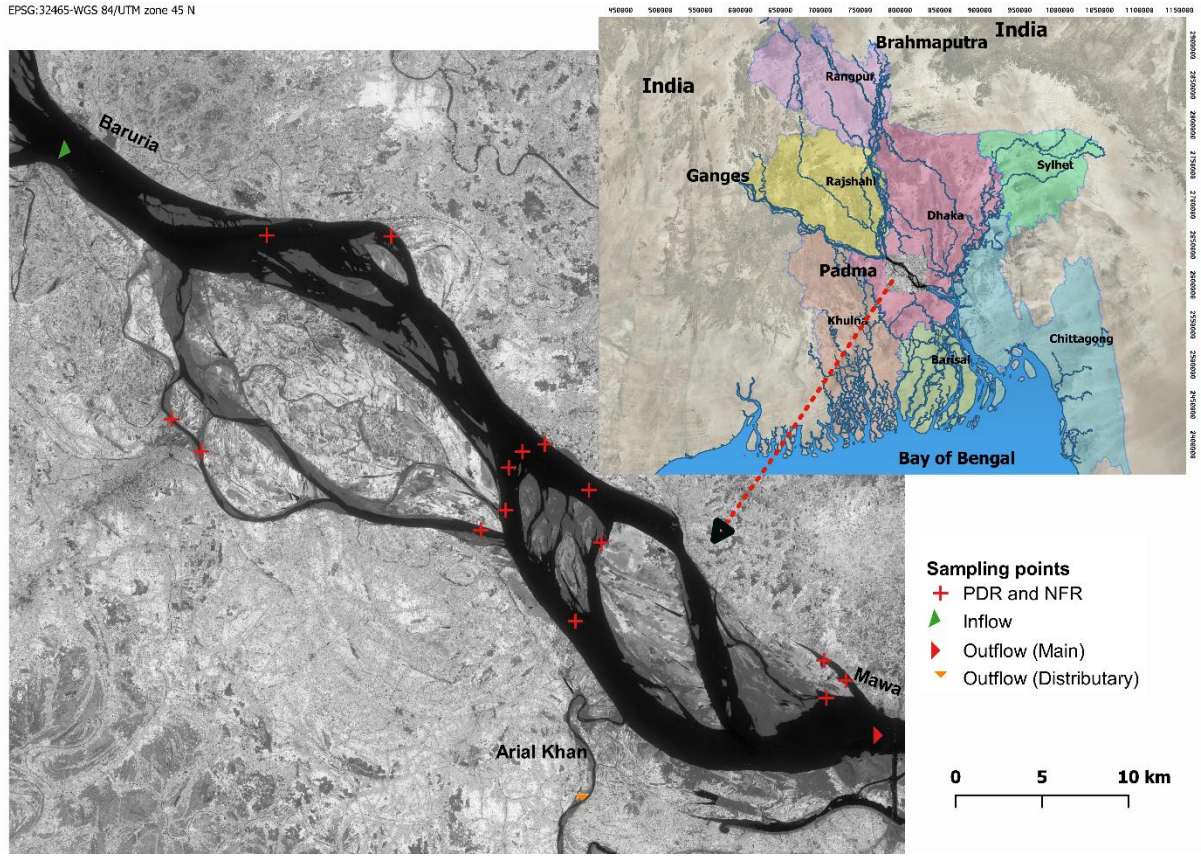

Figure 4. 1 Study reach of the Padma River in Bangladesh. Enlarged view of the reach showing sampling stations of Baruria (inflow), Mawa (outflow) and Arial Khan (outflow). The red cross marks represent sampling points in the river for PDR and NFR estimation during the dry/winter season (Source: GeoDASH, Bing Satellite and Copernicus Open Access Hub (https://scihub.copernicus.eu/dhus/#/home, accessed on 25 January 2022).

2.2. Overall approach

The inflow station, known as Baruria, is located near the city of Aricha, Manikganj, and has two outflow stations: the outflow on the main stem of the river is called Mawa, located in the city of Mawa, Munshiganj and a small distributary was measured at Arial Khan near Sadarpur in Faridpur. After the main outflow of Mawa, the river flows southeast, merging with the Meghna River, finally discharging into the Bay of Bengal (Figure 4. 1). The study reach does not have any significant tributaries, so samplings for the measurement of upstream-downstream transport of total nitrogen (TN) were carried out from an inflow (Baruria), a main outflow (Mawa) and a relatively small outflow (Arial Khan) (Figure 4. 1).

Monthly samplings for water quality were conducted together with the Bangladesh Water Development Board (BWDB) to correspond with their regular monitoring programmes for discharge measurements. Samplings for total dissolved nitrogen (TDN) and total suspended solids (TSS) were carried out from August 2019 to September 2020 at all three stations. Monthly water samples from Baruria (inflow) and Mawa (main outflow) were collected at 20% and 80% of channel depth, mainly from 3 sampling points across the river using a Binkley sampler. Additional samples were collected from 3 sampling points across the river

channel of Arial Khan. The downstream (Mawa) station is considered tidal for seven months of the year. So, more samples were collected during the tidal periods. Seventy samples from Baruria, 107 from Mawa, and 13 from Arial Khan were collected for nitrogen concentration analysis over the 14 months sampling period. Additional field campaigns were conducted from March 2021 to August 2021 to look at the influence of extreme events (storm events) and the relationship between discharge and concentration. During that period, 12 samples from Baruria, 11 from Mawa, and 3 from Arial Khan were collected.

For PDR and NFR, field campaigns were carried out during February 2020 (dry/winter season). Water samples from 15 sampling points of the mid-river reach were collected in triplicate, and separately for PDR and NFR. Immediately after collection, all the samples were transported in an icebox to the research laboratory in the Department of Botany, Jagannath University, Bangladesh.

After field samplings (i) TN (TDN+PN), (ii) PDR, and (iii) NFR were measured in the laboratory, and (iv) discharge (Q), (v) water retention, (vi) flux calculations were done separately. Finally, (vii) retention calculation and partitioning and (viii) net N losses via gaseous phases were estimated.

(i) Total nitrogen (TN)

Total nitrogen (TN) is the sum of TDN and PN. The measurement or estimation procedure for these were:

Total dissolved nitrogen (TDN)

For total dissolved nitrogen (TDN), water samples were filtered through Whatman GF/F filter paper on site and kept in high density polyethene (HDPE) bottles in a cool ice box for transporting as frozen to IHE Delft Institute for Water Education, The Netherlands for analysis. In the laboratory of IHE Delft, TDN was measured by high-temperature combustion (680 ^{o}C) using a Shimadzu TOC-L analyser.

Particulate nitrogen (PN)

To determine the particulate nitrogen (PN), TSS data was used. A volume of 60 mL was passed through dry, pre-weighed Whatman GF/F glass fibre filters for TSS measurement. The filter was dried at 105 ^{o}C, reweighed, and TSS was calculated (APHA, 2005). According to Balakrishna and Probst (2005) the carbon and nitrogen ratio of a large tropical river showed seasonal variation and mainly depended on the sediment fluxes during monsoon and in-channel phytoplankton density during other seasons. In the present study, comparatively higher TSS was found in monsoon, and higher phytoplankton density was counted in non-monsoon months (Appendix 5 and 6). So, PN was calculated following regression equations as modified after Balakrishna and Probst (2005).

$$\mathrm{PC} = \left(\frac{\frac{71.04}{\mathrm{TSS}}\,\mathrm{mg}}{\mathrm{L}} \right) + 1.6068$$

$$\frac{\mathrm{PC}}{\mathrm{PN}} = 0.0354 \times \mathrm{TSS\ mg\ L^{-1}} + 5.5041$$

PC is the concentration of the particulate carbon, and PN is the concentration of the total particulate nitrogen (mg L^{-1}).

(ii) Potential denitrification rate (PDR)

The potential denitrification rate (PDR) was measured by the acetylene inhibition method (Groffman et al., 1999). First, samples for PDR were processed in the research laboratory, Department of Botany, Jagannath University, Dhaka. Here, instead of sediment, water samples of 10, 25, and 50 ml volumes were used for the incubation. The gas samples were stored in evacuated exetainers with vacuum grease applied and then shipped to IHE. In the laboratory of IHE, gas samples for N_2O were quantified by gas chromatography (Scion 456-GC) using an electron capture detector (ECD) at 250 ^oC. Finally, the PDR was calculated as mg N_2O-N L^{-1} h^{-1}.

(iii) Nitrogen fixation rate (NFR)

The nitrogen fixation rate (NFR) was also measured using the acetylene inhibition method (Grimm and Petrone, 1997), in which acetylene was introduced to a sample and reduced to ethylene by the nitrogenase enzyme. Water samples were placed in gas-tight flasks, and purified acetylene was added by bubbling through 10% of acid (H_2SO_4) so as to protenate (and dissolve) any NH_3 from the acetylene tank (98.5% acetylene), which could affect the microbial activity in the jar. After that, flasks were placed on a rotary shaker at 125 rpm for incubation for 4 hours. Gas accumulated in the flask was removed by hand inserting a syringe, then injected into evacuated gas vials (15 mL) and sealed and stored for later analysis of ethylene. All vials were transported to IHE Delft, the Netherlands. In GC (Bruker GC-456), ethylene was quantified using a flame ionisation detector (FID) at 175 ^oC, and the runtime was 2.5 mins. Finally, the NFR was calculated as mg N_2 L^{-1} h^{-1}.

(iv) Discharge (Q)

Monthly observed discharge data with flow velocity from 2019 to 2021 at the Baruria, Mawa and Arial Khan stations were collected from the BWDB. Three hourly water level data during that period were also collected from the BWDB. Daily mean rainfall data from 2019 to 2020 from the eight rainfall stations close to the study area were collected from the BWDB.

The outflow station, Mawa, was tidal from November to May, according to BWDB. So, for measuring the daily discharge of this station, first, the monthly mean discharge of monsoon months (June to October) between Baruria and Mawa was compared, and regression analysis was used to estimate the discharge in Mawa during tidal months, calculated from the discharge in Baruria (Figure 4. 2). For each station using observed monthly discharge data, rating curves were produced, and 3 hourly discharges (Q) were calculated from water level (WL) data.

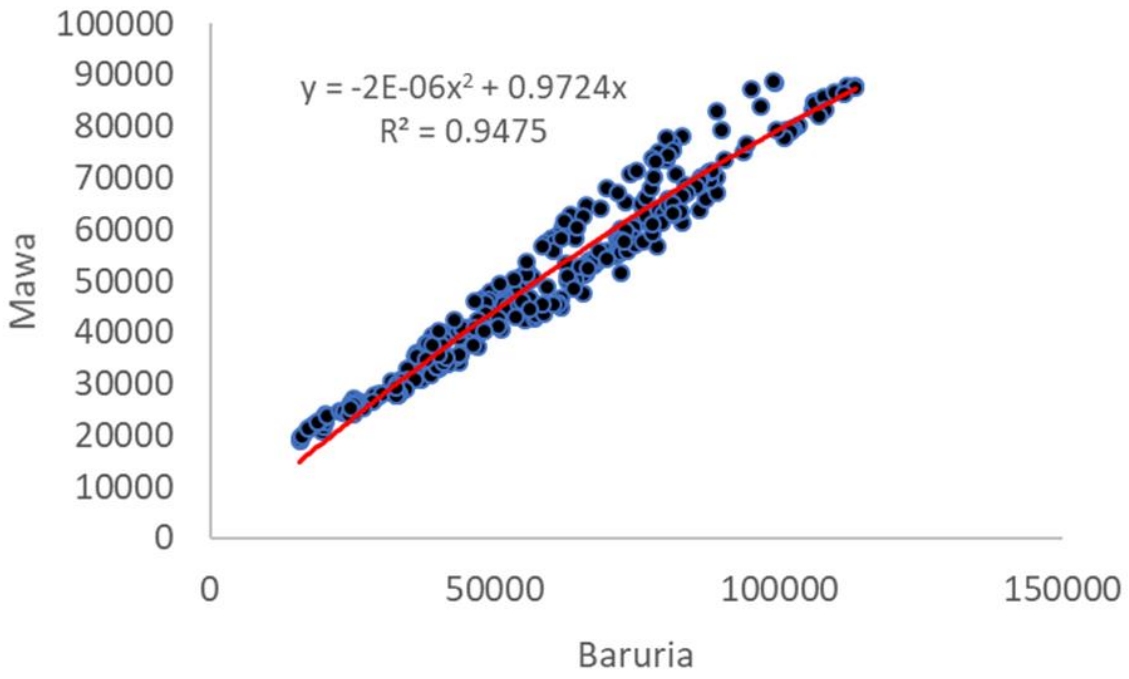

Figure 4. 2 Regression analysis between discharges of Baruria (inflow) and Mawa (outflow) during monsoon months (June-October); showing correlation of coefficient (R^2= 0.9475) and regression equation ($y= -2\times10^{-6} x^2 + 0.9724x$) that used to derive the discharges during non-monsoon months in Mawa.

(v) Water retention

Water retention was observed in the study reach for the duration of the study period, irrespective of season. Monthly outflow discharges were subtracted from the inflow discharges to calculate water retention as:

$$Water\ retention\ (m^3\ month^{-1}) = Inflow\ Q(m^3\ month^{-1}) - Outflow\ Q\ (m^3\ month^{-1})$$

(vi) Flux calculations

To calculate nitrogen flux from the inflow (Baruria) and the outflows (Mawa and Arial Khan), first, the relationship between discharge and nitrogen concentration (TDN and PN) was analysed. The relationship between observed discharge and measured nitrogen concentrations is presented in Figure 4. 3. Observed discharge and measured total dissolved nitrogen (TDN) showed no significant relationship for all the sampling stations (Baruria, Mawa and Arial Khan). Significant relationships were found between discharge and PN data for all stations (Figure 4. 3). So, linear regression equations were used for the PN concentration to estimate the three hourly PN values from the discharges, whereas, for TDN, only a mean value was used. Finally, three hourly discharges were multiplied by concentration values to obtain three hourly PN and TDN fluxes. From 3 hourly, first daily and then monthly fluxes were calculated. Finally, TN flux was obtained from PN and TDN as t $month^{-1}$ (tonnes per month).

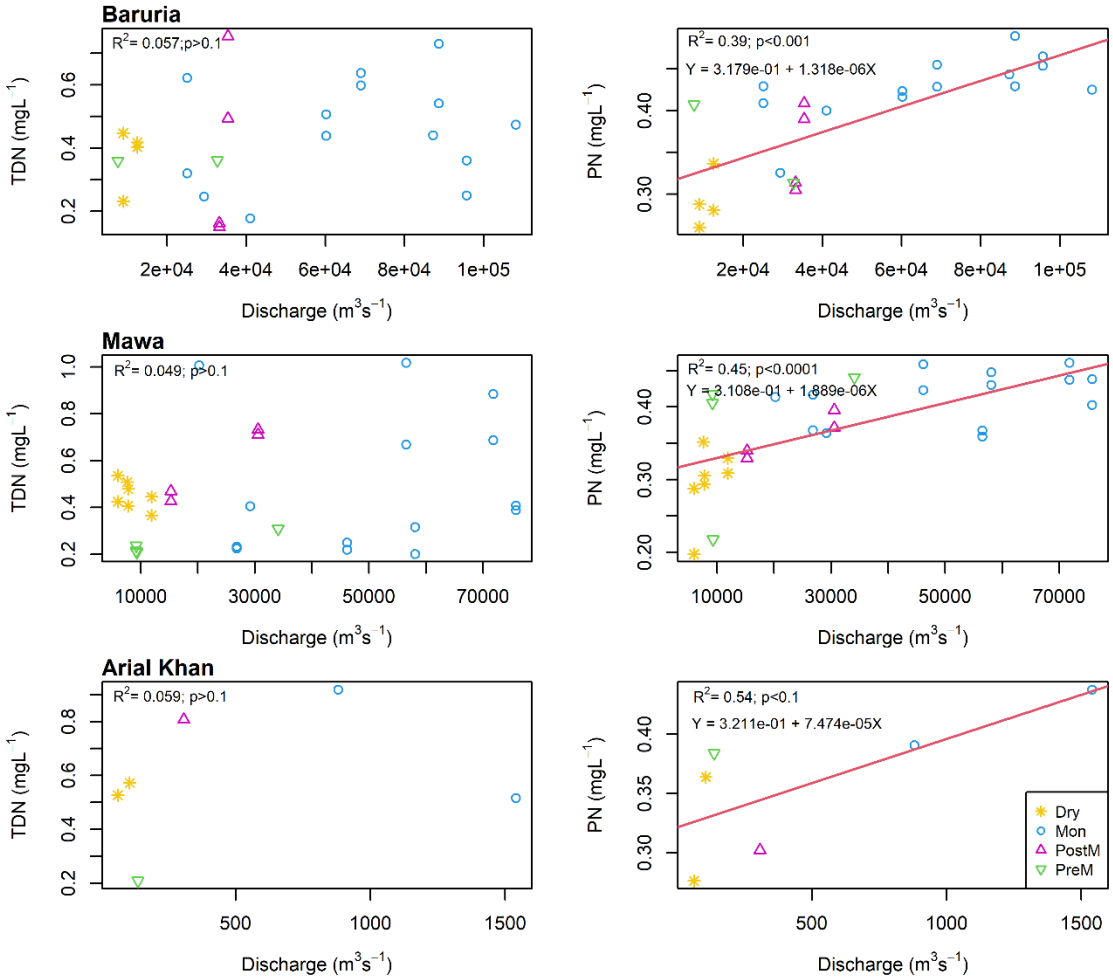

Figure 4. 3 Relationships between discharge and total dissolved nitrogen (TDN) and particulate nitrogen (PN) (where regressions were significant) in the Baruria (inflow), Mawa (outflow), and Arial Khan (outflow) of the Padma River, Bangladesh.

(vii) Retention calculations and partitioning

Overall retention

The mass balance approach involved using discharge and concentration of nitrogen to calculate the difference between loads at the inflow and outflow points that define the study reach. In the nitrogen retention calculation, the lateral input due to anthropogenic activity – e.g., from wastewater input and runoff - was assumed to be trivial compared with upstream input to the study reach. Therefore, lateral inputs were ignored. The mass balance was calculated as:

$$Nitrogen\ retention\ (t\ month^{-1}) = Input\ (inflow)(t\ month^{-1}) - Output\ (outflows)(t\ month^{-1})$$

Nitrogen loss due to water retention

To estimate the nitrogen loss due to water retention (NLWR) through the reach, water retention for every month was multiplied by the inflow TN concentration to quantify monthly N losses. So, N loss due to water retention (NLWR) was calculated as

$$NLWR\ (t\ month^{-1}) = Water\ retention\ (m^3\ month^{-1}) \times Inflow\ TN\ Conc.\ (t\ m^{-3})$$

Sedimentation

The difference in PN concentration from the inflow to outflows can cause sedimentation. So, sedimentation of particulate N in the study reach was estimated by calculating the difference between PN concentrations from inflow and outflows and multiplying this difference by the Q of the outflow:

$$N\ Sedimentation\ (t\ month^{-1}) = [Conc.of\ inflow\ PN\ (t\ m^{-3}) - Conc.of\ outflows\ PN\ (t\ m^{-3})] \times Outflow\ Q\ (m^3\ month^{-1})$$

(viii) Net N losses via gaseous phases

Upscaling of the measured PDR and NFR in the water column

Measured PDR and NFR in the water column were upscaled using the monthly observed flow velocity, discharges in outflows and estimated water travel time in the study reach. Only the amount of water in the outflows was considered for PDR and NFR up-scaling. A travel time factor was used to estimate water travel time from inflow to outflows using the flow velocity and total distance (50 km) of the reach. Finally, the amount of water from every month was multiplied by the measured average PDR or NFR to get an estimation for the whole reach. So, the up-scaling of PDR and NFR is as follows:

$$PDR\ (t\ month^{-1}) = [(Outflow1\ Q1 + Outflow2\ Q2)(L\ month^{-1}) \times k_t\ (d)] \times Mean\ \ PDR\ (t\ L^{-1}\ d^{-1})$$

$$NFR(t\ month^{-1}) = [(Q1 + Q2)(L\ month^{-1}) \times k_t\ (d)] \times Mean\ \ NFR\ (t\ L^{-1}\ d^{-1})$$

$$k_t\ (d) = \frac{\text{reach distance (m)}}{\text{Outflow1 weighted average velocity (m d}^{-1}) + \text{Outflow2 weighted avearge velocity (m d}^{-1})}$$

Q1 and Q2 are the discharges of outflow$_1$ (Mawa) and outflow$_2$ (Arial Khan), respectively. k_t was the travel time factor derived from the monthly water velocities. Mean PDR and NFR were calculated from the measured PDR and NFR at different sampling points.

Estimation and upscaling of PDR in submerged GUs

For estimating PDR in submerged GUs first, the submerged area of GUs was calculated for each season using the surface area of GUs described in Gani et al. (2022) (Appendix 7). After that, mean PDR of each GU was calculated from the measured PDR in GUs during the dry/winter season (Chapter 3) (Appendix 8). Finally, the area of submerged GUs was multiplied by the mean value PDR in each GU to obtain seasonal estimates; and then converted to monthly estimates.

$$PDR\ in\ Submerged\ GUs\ (t\ \ month^{-1}) = Area\ of\ submerged\ GUs\ (m^2) \times Mean\ measured\ PDR\ in\ GUs(t\ m^{-2}\ month^{-1})\ \times k_{dm}$$

Here, k_{dm}= conversion factor from day to month.

3. Results

3.1. River hydrology by month

The highest discharge was found in July 2020 (Baruria: 2.67×10^{11} m^3 $month^{-1}$, Mawa: 2.35×10^{11} m^3 $month^{-1}$and Arial Khan: 5.46×10^{9} m^3 $month^{-1}$) for all the sampling locations, and the lowest discharge was in March 2020 for Baruria ($1.1.8\times10^{10}$ m^3 $month^{-1}$) and February 2020 for Mawa (1.12×10^{10} m^3 $month^{-1}$) and Arial Khan (3.9×10^{8} m^3 $month^{-1}$) (Figure 4. 4). Water retention, i.e. the difference in discharge between inflow and outflows, showed that during monsoon months, the retention was higher than in other months. The highest water retention occurred during September 2019 (3.17×10^{10} m^3 $month^{-1}$), and the lowest in March 2020 (3.59×10^{7} m^3 $month^{-1}$) (Figure 4. 5). During monsoon, river discharge mostly driven by rains, and is therefore closely related to precipitation patterns (Appendix 9).

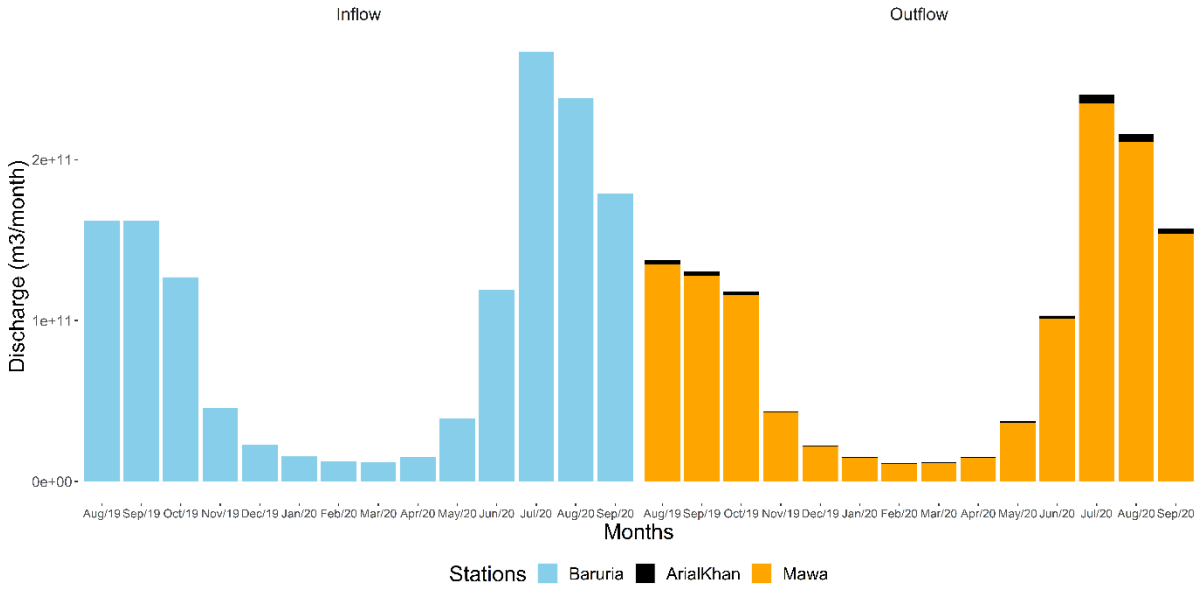

Figure 4. 4 Monthly variation of calculated discharge in the study area of the Padma River, Bangladesh, from August 2019-September 2020.

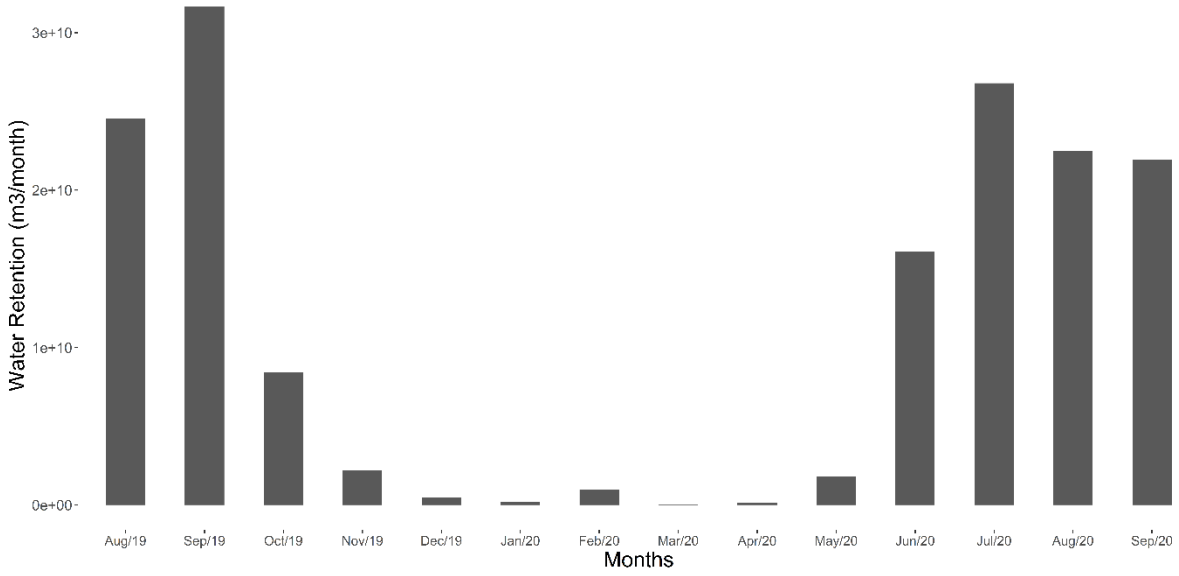

Figure 4. 5 Monthly variation of water retention in the study area of the Padma River Bangladesh, from August 2019 to September 2020.

3.2. Monthly variation of nitrogen concentration and nitrogen flux in the inflow and outflows

Monthly average TN concentrations were higher in the inflow and outflows during the monsoon than in the other months. The TN concentrations were consistently higher in the inflow (Baruria) than in the main outflow (Mawa). However, the TN concentration of distributary was the highest (Arial Khan) (Figure 4. 6). TN fluxes through Baruria, Mawa, and Arial Khan ranged from 6950 − 301777, 6144 − 173805 and 214 − 5696 t month^{-1}, respectively (Fig. 4. 7). Like the rainfall, discharge and average TN concentration, the highest TN flux was estimated in the monsoon months. The highest value was found in July 2020. However, the TN flux pattern during monsoon months differed in both outflows. In Mawa, the highest value was found in July 2020; in Arial Khan, the highest was found in August 2020; and the lowest was in June 2020. More TPN was transported through Mawa during July 2020 and August 2020 and less during August 2019 and September 2019 (Figure 4. 7). So, the two monsoon periods showed a distinct feature in the case of nitrogen flux in Mawa, which is the main outflow of the river.

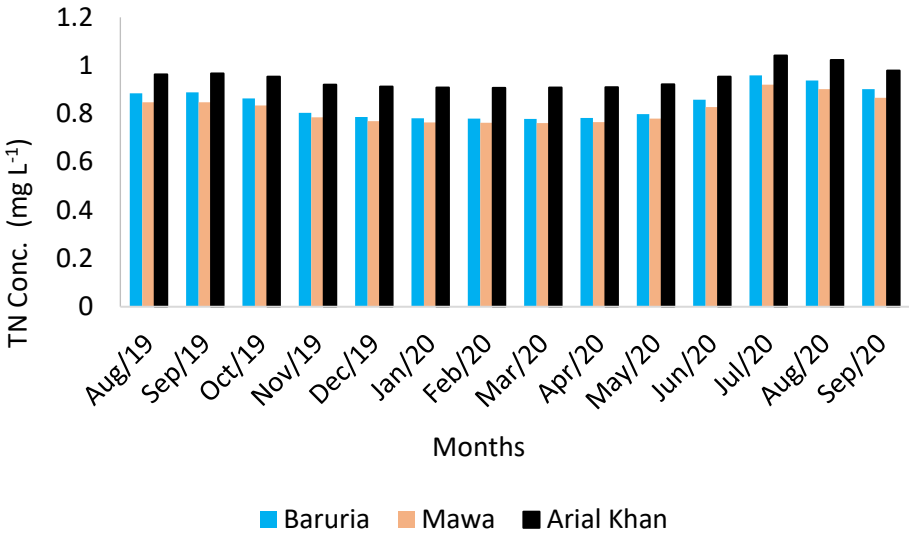

Figure 4. 6 Monthly variation of TN (TDN+TPN) concentration (mg L^{-1}) in the study area of the Padma River, Bangladesh.

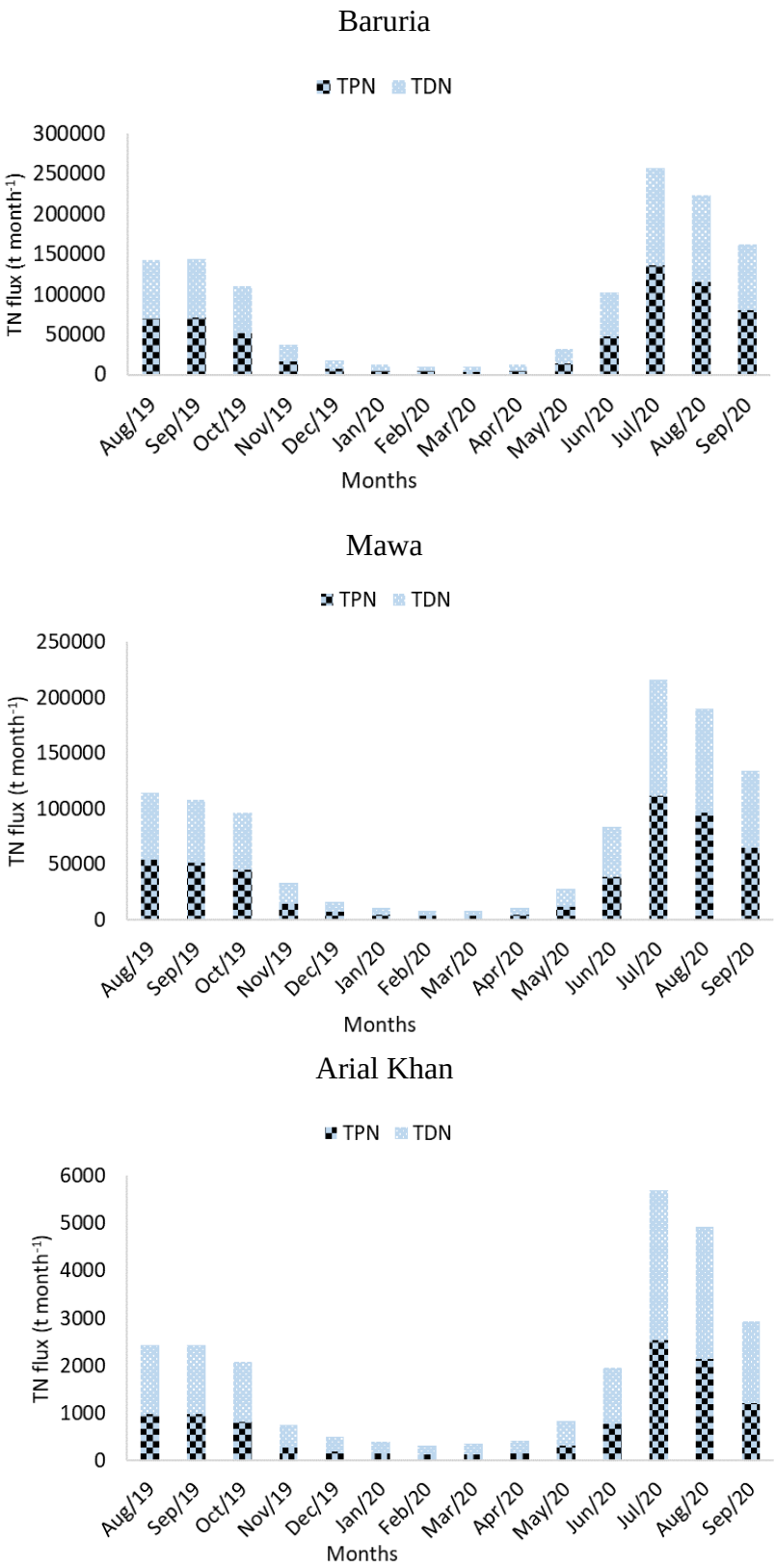

Figure 4. 7 Monthly variation of TN flux (t month^{-1}) in the Baruria (inflow), Mawa (outflow) and Arial Khan (outflow) of the study area of the Padma River, Bangladesh.

3.3. Measured nitrogen retention through a mass balance

The monthly mass balance estimation showed that the maximum TN retention was during July 2020 (120000 t month^{-1}). Retention occurred mainly in monsoon except during September 2019 when the inflow flux was higher than the outflow fluxes. In post-monsoon 2019, comparatively less retention occurred as more TN was transported through Mawa than Baruria during October 2019. A similar scenario was found in dry/winter 2020 and pre-monsoon 2020, where more TN was transported through Mawa than Baruria, resulting in net TN export during those periods (January 2020, February 2020, April 2020, and May 2020) (Figure 4. 8). From October 2019 to September 2020 (hereafter annual) TN retention of the reach was 121715 t which was 11% of the total inflow to the river. Seasonal variation showed that measured TN retention in the post-monsoon, dry/winter, pre-monsoon, and monsoon season was 12928 t (10.6% of annual TN retention), 1946 t (1.6% of annual TN retention), 2493 t (2.1% of annual TN retention) and 104347 t (85.7% of annual TN retention), respectively (Appendix 10).

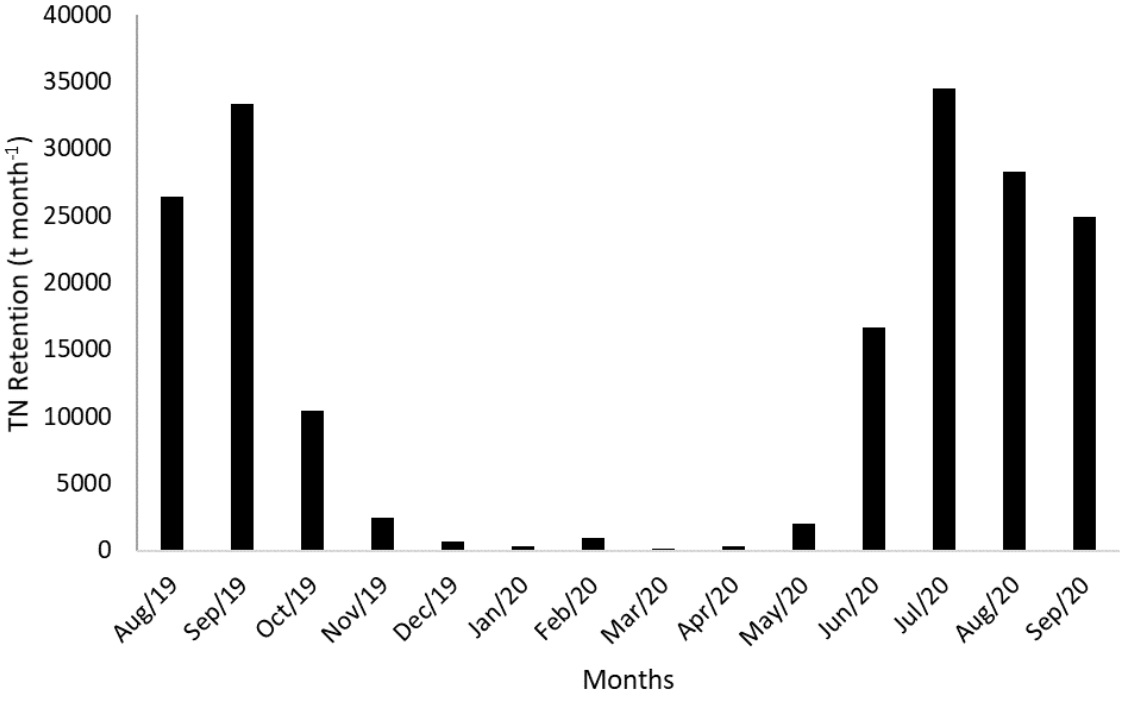

Figure 4. 8 Monthly variation of estimated TN (total nitrogen) retention in the study reach of Padma River during August 2019-September 2020.

3.4. Variation of estimated nitrogen loss due to water retention (NLWR) and sedimentation

In the study area, TN was lost due to water retention (NLWR) to the floodplains and aquifers throughout the study period, but it was comparatively higher in monsoon months. The maximum TN transport as floodplain and aquifer loss occurred during July 2020 (30135 T/month). Some amount of N loss occurred during post-monsoon 2019 (1889 − 7630 t month^{-1}) and pre-monsoon (103 − 1169 t month^{-1}), while in the dry/winter 2020, it was a minimum (21 − 617 t month^{-1}). TN losses also occurred due to sedimentation, and the higher was during monsoon. Among monsoon months, the maximum sedimentation was found in

July 2020 (7014 t month^{-1}) and the minimum was in June 2020 (2066 t month^{-1}), which was 5 times higher than the lowest value during non-monsoon (80 t month^{-1}) (Figur 4. 9). Estimated annual TN retention as NLWR was 92289 t (77% of total measured retention) and estimated annual TN retention via sedimentation was 22176 t (18% of total measured retention) (Appendix 10).

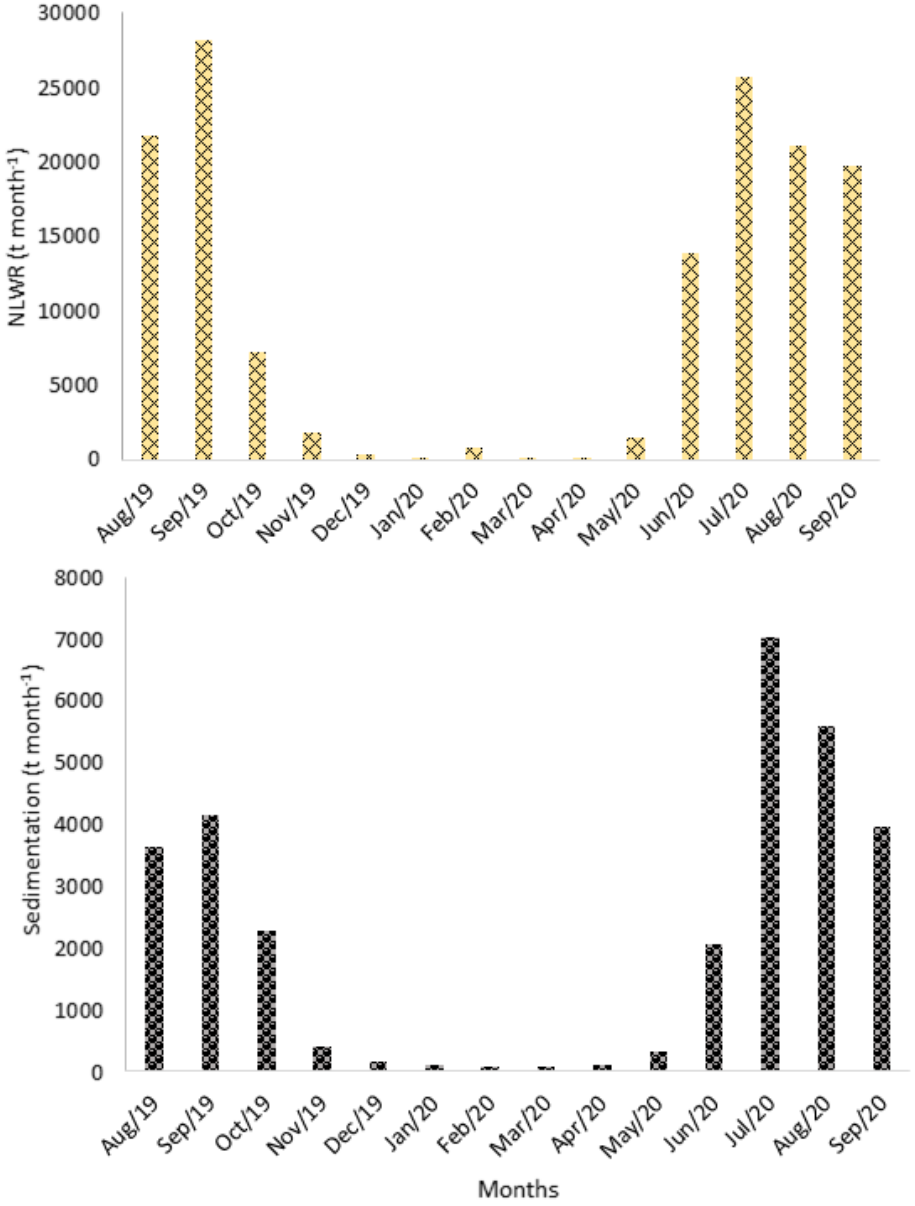

Figure 4. 9 Monthly variation of estimated N loss due to water retention (NLWR) and sedimentation in the study reach of Padma River during August 2019-September 2020.

Variation of estimated potential denitrification rate (PDR) in the water column and submerged GUs and N fixation rate (NFR)

Most of the nitrogen loss by denitrification (PDR) in the water column and submerged GUs occurred in the monsoon months, while at the same time, nitrogen was added through N

fixation (NFR). PDR in submerged GUs showed a comparatively higher value than PDR in water column during non-monsoon months. The highest PDR and NFR values in the water column were found in July 2020 (PDR: 542 t month^{-1}, NFR: 7.34 t month^{-1}), and the lowest values were in March 2020 (PDR: 27 t month^{-1}, NFR: 0.36 t month^{-1}) during monsoon months. In non-monsoon months, the values were higher in October 2019 (PDR: 213 t month^{-1}, NFR: 2.89 t month^{-1}) (Figure 4. 10). Estimated annual PDR in submerged GUs was 2795 t (2.3% of total measured retention) and estimated annual water column PDR was 2152 t (1.8% of total measured retention) (Appendix 10).

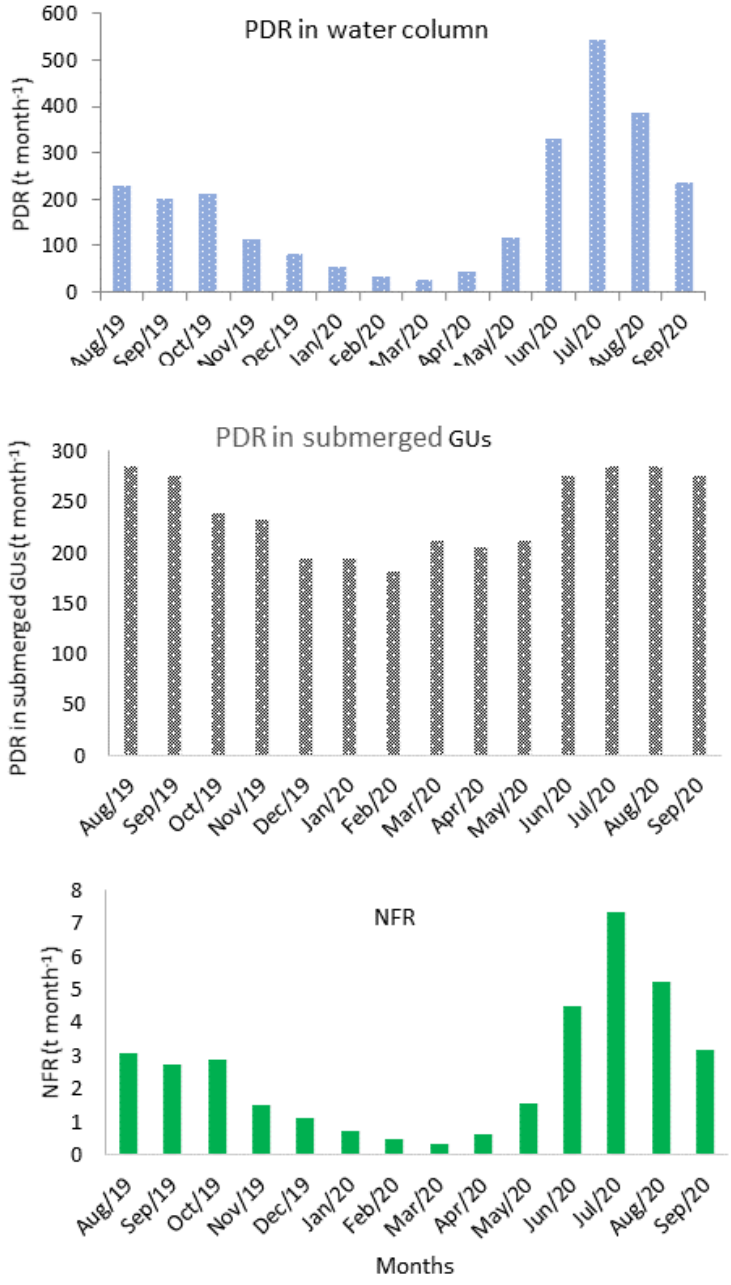

Figure 4. 10 Monthly variation of estimated potential denitrification rate (PDR) and nitrogen fixation rate (NFR) in the study area of Padma River, Bangladesh.

3.5. Comparison of measured retention with estimated retention and contribution of different retention processes

Monthly estimated retention through different retention processes ((NLWR, sedimentation and PDR)) showed same pattern as measured retention (Figure 4. 11, Figure 4. 12). The sum of estimated annual retention was 119412 t, which is 98% of the measured value. Estimated TN retention in the post-monsoon, dry/winter, pre-monsoon and monsoon season was 12500 t, 2380 t, 2904 t and 101629 t, respectively, which corresponds to 97%, 122%, 116% and 97% of the measured retention in those seasons, respectively (Figure 4. 11, Appendix 10).

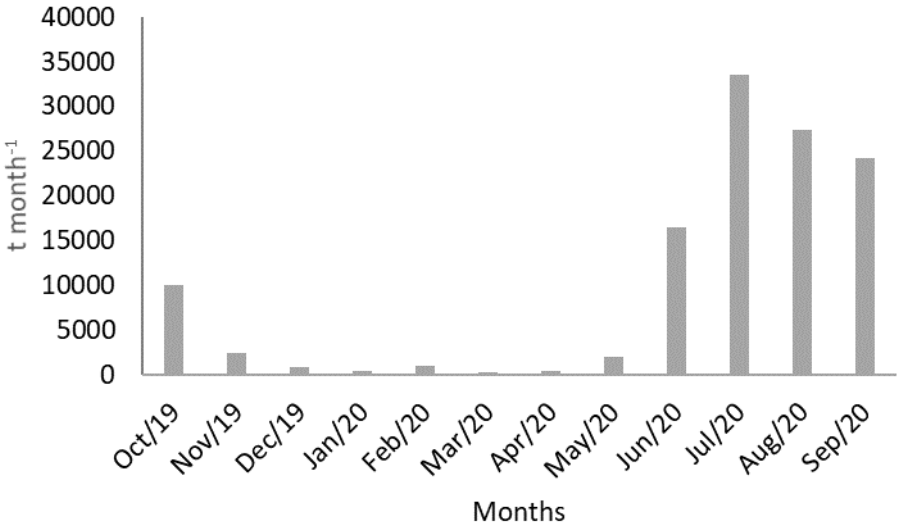

Figure 4. 11 Monthly variation of estimated TN (total nitrogen) retention in the study reach of Padma River during August 2019-September 2020.

During monsoon months, measured retention was higher than estimated retention, while during non-monsoon months, except for October 2019, the measured retention was lower than the estimated retention (Figure 4. 12). A comparison of measured retention and the sum of estimated retention processes is shown in Figure 4. 13. Comparatively, the percentage of NLWR was higher in the monsoon months. In case of sedimentation, the highest percentage was found in March 2020, and the lowest was in February 2020. The percentage of PDR both in the water column and submerged GUs showed a higher value in non-monsoon months. Figure 4. 13 also shows that the difference between measured and estimated retention was negative during non-monsoons.

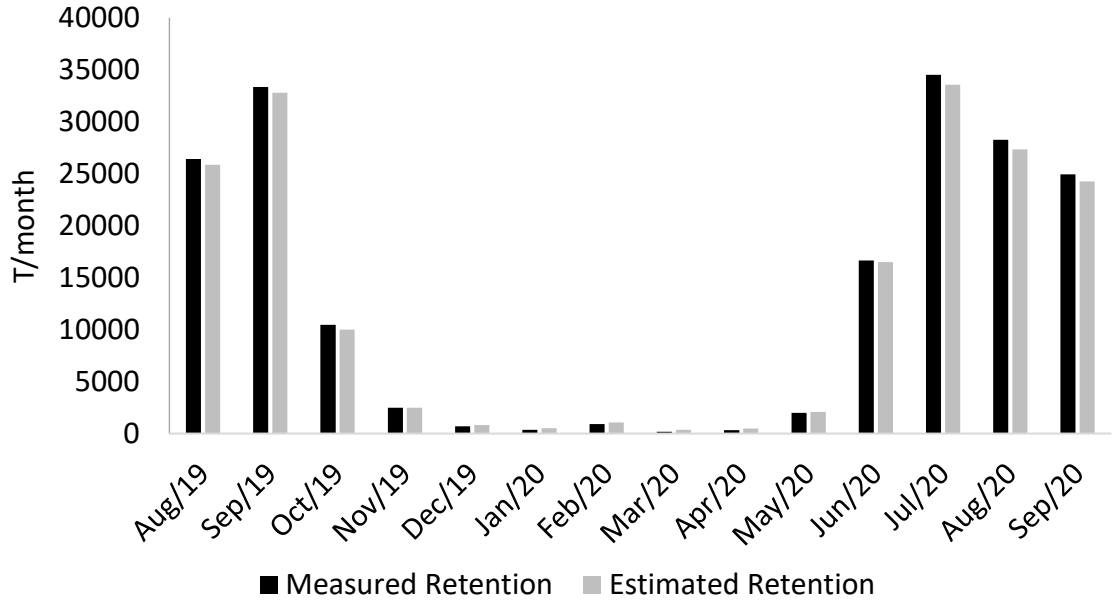

Figure 4. 12 A comparison between measured TN retention (through mass balance calculation) and estimated TN retention (through different retention processes) in the Padma River, Bangladesh.

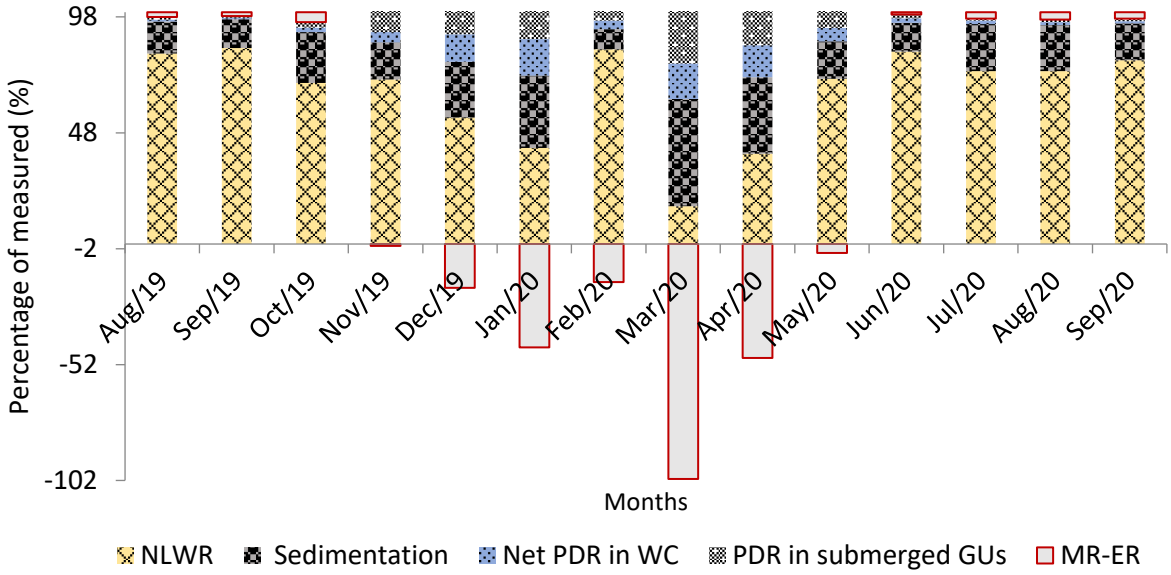

Figure 4. 13 Monthly comparison of NLWR (nitrogen loss due to water retention), sedimentation, and Net PDR in the water column (net potential denitrification rate in the water column), PDR in submerged GUs and MR-ER (MR= measured retention and ER= estimated retention) at the study area of Padma River, Bangladesh (Net PDR = PDR-NFR).

4. Discussion

To our knowledge, this is the first study that has looked at monthly -time steps for nitrogen retention in a monsoon-dominated large tropical river. Other studies in the temperate zone have, however, also shown monthly variation in nitrogen retention (de Klein and Koelmans, 2011; Natho et al., 2013). Considering the mean width of the reach, the measured TN retention during the present study was 556 mg m^{-2} $d^{-1,}$ which can be comparable to the large lowland Elbe River, where the estimated retention was 408 mg m^{-2} d^{-1} (Ritz and Fischer, 2019). All nitrogen retention processes were influenced by discharge, which varied significantly between seasons. Moreover, in all seasons, the studied reach was found to be losing water, as downstream discharge was less than upstream discharge. The annual retention of the Padma River (represented 11% of the total input to the river) was almost similar to other studies (Coupe et al., 2013; Loken et al., 2018). Unlike other studies, about 86% of the retention estimated in the Padma River occurs during monsoon months (Appendix 10). Several factors were apparently involved in regulating TN retention in the studied reach.

4.1. Role of discharge as an influencing factor of TN retention

In the Padma River, strong seasonal differences in precipitation and river discharge were observed, which is similar to other large rivers, where discharge is a major regulatory factor for nitrogen transport (Wang et al., 2020; Pan et al., 2020; Krishna et al., 2016).

In the river, the discharge of primary and secondary channels, that increased in the water flux was associated significantly with estimated TN retention. However, the data showed three scenarios of non-monsoon, monsoon 2019 and monsoon 2020 (Figure 4. 14). The scenarios were observed mainly due to the variation of monsoon discharge events, which varied from 2019 to 2020 (Figure 4. 4). In 2020, flooding started unusually late in June and recorded the highest discharge and second longest residence time since 1989 and 1998, respectively (OCHA, 2023). The maximum TN retention was found during the flood peak in July 2020. In contrast, in 2019, the highest peak was observed in September. Due to a lack of data (June and July 2019), it was not possible to show how flooding influenced retention in the whole monsoon of 2019.

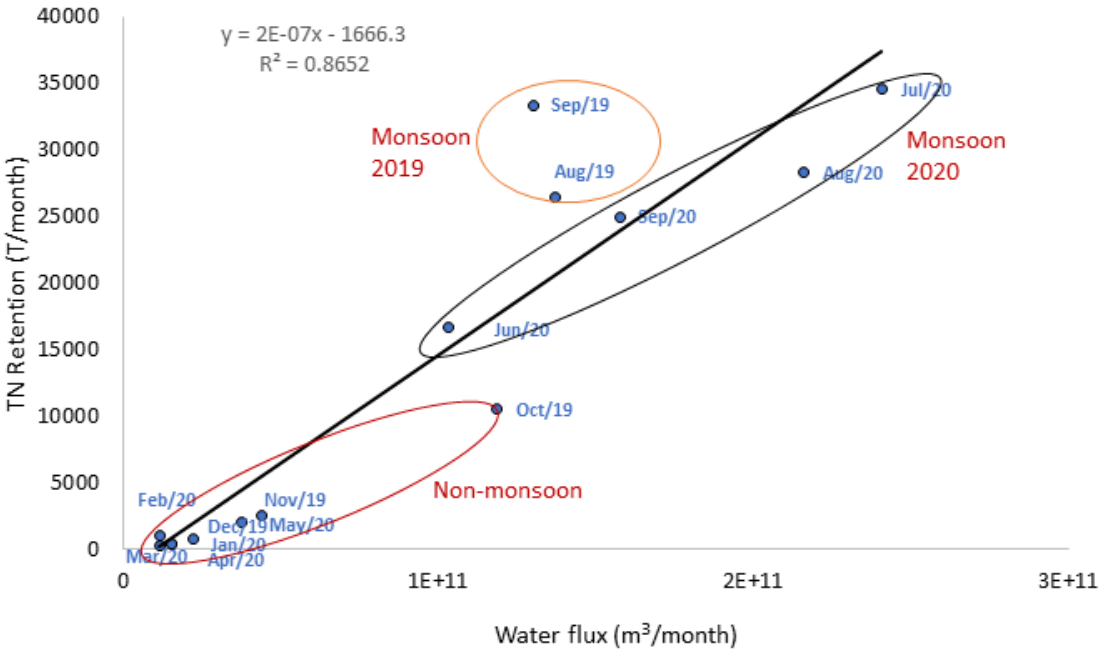

Figure 4. 14 Regression analysis between water flux and nitrogen retention in the Padma River, Bangladesh, showing three scenarios represented by the ovals (non-monsoon, monsoon 2019 and monsoon 2020). Water flux was calculated based on the allocation of inflow discharge to the surface area of primary and secondary channels (C & S).

The increase in discharge is due to increased surface runoff with high nitrogen concentrations increasing river nitrogen load. Due to the positive difference in TN concentration from inflow to outflows, the Padma River showed more TN flux in monsoon 2020 than in monsoon 2019. Different monthly estimations of the nitrogen flux also occurred due to the greater inflow concentrations relative to the main outflow influenced by the discharge. Due to this phenomenon, average retention estimation fluctuated highly between monsoon periods (Figure 4. 15). In the present study, estimated PN concentration was based on the relationship with discharge, which was also a factor that impacts TN concentrations, resulting in more retention in monsoon months.

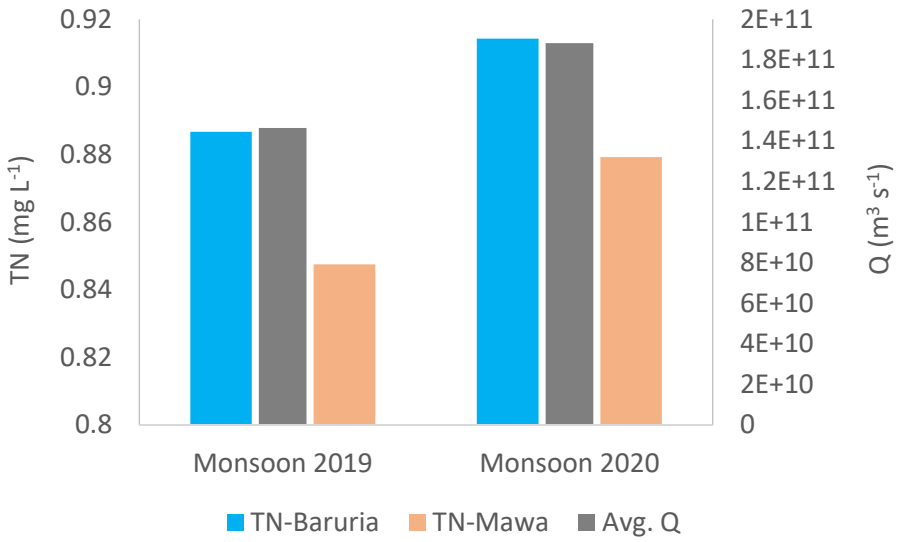

Figure 4. 15 Mean TN concentrations in the Baruria (inflow) and Mawa (outflow) during monsoon 2019 and 2020. Avg. Q (average discharge) from inflow and outflow stations during this period is also depicted in this figure.

4.2. Role of submerged GUs and water column denitrification in TN retention

Net PDR in the water column and PDR in submerged GUs were influenced by the total discharge flowing from the reach in each season. TN retention via net PDR in the water column was a rate per water volume, so the retention value increased or decreased as volume increased or decreased. TN retention via PDR in submerged GUs was a rate per area of submerged GUs, so retention increased or decreased as the area (and type) of submerged GU increased or decreased. Area changed as discharge increased and decreased.

In the study reach, PDR in submerged GUs appears to be much more important than the water column PDR (2795 t year^{-1} vs. 2152 t year^{-1}, respectively). Annually, denitrification associated with GUs increases from 2795 to 3197 due to the inundation of geomorphic units exposed during the post-monsoon, dry/winter and pre-monsoon seasons (Chapter 3). PDR in the water column and in GUs were most significant to total N retention in the pre-monsoon and dry/winter seasons, accounting for 28% and 31% of total N retention, respectively. During the monsoon and post-monsoon seasons, PDR in the water column and in GUs accounted for only 2% and 7% of total N retention, respectively. PDR estimates in submerged GUs were strongly dependent on the assumed depth of hyporheic exchange, which was considered at 10 cm depth during the present study. Other studies have shown exchange up to 1 m (Fischer et al., 2005; Bartoli et al., 2021).

4.3. Role of water retention in TN retention and retention processes

During the present study, NLWR and sedimentation were estimated to contribute a significant portion to TN retention, which occurred due to water retention. Estimated TN retention values for NLWR and sedimentation were influenced by the water retention seasonally in the reach. Differences in downstream versus upstream discharge determined the

amount of water retention, which included the retention of 100% of TN in the retained water (NLWR). Suspended sediment concentrations (and associated PN) were estimated as a function of discharge. Suspended sediment concentrations decreased downstream, and the difference in suspended sediment loads was equated to sedimentation, with associated PN retained. Comparatively higher TN retention was found in September 2019 and July 2020 due to high water retention, which influences NLWR and sedimentation. Unexpectedly, after January 2019, more water retention was observed in February 2020, which enhanced NLWR and sedimentation. However, this appeared mainly due to direct or indirect groundwater recharge during the dry season induced by intensive groundwater abstraction for irrigation (Nowreen et al., 2020). Another factor might be dredging activities during that time, i.e. sediment removal through water showed high NLWR and sedimentation. In addition, during non-monsoon periods, as a percentage, comparatively higher denitrification was estimated in the water column, likely due to low flow velocity (1.65 times lower than monsoon), resulting in nitrogen loss.

4.4. Processes that are responsible for the difference between measured and estimated retention

Measured and estimated N retention were within 2% of each other overall, but differences were higher in the individual seasons. Measured values were higher than estimated in monsoon and post-monsoon seasons, while measured values were less than estimated in pre-monsoon and dry/winter seasons. The differences are small and may fall within the range of uncertainty in measurements and estimations, but other explanations are also possible. During monsoon, the surplus of measured retention suggested that other retention processes might be responsible for the difference, which was not accounted for in the present research. For example, gaseous nitrogen loss to the atmosphere through processes other than denitrification during monsoon can be the cause, which was not considered during the retention process estimation.

The variation of GUs and fertilisation for cropping can explain the surplus of the estimated value during pre-monsoon and dry/winter seasons. The application of fertiliser in the GUs for high crop yield was started during or after post-monsoon. The nitrogen status of the study area was categorised by the Bangladesh Agricultural Research Council as very low and low, where the expected maximum yield ranged from 25-75% without fertiliser. Fertiliser is applied between November and March to increase the crop yield (Ahmmed et al., 2018). As the surface area of terrestrial GUs increased from post-monsoon to the winter/dry season (Gani et al., 2022), an increase in fertiliser application might be expected to increase PDR and be higher in the dry/winter season. However, the submerged surface area was higher in pre-monsoon than dry/winter season (Appendix 7). As the inundation started, the stored N in soil was released due to increased water volume and readily available nitrate for denitrification. So, a higher PDR was observed in March 2020.

4.5. Limitations and scope for future research

In the Padma River, estimating the annual TN budget without measuring all forms of nitrogen and considering a series of data for several years was challenging due to the high monthly

variation of TN flux from inflow to outflow, Frequent changes in channel geomorphology and flooding events were also responsible for this difficulty. These factors alter the nitrogen transport scenario from season to season, so slight temporal scale variation can influence long-term predictions. Beyond these limitations, the current research can explain retention processes like NLWR, sedimentation, and PDR in the water column and submerged GUs monthly. The contributions of these processes to TN retention are highly variable and can impact nitrogen budget estimation. Moreover, flooding events can significantly affect year-to-year retention calculation. So, these facts should be considered in estimating nitrogen budgets in tropical floodplain rivers.

5. Conclusion

In the study area, nitrogen retention mechanisms were strongly influenced by discharge and thus varied on a seasonal basis; most of the retention occurs during monsoon. In other seasons, less retention occurs due to less water retention. Retention as NLWR and sedimentation were the main retention processes in the river; however, during non-monsoon, a comparatively significant amount of nitrogen losses occurred by denitrification. The following conclusions can be drawn:

- Nitrogen retention occurs in the Padma River of Bangladesh, showing monthly or seasonal fluctuations.
- Variation in discharge was the main controlling factor of nitrogen retention in the study reach. However, flooding events can change the retention mechanism from one season to another.
- In addition, PDR, and water retention can also act as regulating factors for TN retention but strongly influenced by seasonality.
- Water retention resulted in sedimentation and nitrogen losses throughout the study period.
- Concentration of nitrogen in the form of particulate and dissolved nitrogen can regulate overall nitrogen retention.
- Estimated potential denitrification and nitrogen retention through flooding varied based on monthly water retention and thus can influence TDN and PN retention.
- There was a slight difference between measured retention (through mass balance) and estimated retention (through retention processes). However, this difference can be explained by other processes that might be occurred during that time.
-

6. References

APHA (American Public Health Association) (2005). Standard Methods for the Examination of Water and Wastewater (21st ed.). Washington DC, American Public Health Association.

Ahmmed S., Jahiruddin M., Razia S., Begum R. S., Biswas J. S., Rahman A. S. M. M., Ali M. M., Islam K. M. S., Hossain M. M., Gani M. N., Hossain G. M. A. & Sultan M. A. (2018). Fertilizer Recomendation Guide- 2018. In Bangladesh Agricultural Research Council (BARC), Farmgate, Dhaka 1215.

Balakrishna K. & Probst J. L. (2005). Organic carbon transport and C/N ratio variations in a large tropical river: Godavari as a case study, India. Biogeochemistry, 73(3), 457–473. https://doi.org/10.1007/s10533-004-0879-2

Bartoli M., Nizzoli D., Zilius M., Bresciani M., Pusceddu A., Bianchelli S., Sundbäck K., Razinkovas-Baziukas A. & Viaroli P. (2021). Denitrification, Nitrogen Uptake, and Organic Matter Quality Undergo Different Seasonality in Sandy and Muddy Sediments of a Turbid Estuary. Frontiers in Microbiology, 11(January). https://doi.org/10.3389/fmicb.2020.612700

Best J. (2019). Anthropogenic stresses on the world's big rivers. Nature Geoscience, 12, 7–21. https://doi.org/10.1038/s41561-018-0262-x

Böck K., Polt R. & Schülting L. (2018). Ecosystem Services in River Landscapes. Riverine Ecosystem Management, 413–433. https://doi.org/10.1007/978-3-319-73250-3_21

Bouwman A. F., Bierkens M. F. P., Griffioen J., Hefting M. M., Middelburg J. J. & Middelkoop H. (2013). Nutrient dynamics, transfer and retention along the aquatic continuum from land to ocean: towards integration of ecological and biogeochemical models. https://doi.org/10.5194/bg-10-1-2013

Bukaveckas P. A. & Isenberg W. N. (2013). Loading, Transformation, and Retention of Nitrogen and Phosphorus in the Tidal Freshwater James River (Virginia). Estuaries and Coasts, 36(6), 1219–1236. https://doi.org/10.1007/s12237-013-9644-x

Campbell I. (2009). Chapter 1 - Introduction, Editor(s): Ian C. Campbell, In Aquatic Ecology, The Mekong, Academic Press, Pages 1-11, ISBN 9780123740267, https://doi.org/10.1016/B978-0-12-374026-7.00001-2.https://www.sciencedirect.com/science/article/pii/B9780123740267000012

Chen D., Lu J., Wang H., Shen Y. & Kimberley M. O. (2009). Seasonal variations of nitrogen and phosphorus retention in an agricultural drainage river in East China. Environmental Science and Pollution Research, 17(2), 312–320. https://doi.org/10.1007/s11356-009-0246-x

Cotrim da Cunha L., Buitenhuis E. T., Le Quéré C., Giraud X. & Ludwig W. (2007). Potential impact of changes in river nutrient supply on global ocean biogeochemistry. Global Biogeochemical Cycles, 21(4), 1–15. https://doi.org/10.1029/2006GB002718

Coupe R. H., Goolsby D. A., Battaglin W. A., Böhlke J. K., McMahon P. B. & Kendall C. (2013). Transport of nitrate in the Mississippi River in July-August 1999. Annals of Environmental Science, 7(3), 31–46.

Davidson E. A., De Araüjo A. C., Artaxo P., Balch, J. K., Brown I. F., Mercedes M. M., Coe M. T., Defries R. S., Keller M., Longo M., Munger J. W., Schroeder W., Soares-Filho B. S., Souza C. M. & Wofsy S. C. (2012). The Amazon basin in transition. Nature, 481(7381), 321–328. https://doi.org/10.1038/nature10717

de Klein J. J. M. & Koelmans A. A. (2011). Quantifying seasonal export and retention of nutrients in West European lowland rivers at catchment scale. Hydrological Processes, 25(13), 2102–2111. https://doi.org/10.1002/hyp.7964

Eisner S. Flörke M., Chamorro A. & Daggupati P. (2017). An ensemble analysis of climate change impacts on streamflow seasonality across 11 large river basins. 401–417. https://doi.org/10.1007/s10584-016-1844-5

Fischer H., Kloep F., Wilzcek S. & Pusch M. T. (2005). A river's liver - Microbial processes within the hyporheic zone of a large lowland river. Biogeochemistry, 76(2), 349–371. https://doi.org/10.1007/s10533-005-6896-y

Gani M. A., van der Kwast J., McClain M. E., Gettel M. G. & Irvine K. (2022). Classification of Geomorphic Units and Their Relevance for Nutrient Retention or Export of a Large Lowland Padma River, Bangladesh: A NDVI Based Approach. Remote Sensing, 14(6). https://doi.org/10.3390/rs14061481

Grimm N. B. & Petrone K. C. (1997). Nitrogen Fixation in a Desert Stream Ecosystem Author (s): Nancy B . Grimm and Kevin C . Petrone Published by : Springer Stable URL : http://www.jstor.org/stable/1469163 REFERENCES Linked references are available on JSTOR for this article : You may need. 37(1), 33–61.

Grizzetti B., Passy P., Billen G., Bouraoui F., Garnier J. & Lassaletta L. (2015). The role of water nitrogen retention in integrated nutrient management: Assessment in a large basin using different modelling approaches. Environmental Research Letters, 10(6), 65008. https://doi.org/10.1088/1748-9326/10/6/065008

Groffman P. M., Holland E. A., Myrold D. D., Robertson G. P. & Zou X. (1999). Denitrification. In S. P. Robertson G. P., Coleman D. C., Bledose C. S. (Ed.), Standard soil methods for long-term ecological research. pp. 272–288. Oxford University Press.

Hamilton S. K. (2010). Biogeochemical implications of climate change for tropical rivers and floodplains. Hydrobiologia, 657(1), 19–35. https://doi.org/10.1007/s10750-009-0086-1

Hauer C., Leitner P., Unfer G., Pulg U., Habersack H. & Graf W. (2018). The Role of Sediment and Sediment Dynamics in the Aquatic Environment. In Riverine Ecosystem Management (pp. 151–169). https://doi.org/10.1007/978-3-319-73250-3_8

Islam S. N. (2016). Deltaic floodplains development and wetland ecosystems management in the Ganges–Brahmaputra–Meghna Rivers Delta in Bangladesh. Sustainable Water Resources Management, 2(3), 237–256. https://doi.org/10.1007/s40899-016-0047-6

Krishna M. S., Prasad M. H. K., Rao D. B., Viswanadham R., Sarma V. V. S. S. & Reddy N. P. C. (2016). ScienceDirect Export of dissolved inorganic nutrients to the northern Indian Ocean from the Indian monsoonal rivers during discharge period. Geochimica et Cosmochimica Acta, 172, 430–443. https://doi.org/10.1016/j.gca.2015.10.013

Latrubesse E. M., Stevaux J. C. & Sinha R. (2005). Tropical rivers. Geomorphology, 70(3-4 SPEC. ISS.), 187–206. https://doi.org/10.1016/j.geomorph.2005.02.005

Loken L. C., Crawford J. T., Dornblaser M. M., Striegl R. G., Houser J. N., Turner P. A. & Stanley E. H. (2018). Limited nitrate retention capacity in the Upper Mississippi River. Environmental Research Letters, 13(7), 74030. https://doi.org/10.1088/1748-9326/aacd51

Mckee L. J., Eyre B. D. & Hossain S. (2000). Transport and retention of nitrogen and phosphorus in the sub-tropical Richmond River estuary, Australia-A budget approach. Biogeochemistry, 50, 241–278. https://link.springer.com/content/pdf/10.1023%2FA%3A1006339910533.pdf

Metcalfe I. (2003). Environmental concerns for Bangladesh. South Asia: Journal of South Asia Studies, 26(3), 423–438. https://doi.org/10.1080/0085640032000178961

Mulholland P. J. & Webster J. R. (2010). Nutrient dynamics in streams and the role of J-NABS. Journal of the North American Benthological Society, 29(1), 100–117. https://doi.org/10.1899/08-035.1

NASA Earth Observatory (2019). Available online: https://earthobservatory.nasa.gov/world-of-change/PadmaRiver (accessed on 27 March 2019).

Natho S., Venohr M., Henle K. & Schulz-Zunkel C. (2013). Modelling nitrogen retention in floodplains with different degrees of degradation for three large rivers in Germany. Journal of Environmental Management, 122, 47–55. https://doi.org/10.1016/J.JENVMAN.2013.02.049

Nicole A. (2003). The Nile: Moving Beyond Cooperation (SC-2003/WS/61). UNESCO / IHP / WWAP | Paris, France.

Nowreen S., Taylor R. G., Shamsudduha M., Salehin M., Zahid A. & Ahmed K. M. (2020). Groundwater recharge processes in an Asian mega-delta: hydrometric evidence from Bangladesh. Hydrogeology Journal, 28(8), 2917–2932. https://doi.org/10.1007/s10040-020-02238-3

OCHA (2023). https://www.unocha.org/our-work/humanitarian-financing/anticipatory-action/summary-bangladesh-pilot. Accessed on 16 February 2023.

Pan L., Dai J., Wu Z., Wan Z., Zhang Z., Han J., Li Z., Xie X. & Xu B. (2020). Spatio-Temporal Dynamics of Riverine Nitrogen and Phosphorus at Different Catchment Scales in Huixian Karst Wetland, Southwest China. Water, 12(10), 2924. https://doi.org/10.3390/w12102924

Ritz S. & Fischer H. (2019). A Mass Balance of Nitrogen in a Large Lowland River (Elbe, Germany). Water, 11(11), 2383. https://doi.org/10.3390/w11112383

Sarker M. H. & Thorne C. R (2006). in Braided Rivers: Process, Deposits, Ecology and Management (eds Sambrook Smith, G. H. et al.) 289–310 (Blackwell, Oxford).

Sattar M. A., Kroeze C. & Strokal M. (2014). The increasing impact of food production on nutrient export by rivers to the Bay of Bengal 1970-2050. Marine Pollution Bulletin, 80(1–2), 168–178. https://doi.org/10.1016/j.marpolbul.2014.01.017

Seitzinger S. P., Styles R. V., Boyer E. W., Alexander R. B., Billen G., Howarth R. W., Mayer B. & Van Breemen N. (2002). Nitrogen retention in rivers: Model development and application to watersheds in the northeastern U.S.A. Biogeochemistry, 57–58, 199–237. https://doi.org/10.1023/A:1015745629794

Shaika N. A., Khan S. & Sultana S. (2022). Harmful algal blooms in the coastal waters of Bangladesh: an overview. J Aquac Mar Biol., 11(3):105-111. doi: 10.15406/jamb.2022.11.00344

Subramanian V. (2008). Nitrogen transport by rivers of south Asia. Current Science, 94(11), 1413–1418.

Syvitski J. P. M., Cohen S., Kettner A. J. & Brakenridge G. R. (2014). How important and different are tropical rivers? - An overview. Geomorphology, 227, 5–17. https://doi.org/10.1016/j.geomorph.2014.02.029

Tanaka Y., Minggat E. & Roseli W. (2021). The impact of tropical land-use change on downstream riverine and estuarine water properties and biogeochemical cycles: a review. Ecological Processes, 10(1). https://doi.org/10.1186/s13717-021-00315-3

Wang A., Yang D. & Tang L. (2020). Spatiotemporal variation in nitrogen loads and their impacts on river water quality in the upper Yangtze River basin. Journal of Hydrology, 590:125487, ISSN 0022-1694. https://doi.org/10.1016/j.jhydrol.2020.125487.

Wang J., Xia X., Liu S., Zhang S., Zhang L., Jiang C., Zhang Z., Xin Y., Chen X., Huang J., Bao J., McDowell W. H., Michalski G., Yang Z. & Xia J. (2022). The Dominant Role of the Water Column in Nitrogen Removal and N2O Emissions in Large Rivers. Geophysical Research Letters, 49(12), 1–12. https://doi.org/10.1029/2022GL098955

Weigelhofer G., Hein T. & Bondar-Kunze E. (2018). Phosphorus and Nitrogen Dynamics in Riverine Systems: Human Impacts and Management Options. In Riverine Ecosystem Management (pp. 187–202). Springer International Publishing. https://doi.org/10.1007/978-3-319-73250-3_10

Winemiller K. O., McIntyre P. B., Castello L., Fluet-Chouinard E., Giarrizzo T., Nam S., Baird I. G., Darwall W., Lujan N. K., Harrison I., Stiassny M. L. J., Silvano R. A. M., Fitzgerald D. B., Pelicice F. M., Agostinho A. A., Gomes L. C., Albert J. S., Baran E., Petrere M., … & Sáenz L. (2016). Balancing hydropower and biodiversity in the Amazon, Congo, and Mekong. Science, 351(6269): 128–129. https://doi.org/10.1126/science.aac7082

Wollheim W. M., Vörösmarty C. J., Peterson B. J., Seitzinger S. P. & Hopkinson C. S. (2006). Relationship between river size and nutrient removal. Geophysical Research Letters, 33(6). https://doi.org/10.1029/2006GL025845

Zinia N.J. & Kroeze C. (2015). Future trends in urbanization and coastal water pollution in the Bay of Bengal: the lived experience. Environment, Development and Sustainability, 17: 531–546.https://doi.org/10.1007/s10668-014-9558-1

Chapter 5

DISCUSSIONS AND CONCLUSION

1. Synthesis of the main findings

The research presented in this thesis focuses on nitrogen retention in distinct geomorphic units of the large lowland Padma River in Bangladesh. The first chapter of the thesis discusses the background of the study, the importance of nitrogen dynamics and retention in large lowland rivers, and how these are influenced by the nature of geomorphic units (GUs). The following three chapters of research results identify key hydromorphological and nutrient retention processes in the river.

The second chapter describes the geomorphology of the river and the identification and classification of geomorphic units using NDVI of Sentinel-2 data and validation with field observation, mapping nutrient retention/export relevant geomorphic units (NREGUs). The GUs and NREGUs change in response to river discharge.

The third chapter focused on the spatiotemporal dynamics of the potential denitrification rate (PDR) as a retention process. Linear mixed models were developed using measured PDR in one season to predict PDR in other seasons. The model estimated the spatial distribution of PDR for every GU in post-monsoon, dry/winter and pre-monsoon; this showed that the number and surface area of GUs could impact PDR in the study area seasonally.

The fourth chapter was constructed based on the mass balance measurement in the study reach to show monthly total nitrogen (TN) retention. Besides mass balance, this chapter describes different retention processes of sedimentation, nitrogen loss due to water retention, net PDR (denitrification − N_2 fixation) in the water column, and PDR in submerged GUs. A comparison of estimated retention through the processes with mass balance measurement showed that the difference could be explained by other retention processes in the river reach. Finally, the chapter discusses the importance of river discharge, geomorphology and water retention as influencing factors for TN retention.

All the thesis chapters mainly focus on river nitrogen retention, including river geomorphology. The key findings from the thesis chapters 2, 3 and 4 and their relevance to river management, policy and society are presented in Table 5. 1.

Table 5. 1 Summary of the key findings of different chapters (2, 3 and 4) and relevance with management, policy and society.

Chapter	Key findings	Relevance with the management, policy and society
Two	(i) Eight geomorphic units are present in the study reach of the Padma River, which shows seasonal variation.	(i) The present NDVI-based approach can be implemented for other rivers in the country
	(ii) Mapping nutrient retention and export relevant GUs (NREGUs) showed river discharge can alter the	(ii) Using the present approach, identifying NREGUs might help detect nutrient retention potential

Chapter	Key findings	Relevance with the management, policy and society
	number and types of NREGUs. (iii) The channel bar types can be distinguished based on the shape index where NDVI is ineffective. Bar perimeter is the primary responsible factor, and this might help estimate the spatiotemporal variation of nutrient retention processes.	areas, which can be used to assess ecological conditions regarding nutrient pollution. (iii) Importance of shape indexes for the analysis of river geomorphology. Using this index, the potential impact of GUs on the nitrogen retention process can be identified, showing the effects of implementing dredging works in the rivers. Thus, eco-friendly river management programmes can be implemented by enforcing sustainable management policies.
Three	(i) Estimating denitrification in the emerged GUs of large rivers as a retention process. (ii) Modelling spatiotemporal denitrification rate in the GUs using remote sensing. (iii) Importance of surface area and number of GUs in regulation denitrification.	(i) Indication of nitrogen pollution in the rivers and the role of GUs in removing nitrogen permanently from the systems. (ii) Establish a new tool for the estimation of denitrification, which is helpful for river nitrogen retention monitoring and can be used to implement restoration programmes. (iii) Sustainable dredging can be implemented considering the dynamics of GUs. The Policies lacking effective measures for dredging activities may result in environmental degradation.
Four	(i) Both, mass balance measurement and estimation through retention processes showed that nitrogen retention occurs throughout year in the study reach. (ii) Estimation of nitrogen retention through different retention processes showed that nitrogen loss due to water retention is the most important process for retention, followed by	(i) Provide evidence that the study reach is an essential site for nitrogen retention. (ii) Suggest implementation of river management and policy for reducing coastal pollution where attention should be given. (iii) The present concept of retention estimation through modelling can be

Chapter	Key findings	Relevance with the management, policy and society
	sedimentation and denitrification. (iii) The difference between the mass balance measurement and estimation through different retention processes was negligible. (iv) Variations in river discharge, flooding events, and activities in GUs can impact nitrogen retention and export in the study reach.	implemented in other rivers at more or less the same conditions. (iv) To promote ecosystem services from the Padma River, local authorities should focus on the research findings, and national policy should be amended, focusing on the importance of GUs to manage such kinds of rivers in the country.

2. Role of river geomorphology on nitrogen retention as an indicator of water quality in large rivers

River geomorphology and nitrogen retention are interconnected factors that play a crucial role for water quality in large rivers. Understanding the relationship between geomorphology and nitrogen retention is important because excessive nitrogen can lead to water pollution and ecosystem degradation. Geomorphology, which includes the shape, size, and structure of GUs influence nitrogen retention. To date, very few studies have investigated nitrogen retention in GUs (Lin et al., 2016; Wagenschein and Rode, 2008). Chapters 3 and 4 of this thesis showed that nitrogen retention can vary spatially and temporally in large rivers such as the Padma, building on the work by Wang et al. (2020). The retention potential of GUs in a river channel can change with the seasons and human pressures. Nitrogen retention, therefore, is an important ecosystem service in regulating nitrogen mobility. Retention can enhance nutrient pollution downstream, with consequences for coastal water bodies, eutrophication, and the manifestation of algal blooms and hypoxia.

In Bangladesh, large river networks are crucial in shaping the landscape and associated ecosystems. The rivers in the country are primarily fed by silt and sand from water flowing from the Himalayas. The dynamic nature of these rivers contributes to the continuously changing geomorphology of the delta region. The deposition of sediments and erosion along the riverbanks are common geomorphic processes in this study reach, leading to the formation of river islands (chars), bars and the reshaping of river channels. In monsoons, high flow creates flooding, and less flow in the dry season initiates water scarcity resulting in less active channels for navigation. Both types of features can alter river geomorphology and water quality.

Declining water resources and the contamination of surface and groundwaters is a growing concern in Bangladesh. Sewage and industrial waste discharge into water bodies deteriorates water quality. Bangladesh is a densely populated country with rapid economic growth, with increased industrialisation and agricultural intensification. The Padma River, situated in the

world's most flood-prone area, geomorphology and water quality are intricately linked with the country's geography, climate change, agricultural practices, and other human activities. The river is crucial for water supply for irrigation and domestic and industrial consumption but, at the same time, is responsible for heavy losses of life and property from floods (Mirza et al., 2003). In addition, the river transports nutrients to the Bay of Bengal in conjunction with other coastal rivers and estuaries. Modelling studies have indicated that nitrogen export to the Bay of Bengal is increasing and will continue to increase in the future (Pedde et al., 2017). One of the reasons for that is the increasing nitrogen loads in rivers draining into the Bay of Bengal (Sattar et al., 2014). This thesis has shown that seasonal changing patterns within the river's GUs, can significantly influence nitrogen retention and export. Monitoring geomorphological change and water quality deterioration in the river can identify important zones for both nitrogen retention and export. Such knowledge can help local river management. For instance, agriculture management; irrigation plan, *char* (bar or island) development and human settlement.

3. The overall role of GUs for nitrogen retention in the Padma River

In the 3rd chapter of this thesis, the contribution of terrestrial GUs in denitrification (PDR) as a retention process was discussed. In the 4th chapter, the contribution of submerged GUs and river channels for denitrification was highlighted. If PDR in the GUs and water column of the study reach is considered, then out of the total, 46%, 60%, 80%, and 80% of PDR occurred in the GUs of the river during monsoon, post-monsoon, dry/winter and pre-monsoon, respectively (Appendix 11). It is evident that the GUs play a significant role in removing nitrogen by denitrification (Chapters 3 and 4). Comparatively higher PDR was found in dry/winter (Robi), and pre-monsoon (Kharif-I) due to fertiliser application, as discussed in Chapter 4, but this amount contributes about 50% and 40% of the PDR, respectively. PDR was estimated to contribute about 11% of the total retention. However, most of retention occurred during monsoon due to water retention and sedimentation. Water retention resulted in the study reach due to the difference between inflow and outflow discharges and might be unique in other tropical rivers but quite common in floodplain rivers. Denitrification also occurred in the portion of water retention, which was not considered. In that sense, the percentage of PDR will be higher than that calculated, and the role of GUs will be more significant than shown in the present study. On the other hand, during monsoons, higher water retention was due to the presence of in-channel GUs, and it was assumed that the retention might be less if there were no exposed GUs. In that case, less water might overflow through the river banks.

4. The impact of river engineering programmes on nitrogen retention

River engineering, including dredging, can impact the hydroecology of rivers. This includes alterations in water flow velocity, sedimentation, channel bed modification and habitat destruction (Rahman and Yunus, 2016; Okoyen et al., 2020). These changes can have wide-ranging effects on the river ecology and nitrogen cycling. In addition, large-scale channel alterations through dredging can affect flood dynamics in lowland rivers (Saad and Habib, 2021) and can result in the formation of dredge spoil mounds, which can enrich nitrogen

concentration (Mossa and Chen, 2021). Dredging in large rivers can impact bridge foundations and abutments if the choice of dredging locations is not guided correctly. This can make these structures vulnerable to scour and erosion, compromising their stability (Abam et al., 2023). Therefore, effective management of dredging problems requires enforcing relevant environmental laws and monitoring, as shown in the Niger Delta (Okoyen et al., 2020). Moreover, some indirect effects of dredging have been observed. For instance, dredging-induced sound can aggravate aquatic life, and changes in the ratio of freshwater to salt in coastal water can adversely affect marine life (Suedel et al., 2019; Wenger et al., 2017). All these activities can alter the overall ecological quality, which may indirectly affect nitrogen retention in rivers.

It is evident that river dredging affects geomorphology. In tropical regions, in-channel GUs are influential in restructuring river channels, and their depth and flow path, conditions due to rainfall and seasonal flooding. Changes in rainfall patterns and increasing frequency of floods and cyclones from a changing climate affect agriculture, water availability, and water quality. The large lowland rivers of Bangladesh follow the same pattern. The direct and indirect impact of river engineering programmes, e.g. sediment extraction for navigation, channelisation for maintaining river flow and preventing river bank erosion, has been shown by different researchers (Yuan and Zhu, 2015; Chen, 2021). Most of the time, these river management activities are considered the preferred solution to mitigate the negative effects of river modifications. Few studies have been conducted on large rivers to show the impact on river ecosystems of the above river engineering programs (Rahman et al., 2021; Rahman and Ali, 2022). In the case of Padma River, it was assumed that these kinds of activities would impact the river ecosystems by mainly removing in-channel GUs, with the reduction in nitrogen retention capacity affecting river health.

5. The dilemma in implementing present research for sustainable river management

Despite several adverse impacts of dredging, river engineering programmes consider dredging as a specific activity. It depends on the river's structure, sediment quality, dredging technique, the degree to which the floodplain is connected, and the nature of the river flow. The government of Bangladesh has taken the initiative for a 50-year plan to restore the navigability of the major rivers of the country, including the Padma River. Under this plan, different river training programmes, including sediment removal through capital dredging, will be implemented. The Padma River, whose width ranges from 5-20 km, will be reduced to 5 km to recover land for agricultural activities or human settlement (Sultana et al., 2017). The research presented in this thesis shows that removing all the in-channel GUs might not be an ideal plan, or the results of implementing such a plan might not be effective. There are several arguments for this view:(i) In-channel GUs in the Padma River are used for multiple purposes, e.g. human settlements, cultivation, grazing land and touristic activities, although seasonal flooding makes these activities vulnerable. Removing GUs through dredging can introduce the loss of all the above activities;

(ii) Seasonal flooding makes all GUs the source of nitrogen; due to this denitrification occurs other than monsoon in terrestrial GUs, so if all GUs are removed, all the nutrients will mostly be transported downstream, with increased risk of eutrophication, the consequence formation of harmful algal blooms and hypoxia in the coastal areas of the country;
(iii) Appearance of in-channel GUs responsible for reducing river flow and increasing water retention time. The thesis has shown that the maximum surface area of terrestrial GUs observed in the dry/winter season enhanced the interaction between the edge of GUs and the water column, which altered the retention scenarios. It is expected that this phenomenon strengthens the capacity of nitrogen retention. Due to this, the rate of PDR was higher in pre-monsoon. So, removing GUs from the river can affect nutrient retention;
(iv) Water retention occurred in the river reach throughout the year, leading to a significant portion of nitrogen retention. In the study reach, due to GUs, water overflows through the river banks mainly in monsoon. So, removing all the GUs will result in less water retention, so that less nitrogen will be retained;
(v) Sedimentation is another important retention process in the studied reach of the river. GUs can slow down water flow, and promoting sedimentation in the reach, and less transport to the downstream part.

Despite the considerations presented above, there might be several reasons for implementing capital dredging. The most important one is that removing GUs can increase the capacity of water retention of the river itself without overflowing water through banks, which can reduce flooding and bank erosion. In addition, river flow will be undisturbed in the channel due to the absence of GUs and interaction with water. Removing GUs will also increase water depth, which can solve the navigation problem throughout the year.

6. Existing gaps in river research and applications in Bangladesh

Many studies have addressed river morphology, changing patterns, bank erosion and accretion in Bangladesh (Alam et al., 2023; Islam and Nahar, 2023). The impact of flooding and river discharge on morphology has been shown by Rahman et al. (2023) and Giri et al. (2021). On the other hand, a large number of research articles are published about the water quality, nutrient loads, pollution conditions and ecological status of the rivers in Bangladesh (Hasan et al., 2023; Gani et al., 2023; Kabir et al., 2021; Haque et al., 2019; Bhuiyan et al., 2018; Zerin et al., 2017). Humans and the surrounding environment are the main initiators of pollution and water quality deterioration of the rivers. However, a central gap exists between research and the application of river management programmes. As a densely populated country, management and investment have always been going forward to protect human life and properties and implementing small management works. Thus, focusing on ecological issues and river ecosystem services has come after. In addition, most of the research investigations focus on identifying problems and monitoring rather than implementing actions. Due to the lack of an integrated approach, it has been impossible for the policymakers or respective authorities to apply protected measures sustainably to solve the problems identified by researchers. Thus, sustainable river management programmes in Bangladesh have not been successful so far. In addition, the river management programmes

are directly linked with coastal management programmes. However, few efforts have been made to connect river restoration programs with coastal conservation activities. A comprehensive approach to river restoration or management in terms of geomorphological set-up and planning, scientific management of GUs in large rivers, transportation and discharge of nutrients, including nitrogen, must be adopted rapidly to succeed in river management.

7. Recommendations and policy implementations for sustainable river management

The problem of river water pollution, flooding and bank erosion is not limited to Bangladesh. Still, it concerns other countries and is a part of the global crisis that partly occurs due to climate change and requires combined action to mitigate this. The source of the Padma River is two transboundary rivers, the Ganges and the Brahmaputra, which also suffer the same problem after their origin in India and partly in China. The main effects are in the lower part that flows through Bangladesh. The river flow path alteration, and human-induced activities are responsible for this. The same scenario can be found in other transboundary rivers in the subtropical and tropical regions. Examples include the Indus River in India and Pakistan; the Mekong River in China, Myanmar, Thailand, Laos, Cambodia and Vietnam; and the Zambezi River in Angola, Namibia, Botswana, Zimbabwe and Mozambique. All these rivers are at risk of a consistent increase in flooding in the near future due to climate change (Hirabayashi, 2008; Dankers et al., 2014; Eccles et al., 2019).

Due to the combined effect of climate and land use change and increasing pollution pressures, the geomorphology and ecology of large rivers in the tropics have changed significantly (Gabiri et al., 2020; Tanaka et al., 2021; Iqbal et al., 2022). Even flooding and extreme events accelerate this change dramatically and rapidly, affecting river erosion and deposition processes. River engineering programmes such as constructing embarkment, dams, and channelisation are frequent scenarios in these rivers. In this thesis it is shown that changes in the river geomorphology can affect nitrogen retention and export capacity of the river, which can have adverse effects on the estuary and coast in the long run. Preventing or implementing river management activities is not a sustainable measure. Present research can address this issue. For instance, removing all the GUs from the river channel or keeping them as they appear in the channel is not the solution; even the local people face enormous challenges due to extreme events. Instead, before implementing management programmes, it should be addressed where and how different river restoration activities should be conducted. In addition, the impact of implementing the management programmes should be considered. The existing policies for sustainable management of rivers in tropical countries typically involve integrated management mechanisms at the river basin level. Key aspects of these policies include (i) integrated river basin management; (ii) cooperation between stakeholders, (iii) equitable benefits, (iv) protection between water resources and (v) recognition of water crisis (Marques et al., 2019; Prodhan et al., 2021; Amin et al., 2023; Hadi, 2019). The policies aim to balance economic development, social needs, and environmental conservation in the context of tropical river management. These are designed to address the unique

challenges and opportunities presented by rivers in tropical regions. International river management efforts covering over 260 basins have demonstrated success when cooperation and collaboration are effective (Bernauer, 2002). Policies for transboundary river water sharing exhibit varied outcomes; for instance, the Nile is a success, while the Teesta and Euphrates–Tigris are considered failures (Hossen et al., 2023). Acknowledging the increasing climate and human-introduced pressures, a comprehensive review of river management policies may be essential for sustainable development.

The Government of Bangladesh has approved the Bangladesh Delta Plan (BDP) 2100, aiming to achieve a safe, climate change and natural disaster-resilient prosperous delta. Among the most priority areas of the BDP, flood control, river erosion, and river management, including dredging, training, and navigability, will likely absorb 35% of total investments. But there will be an ecological impact of dredging if it is not implemented in a sustainable way (Bashir, 2020). Dredging is necessary to maintain navigation river flows and prevent bank erosion, but not as the government plans to do, such as capital dredging. Instead, dredging can be implemented partly considering the position, shape and mechanisms of biogeochemical processes of GUs and impacts on river health. The present research shows that the degree of effect on nitrogen retention is variable according to the types and positions of GUs. For instance, the retention capacity as denitrification for islands and bars differs. Even in the bars, denitrification might be variable according to the shape (transverse and longitudinal bars) and position (side and mid bars) of the GUs, which have been discussed in Chapter 2, the potential importance of shape indexes for nutrient retention. So, planned sediment removal activities in the rivers might be helpful for the sustainable management of water resources.

The National Water Policy (NWP, 1999) of Bangladesh ensures the protection and preservation of natural environments and water resources of the country for sustainable development. NWP emphasises water resource management actions to avoid or minimise environmental damage. NWP also states that “dredging and other suitable measures would be undertaken, wherever needed, to maintain the navigational capability of designated waterways”. To support this, the Bangladesh Water Act (BWA, 2013) has been formulated, which also ensures the (i) best use of water resources and (ii) control of uncontrolled/unaccounted abstraction, diversion, and pollution. In addition, one of the key measures of the BWA is water resource protection or pollution control and maintaining water quality standards.

Under the Ministry of Water Resources, different regulatory organisations, e.g. Bangladesh Water Development Board (BWDB), Water Resources Planning Organization (WARPO), River Research Institute (RRI), and Joint Rivers Commission (JRC) institutes are working for the betterment of river management programs and supervise the noted activities according to various policies and acts on water. However, the guidelines are focused on river engineering programs to reduce the loss of human life and property. But, more than pollution prevention and water quality measures are required. So, there is a considerable knowledge gap in implementing dredging projects considering river health. Although some initiatives have been started (Mongla Port Authority, 2017). So, now it is high time to address this issue in

the water policy for the sustainable management of the rivers in the country and share this knowledge with other stakeholders working on this issue.

8. Conclusion

Padma River in Bangladesh faces numerous natural and human-derived problems, which affects its geomorphology and nitrogen retention. This thesis concludes that changes in geomorphic units in the river can impact nitrogen retention capacity and alter nitrogen export scenarios to the coastal areas. Thus, removing these GUs is not a scientific solution for river management. Although, this type of river is always accountable for flooding, bank erosion and loss of human resources. All these factors are interlined with river health and can cause a significant loss of ecological and economic resources for extended periods. It can be assumed small and planned dredging works can impact river geomorphology, thus nitrogen retention processes differently, thus having less impact on the river ecosystems and health. So, sustainable dredging works can be done for river management considering the minimum influence on river geomorphology and less effect on nitrogen retention and export mechanisms. It is also advisable to ensure the estimation of nitrogen retention as an indicator of water quality, which is considered a priority issue for sustainable development. The thesis focuses on the Padma River due to its highly diversified nature in terms of geomorphology, hydrology and biogeochemistry. Thus, the results of the present work can be implemented in other geomorphologically complex floodplain river systems in the sub-tropical and tropical regions.

9. References

Abam T., Giadom F. & Iduma R. (2023). Impact of Dredging on Coastal Infrastructure: Case Studies from Okrika and Port Harcourt, Niger Delta. Journal of Geoscience and Environment Protection, 11, 349-362. doi: 10.4236/gep.2023.115021

Alam S., Hasan F., Debnath M. & Rahman A. (2023). Morphology and land use change analysis of lower Padma River floodplain of Bangladesh. Environ. Monit. Assess., 195, 886. https://doi-org.unesco-ihe.idm.oclc.org/10.1007/s10661-023-11461-w

Amin F., Dar M. A. & Gupta A. K. (2023). Sustainability Through Integrated Resilience and Risk Management: Rivers and Disasters in Changing Climate. In: Pandey, M., Gupta, A.K., Oliveto, G. (eds) River, Sediment and Hydrological Extremes: Causes, Impacts and Management. Disaster Resilience and Green Growth. Springer, Singapore. https://doi.org/10.1007/978-981-99-4811-6_25

Bashir M. O. I. (2020). Sustainable River Management in Bangladesh through Capital Dredging: Mitigation of Environmental Impacts through Project Management & Operational Best Practices. BMJ Vol 6 (1), 79-98. ISSN 2519-5972\

Bernauer T. (2002). Explaining success and failure in international river management. Aquat. sci. 64, 1–19. https://doi.org/10.1007/s00027-002-8050-4

Bhuyan M. S., Bakar M. A., Sharif A. S. M., Hasan M. & Islam M. S. (2018). Water Quality Assessment Using Water Quality Indicators and Multivariate Analyses of the Old Brahmaputra River. Pollution, 4(3), 481-493. doi: 10.22059/poll.2018.246865.350

BWA (2013). Bangladesh Water Act. Legislative and Parliamentary Affairs Division, Ministry of Law, Justice and Parliamentary Affairs Government of the People's Republic of Bangladesh, S.R.O.No.348-Law/201. pp 24

Dankers R., Arnell N. W., Clark D. B., Falloon P. D., Fekete B. M., Gosling S. N., ... & Wisser D. (2014). First look at changes in flood hazard in the Inter-Sectoral Impact Model Intercomparison Project ensemble. Proceedings of the National Academy of Sciences, 111(9), 3257-3261.

Eccles R., Zhang H. & Hamilton D. (2019). A review of the effects of climate change on riverine flooding in subtropical and tropical regions. Journal of Water and Climate Change, 10 (4), 687–707. https://doi.org/10.2166/wcc.2019.175

Gabiri G., Diekkrüger B., Näschen K., Leemhuis C., van der Linden R., Majaliwa J-G. M. & Obando J. A. (2020). Impact of Climate and Land Use/Land Cover Change on the Water Resources of a Tropical Inland Valley Catchment in Uganda, East Africa. Climate, 8(7), 83. https://doi.org/10.3390/cli8070083

Gani M. A., Sajib A. M., Siddik M. A. & Moniruzzaman M. (2023). Assessing the impact of land use and land cover on river water quality using water quality index and remote sensing techniques. Environ. Monit. Assess., 195(4), 449. doi: 10.1007/s10661-023-10989-1. PMID: 36882593.

Giri S., Thompson A., Donchyts G., Oberhagemann K., Mosselman E. & Alam J. (2021). Stabilization of the Lower Jamuna River in Bangladesh—Hydraulic and Morphological Assessment. Geosciences, 11, 389. https://doi.org/10.3390/geosciences11090389

Hadi T. (2019). An Analysis of Water Policies and Strategies of Bangladesh in the Context of Climate Change. Asia-Pacific Journal of Rural Development, 29 (1), 111-123. https://doi.org/10.1177/1018529119860958

Haque M. A., Jewel M A S. & Sultana M. P (2019). Assessment of physicochemical and bacteriological parameters in surface water of Padma River, Bangladesh. Appl. Water Sci., 9, 10. https://doi.org/10.1007/s13201-018-0885-5

Hasan M. M., Gani M. A., Alfasane M. A., Ayesha M. & Nahar K. (2023) Benthic diatom communities and a comparative seasonal-based ecological quality assessment of a transboundary river in Bangladesh. PLoS One, 18(10), e0291751. https://doi.org/10.1371/journal.pone.0291751

Hirabayashi Y., Kanae S., Emori S., Oki T. & Kimoto M. (2008). Global projections of changing risks of floods and droughtsin a changing climate. Hydrological Sciences Journal 53 (4), 754–772.https://doi:10.1623/hysj.53.4.754

Hossain S. & Chowdhury M. A. I. (2019). Hydro-morphology monitoring, water resources development and challenges for Turag Riverat Dhaka in Bangladesh. Climate Change, 5(17), 34-40.

Hossen M. A., Connor J., Ahammed F. (2023). How to Resolve Transboundary River Water Sharing Disputes. Water, 15(14), 2630. https://doi.org/10.3390/w15142630

Iqbal M., Wen J., Masood M., Masood M. U. & Adnan M. (2022). Impacts of Climate and Land-Use Changes on Hydrological Processes of the Source Region of Yellow River, China. Sustainability, 14(22), 14908. https://doi.org/10.3390/su142214908

Islam M. S. & Nahar N. (2023). Assessment of Flood Risk in the Brahmaputra-Jamuna Floodplain, Bangladesh. In: Islam A., et al. Floods in the Ganga–Brahmaputra–Meghna Delta. Springer Geography. Springer, Cham. https://doi-org.unesco-ihe.idm.oclc.org/10.1007/978-3-031-21086-0_17

Kabir M. H., Tusher T. R., Hossain M. S.,Islam M. S., Shammi R. S., Kormoker T., Proshad R. & Islam M. (2021). Evaluation of spatio-temporal variations in water quality and suitability of an ecologically critical urban river employing water quality index and multivariate statistical approaches: A study on Shitalakhya river, Bangladesh. Human and Ecological Risk Assessment: An International Journal, 27 (5), 1388-1415. doi: 10.1080/10807039.2020.1848415

Lin L., Davis L., Cohen S., Chapman E. & Edmonds J. W. (2016). The influence of geomorphic unit spatial distribution on nitrogen retention and removal in a large river. Ecological Modelling, 336, 26–35. https://doi.org/10.1016/j.ecolmodel.2016.05.01

Marques É. T., Gunkel G. & Sobral M. C. (2019). Management of Tropical River Basins and Reservoirs under Water Stress: Experiences from Northeast Brazil. Environments, 6, 62. https://doi.org/10.3390/environments6060062

Mirza M., Warwick R. A. & Erickso N. J. (2003). The implications of climate change on floods of the Ganges, Brahmaputra and Meghna rivers in Bangladesh. Climatic Change 57:287–318. https://doi.10.1023/A: 1022825915791

Mongla Port Authority (2017). Report on the "Environmental Impact Assessment (EIA) of the Proposed Dredging Project at the Outer Bar area of Pussur Channel". IWM. pp 90

Mossa J. & Chen Y. (2021). Geomorphic insights from eroding dredge spoil mounds impacting channel morphology. Geomorphology, 376, 107571, ISSN 0169-555X. https://doi.org/10.1016/j.geomorph.2020.107571.

NWP (1999). National Water Policy. The Ministry of Water Resources, Government of the Peoples Republic of Bangladesh, Dhaka, Bangladesh. pp 22

Okoyen E., Raimi M. O., Omidiji A. O. & Ebuete A. W. (2020). Governing the Environmental Impact of Dredging: Consequences for Marine Biodiversity in the Niger Delta Region of Nigeria. Insights Mining Science and Technology, 2(3), 555586. doi: 10.19080/IMST.2020.02.555586.

Pedde S., Kroeze C., Mayorga E. & Seitzinger S. P. (2017). Modeling sources of nutrients in rivers draining into the Bay of Bengal—a scenario analysis. Reg Environ Change, **17**, 2495–2506. https://doi.org/10.1007/s10113-017-1176-7

Pradhan N. S., Das P. J., Gupta N. & Shrestha A. B. (2021). Sustainable Management Options for Healthy Rivers in South Asia: The Case of Brahmaputra. Sustainability, 13, 1087. https://doi.org/10.3390/su13031087

Rahman A. & Yunus A. (2016). Study on hydrodynamic response of Gorai river to dredging using delft 3D. In: Proceedings of 3rd International Conference on Advances in Civil Engineering, ICACE, Nashik, India, pp. 21–23.

Rahman M. & Ali M. S. (2022). Morphological response of the Pussur River, Bangladesh to modern-day dredging: Implications for navigability, Journal of Asian Earth Sciences: X, 7:100088, ISSN 2590-0560. https://doi.org/10.1016/j.jaesx.2022.100088.

Rahman M. M., Hasan M. S., Eusufzai M. K. & Rahman M. M. (2021). Impacts of Dredging on Fluvial Geomorphology in the Jamuna River, Bangladesh. Journal of Geoscience and Environment Protection, 9, 1-20. doi: 10.4236/gep.2021.96001.

Rahman M. R., Sweet S. A. & Islam A. H. M. H. (2023). Flood Dynamics, River Erosion, and Vulnerability in the Catchment of Dharla and Dudhkumar Rivers in Bangladesh. In: Islam, A., et al. Floods in the Ganga–Brahmaputra–Meghna Delta. Springer Geography. Springer, Cham. https://doi-org.unesco-ihe.idm.oclc.org/10.1007/978-3-031-21086-0_5

Saad H. A. & Habib E. H. (2021). Assessment of Riverine Dredging Impact on Flooding in Low-Gradient Coastal Rivers Using a Hybrid 1D/2D Hydrodynamic Model. Frontiers in Water, 3, ISSN=2624-9375. doi:10.3389/frwa.2021.628829

Sattar M. A., Kroeze C. & Strokal M. (2014). The increasing impact of food production on nutrient export by rivers to the Bay of Bengal 1970–2050. Mar. Pollut. Bull., 80 (1), 168-178.

Suedel B. C., McQueen A. D., Wilkens J. L. & Fields M. P. (2019). Evaluating Effects of Dredging-Induced Underwater Sound on Aquatic Species: A Literature Review. ERDC/EL T R-19-18.

Sultana P., Khondker M. R. H., Uddin M. M., Uddin M. R. & Hossain M. A. (2017). Dredging and land reclamation in Bangladesh perspective: A state-of-the-art overview. In Proceedings of the 1st International Conference on Mechanical Engineering and Applied Science (ICMEAS), MIST, Dhaka. 0–4.

Tanaka Y., Minggat E. & Roseli W. (2021). The impact of tropical land-use change on downstream riverine and estuarine water properties and biogeochemical cycles: a review. Ecol Process, 10, 40. https://doi.org/10.1186/s13717-021-00315-3

Wagenschein D. & Rode M. (2008). Modelling the impact of river morphology on nitrogen retention—A case study of the Weisse Elster River (Germany). Ecological Modelling, 211, 1–2, ISSN 0304-3800. https://doi.org/10.1016/j.ecolmodel.2007.09.009

Wang A., Yang D. & Tang L. (2020). Spatiotemporal variation in nitrogen loads and their impacts on river water quality in the upper Yangtze River basin. Journal of Hydrology, 590, 125487, ISSN 0022-1694. https://doi.org/10.1016/j.jhydrol.2020.125487

Weng C. N. (2005). Sustainable management of rivers in Malaysia: Involving all stakeholders. International Journal of River Basin Management, 3(3), 147-162. doi: 10.1080/15715124.2005.9635254

Wenger A. S., Harvey E., Wilson S., et al. (2017). A critical analysis of the direct effects of dredging on fish. Fish and Fisheries, 18, 967–985. https://doi.org/10.1111/faf.12218

Yuan R. & Zhu J. (2015). The effects of dredging on tidal range and saltwater intrusion in the Pearl River estuary. Journal of Coastal Research, 31 (6), 1357–1362.

Zerin L., Gani M. A. & Khondker M. (2017). Comparative water quality assessment of the river Buriganga near Dhaka metropolis. Bangladesh. Bangladesh Journal of Botany, 46(2), 589.

APPENDIXES

Appendix 1. Structure of linear mixed models (LMMs)

Model	Model description	Equation
F-0	Linear covariance model	$Y_{ij}=\alpha+\alpha_l+\beta 1_j X1_{ij}+\beta_j 2X2_{ij}+\varepsilon_{ij}$
F-1, FS-1 and S-1	Generalized least-square model	$Y_{ij}=\alpha+\alpha_l+\beta 1_j X1_{ij}+\beta 2_j X2_{ij}+\varepsilon_{ij}$ and $\varepsilon_{ij}\sim N(0,\sigma^2)$
F-2, FS-2 and S-2	Random intercept model	$Y_{ij}=\alpha+b_j+\beta 1_j X1_{ij}+\beta 2_j X2_{ij}+\varepsilon_{ij}$ $b_j\sim(0,\sigma^2)$ and $\varepsilon_{ij}\sim N(0,\sigma^2)$
F-3, FS-3 and S-3	Generalised least-square model specifying the variance structure	$Y_{ij}=\alpha+\beta 1X1_i+\beta 2X2_i+\varepsilon_{ij}$ $\varepsilon_{ij}\sim N(0,\sigma^2)$; $Var(Y_{ij})=Var(\varepsilon_{ij})=\sigma^2$ $Cov(Y_{ij},Y_{kj})=\begin{cases}0, & \text{if } i\neq k\\ \sigma^2, & \text{if } i=k\end{cases}$
F-4, FS-4 and S-4	Random intercept model specifying the variance structure	$Y_{ij}=\alpha+b_j+\beta 1X1_{ij}+\beta 2X2_{ij}+\varepsilon_{ij}$ where, $b_j\sim(0,\sigma_a^2)$ and $\varepsilon_{ij}\sim N(0,\sigma^2)$ $Var(Y_{ij})=Var(b_j+\varepsilon_{ij})=\sigma_b^2+\sigma^2$ $Cov(Y_{ij},Y_{kj})=Cov(b_j+\varepsilon_{ij},b_j+\varepsilon_{kj})=\begin{cases}\sigma_b^2, & \text{if } i\neq k\\ \sigma_b^2+\sigma^2, & \text{if } i=k\end{cases}$

*Where *j*= 1 to 4 LULC types and *i*= observed or measured sample data in LULC types, Yij = log [PDR]ij is the log of the PDR; α is the fixed intercept, α_l is LULC types specific intercept fitted by REML in case of Model F-1, FS-1 and S-1, and b_j is the random intercept for LULC types fitted by REML. X1 is observed vegetation cover (%) or calculated NDVI, and X2 measures soil moisture (%), or band 11 value. β1 and β2 are fixed slopes for the independent variables X1 and X2, and ε_{ij} represents residual error.

Appendix 2. Pearson correlation among field-based parameters

	VC	SM	Elevation	Bulk density	PDR	PDR (log transformed)
VC	1	-0.026	0.163	-0.238	0.234	0.269
SM	-0.027	1	-0.168	-0.033	0.231	0.414
Elevation	0.164	-0.168	1	0.012	-0.029	-0.112
Bulk density	-0.238	-0.034	0.012	1	-0.104	-0.135
PDR	0.234	0.231	-0.029	-0.104	1	0.566
PDR (log transformed)	0.269	0.414	-0.112	-0.135	0.566	1

Appendix 3a. Pearson correlation coefficient (r) vegetation cover (VC), soil moisture (SM), Sentinel-2 bands and derived indexes.

	Veg.	Moistur	NDVI	NDMI_B8	SCI	SAVI	NDW	NDM	B01	B02	B03	B04	B05	B06	B07	B08	B09	B10	B11	B12	B8A	IPVI	mNDV
Veg.	1.00	-0.03	0.81	0.26	-	0.81	-0.80	0.22	-	-	-	-	-	0.28	0.35	0.38	0.35	-	-	-	0.40	0.65	0.71
Moisture	-0.03	1.00	-0.09	0.37	-	-	-0.02	0.33	-	-	-	-	-	-	-	-	-	-	-	-	-	0.16	-0.03
NDVI	0.81	-0.09	1.00	0.05	-	1.00	-0.95	0.05	-	-	-	-	-	0.51	0.57	0.61	0.52	0.06	0.17	-	0.60	0.70	0.87
NDMI_B8	0.26	0.37	0.05	1.00	-	0.03	-0.14	0.96	-	-	-	-	-	-	-	-	-	-	-	-	-	0.30	0.13
SCI	-0.22	-0.33	-0.05	-0.96	1.00	-	0.11	-1.00	0.60	0.57	0.57	0.61	0.69	0.47	0.40	0.32	0.36	0.57	0.71	0.72	0.40	-	-0.10
SAVI	0.81	-0.09	1.00	0.03	-	1.00	-0.96	0.03	-	-	-	-	-	0.51	0.58	0.62	0.52	0.07	0.18	-	0.61	0.70	0.87
NDWI	-0.80	-0.02	-0.95	-0.14	0.11	-	1.00	-0.11	0.49	0.49	0.44	0.38	0.21	-	-	-	-	-	-	0.14	-	-	-0.87
NDMI	0.22	0.33	0.05	0.96	-	0.03	-0.11	1.00	-	-	-	-	-	-	-	-	-	-	-	-	-	0.19	0.10
B01	-0.41	-0.31	-0.36	-0.62	0.60	-	0.49	-0.60	1.00	0.84	0.82	0.80	0.78	0.37	0.30	0.22	0.35	0.64	0.66	0.75	0.26	-	-0.45
B02	-0.45	-0.38	-0.33	-0.65	0.57	-	0.49	-0.57	0.84	1.00	0.99	0.97	0.89	0.46	0.37	0.35	0.21	0.51	0.75	0.85	0.33	-	-0.40
B03	-0.43	-0.38	-0.28	-0.65	0.57	-	0.44	-0.57	0.82	0.99	1.00	0.98	0.91	0.52	0.43	0.42	0.25	0.51	0.78	0.88	0.39	-	-0.34
B04	-0.40	-0.38	-0.24	-0.69	0.61	-	0.38	-0.61	0.80	0.97	0.98	1.00	0.94	0.56	0.47	0.46	0.31	0.57	0.83	0.92	0.43	-	-0.30
B05	-0.24	-0.37	-0.07	-0.70	0.69	-	0.21	-0.69	0.78	0.89	0.91	0.94	1.00	0.75	0.67	0.61	0.49	0.64	0.94	0.97	0.64	-	-0.10
B06	0.28	-0.31	0.51	-0.44	0.47	0.51	-0.39	-0.47	0.37	0.46	0.52	0.56	0.75	1.00	0.98	0.95	0.78	0.56	0.87	0.75	0.98	0.22	0.54
B07	0.35	-0.30	0.57	-0.37	0.40	0.58	-0.45	-0.40	0.30	0.37	0.43	0.47	0.67	0.98	1.00	0.95	0.79	0.52	0.81	0.67	0.99	0.31	0.62
B08	0.38	-0.32	0.61	-0.33	0.32	0.62	-0.50	-0.32	0.22	0.35	0.42	0.46	0.61	0.95	0.95	1.00	0.74	0.46	0.76	0.63	0.96	0.28	0.69
B09	0.35	-0.22	0.52	-0.32	0.36	0.52	-0.46	-0.36	0.35	0.21	0.25	0.31	0.49	0.78	0.79	0.74	1.00	0.69	0.65	0.52	0.80	0.56	0.53
B10	-0.03	-0.34	0.06	-0.58	0.57	0.07	-0.01	-0.57	0.64	0.51	0.51	0.57	0.64	0.56	0.52	0.46	0.69	1.00	0.70	0.67	0.52	0.06	0.02
B11	-0.03	-0.41	0.17	-0.72	0.71	0.18	-0.04	-0.71	0.66	0.75	0.78	0.83	0.94	0.87	0.81	0.76	0.65	0.70	1.00	0.97	0.80	-	0.16
B12	-0.20	-0.40	-0.01	-0.75	0.72	-	0.14	-0.72	0.75	0.85	0.88	0.92	0.97	0.75	0.67	0.63	0.52	0.67	0.97	1.00	0.66	-	-0.05
B8A	0.40	-0.31	0.60	-0.36	0.40	0.61	-0.50	-0.40	0.26	0.33	0.39	0.43	0.64	0.98	0.99	0.96	0.80	0.52	0.80	0.66	1.00	0.35	0.66
IPVI	0.65	0.16	0.70	0.30	-	0.70	-0.79	0.19	-	-	-	-	-	0.22	0.31	0.28	0.56	0.06	-	-	0.35	1.00	0.77
mNDVI	0.71	-0.03	0.87	0.13	-	0.87	-0.87	0.10	-	-	-	-	-	0.54	0.62	0.69	0.53	0.02	0.16	-	0.66	0.77	1.00

Appendix 3b. Pearson correlation coefficient (r) among vegetation cover (VC), soil moisture (SM), Sentinel-2 derived indexes.

	Veg.	Mois	Pan	SBI	SI	R_B	RD	GE	GV	SB	SR	I	GL	BW	AR	BR	CC	CG	CI	CI	CR	CI	CV	LCI	N	ND	ND	ND	SI	EV
Veg.	1.00	-0.03	0.54	-	-	0.53	0.	0.5	0.2	0.	-	-	-	0.69	0.	0.	0.	-	0.	0.	-	0.	0.	0.	0.	-	-	0.6	-	0.
Moist	-0.03	1.00	0.03	-	-	0.00	-	-	0.3	0.	-	-	-	0.10	0.	0.	0.	-	0.	0.	0.	0.	0.	-	-	-	-	0.2	0.	0.
PanN	0.54	0.03	1.00	0.11	-	0.99	0.	0.9	0.2	0.	-	-	-	0.76	0.	-	0.	-	0.	0.	-	0.	0.	0.	0.	-	-	0.6	-	0.
SBI_	-0.03	-0.39	0.11	1.00	0.	0.17	0.	0.1	-	-	0.5	0.	0.	0.01	-	-	-	0.	-	-	-	0.	-	0.	0.	0.4	0.4	-	0.	-
SIPI	-0.04	-0.04	-0.02	0.11	1.	-0.01	-	0.0	-	-	0.1	0.	0.	-	-	-	-	0.	-	-	0.	-	-	0.	-	0.0	0.1	-	0.	-
R_B	0.53	0.00	0.99	0.17	-	1.00	0.	0.9	0.1	0.	0.0	-	-	0.75	0.	-	0.	-	0.	0.	-	0.	0.	0.	0.	-	-	0.5	0.	0.
RDVI	0.70	-0.08	0.67	0.30	-	0.68	1.	0.7	0.0	0.	-	-	-	0.78	0.	-	0.	-	0.	0.	-	0.	0.	0.	0.	0.0	-	0.5	-	0.
GEMI	0.55	-0.04	0.93	0.19	0.	0.93	0.	1.0	0.2	0.	-	-	-	0.74	0.	-	0.	-	0.	0.	-	0.	0.	0.	0.	-	-	0.5	0.	0.
GVMI	0.29	0.38	0.22	-	-	0.17	0.	0.2	1.0	0.	-	-	-	0.32	0.	0.	0.	-	0.	0.	-	-	0.	0.	0.	-	-	0.4	-	0.
SBL	0.49	0.35	0.45	-	-	0.38	0.	0.4	0.8	1.	-	-	-	0.53	0.	0.	0.	-	0.	0.	-	0.	0.	0.	0.	-	-	0.7	-	0.
SRMS	-0.29	-0.32	-0.01	0.59	0.	0.01	-	-	-	-	1.0	0.	0.	-	-	-	-	0.	-	-	0.	-	-	-	-	0.1	0.5	-	0.	-
I	-0.34	-0.45	-0.20	0.75	0.	-0.15	-	-	-	-	0.7	1.	0.	-	-	-	-	0.	-	-	0.	-	-	-	-	0.4	0.8	-	0.	-
GLI	-0.58	-0.30	-0.59	0.35	0.	-0.53	-	-	-	-	0.2	0.	1.	-	-	-	-	0.	-	-	0.	-	-	-	-	0.6	0.8	-	-	-
BWD	0.69	0.10	0.76	0.01	-	0.75	0.	0.7	0.3	0.	-	-	-	1.00	0.	-	0.	-	0.	0.	-	0.	0.	0.	0.	-	-	0.7	-	0.
ARI	0.54	0.39	0.48	-	-	0.43	0.	0.4	0.7	0.	-	-	-	0.65	1.	0.	0.	-	0.	0.	-	0.	0.	0.	0.	-	-	0.8	-	0.
BRI	0.06	0.41	-0.20	-	-	-0.25	-	-	0.6	0.	-	-	-	-	0.	1.	0.	-	0.	-	0.	-	0.	-	-	-	-	0.3	-	0.
CCCI	0.25	0.13	0.14	-	-	0.13	0.	0.2	0.2	0.	-	-	-	0.28	0.	0.	1.	-	0.	0.	-	0.	0.	0.	0.	-	-	0.2	-	0.
CG	-0.74	-0.09	-0.73	0.00	0.	-0.70	-	-	-	-	0.1	0.	0.	-	-	-	-	1.	-	-	0.	-	-	-	-	0.2	0.6	-	0.	-
CIG	0.69	0.16	0.78	-	-	0.75	0.	0.7	0.4	0.	-	-	-	0.92	0.	0.	0.	-	1.	0.	-	0.	0.	0.	0.	-	-	0.8	0.	0.
CIRE	0.60	0.07	0.82	-	-	0.81	0.	0.8	0.4	0.	-	-	-	0.88	0.	-	0.	-	0.	1.	-	0.	0.	0.	0.	-	-	0.6	0.	0.
CRE	-0.75	0.09	-0.71	-	0.	-0.71	-	-	-	-	0.0	0.	0.	-	-	0.	-	0.	-	-	1.	-	-	-	-	-	0.4	-	0.	-
CI	0.40	0.01	0.21	0.16	-	0.22	0.	0.1	-	0.	-	-	-	0.58	0.	-	0.	-	0.	0.	-	1.	0.	0.	0.	0.6	-	0.4	-	0.
CVI	0.71	0.18	0.72	-	-	0.69	0.	0.7	0.4	0.	-	-	-	0.91	0.	0.	0.	-	0.	0.	-	0.	1.	0.	0.	-	-	0.8	-	0.
LCI	0.77	-0.13	0.61	0.20	0.	0.63	0.	0.6	0.0	0.	-	-	-	0.79	0.	-	0.	-	0.	0.	-	0.	0.	1.	0.	0.1	-	0.4	-	0.
NVI	0.60	-0.09	0.78	0.21	-	0.79	0.	0.8	0.1	0.	-	-	-	0.85	0.	-	0.	-	0.	0.	-	0.	0.	0.	1.	-	-	0.5	0.	0.
NDPP	-0.16	-0.22	-0.30	0.40	0.	-0.25	0.	-	-	-	0.1	0.	0.	-	-	-	-	0.	-	-	-	0.	-	0.	-	1.0	0.4	-	-	-
NDPV	-0.46	-0.37	-0.50	0.48	0.	-0.44	-	-	-	-	0.5	0.	0.	-	-	-	-	0.	-	-	0.	-	-	-	-	0.4	1.0	-	0.	-
NDGR	0.64	0.28	0.60	-	-	0.54	0.	0.5	0.4	0.	-	-	-	0.72	0.	0.	0.	-	0.	0.	-	0.	0.	0.	0.	-	-	1.0	-	0.
SI	-0.06	0.05	-0.01	0.13	0.	0.00	-	0.0	-	-	0.0	0.	-	-	-	-	-	0.	0.	0.	0.	-	-	-	0.	-	0.0	-	1.	0.
EVI	0.58	0.29	0.64	-	-	0.61	0.	0.6	0.7	0.	-	-	-	0.78	0.	0.	0.	-	0.	0.	-	0.	0.	0.	0.	-	-	0.7	0.	1.

Appendix 4a. Accuracy assessment of LULC classification during post-monsoon 2019 based on the confusion matrix, producer's accuracy, user's accuracy and kappa hat coefficient values.

Class	NV	LW	DBL	WB	Total
NV	27	6	0	0	33
LW	1	4	0	0	5
DBL	2	0	6	0	8
WB	2	2	0	28	32
Total	32	12	6	28	78
Producer's accuracy [%]	97.31	6.61	100.0	100.0	
User's accuracy [%]	81.82	80.0	75.0	87.5	
Overall accuracy [%]					82.38
Kappa hat	0.42	0.76	0.74	0.86	
Overall Kappa hat					0.57

Appendix 4b. Accuracy assessment of LULC classification during dry/winter 2020 based on the confusion matrix, producer's accuracy, user's accuracy and kappa hat coefficient values.

Class	CL	NV	LW	DBL	WB	Total
CL	26	1	0	0	0	27
NV	4	54	3	0	0	61
LW	1	2	53	0	7	62
DBL	0	0	2	25	0	27
WB	0	0	3	0	1591	1591
Total	30	57	58	25	1598	1768
Producer's accuracy [%]	90.89	64.29	99.39	92	47.16	
User's accuracy [%]	96.29	88.52	85.48	92.59	100	
Overall accuracy [%]						87.38
Kappa hat	0.96	0.88	0.53	0.92	1.00	
Overall Kappa hat						0.7

Appendix 4c. Accuracy assessment of LULC classification during pre-monsoon 2020 based on the confusion matrix, producer's accuracy, user's accuracy and kappa hat coefficient values.

Class	CL	NV	LW	DBL	WB	Total
CL	21	0	3	0	0	24
NV	4	26	5	0	0	35
LW	1	4	16	0	0	21
DBL	0	0	2	12	0	14
WB	0	2	1	0	44	47
Total	26	32	27	12	44	141
Producer's accuracy [%]	71.15	58.64	21.25	100.0	100.0	
User's accuracy [%]	87.5	74.29	76.19	85.71	93.62	
Overall accuracy [%]						91.72
Kappa hat	0.87	0.72	0.75	0.86	0.64	
Overall Kappa hat						0.69

Appendix 5. Seasonal variation of TSS (total suspended solids) in the study area of the Padma River, Bangladesh

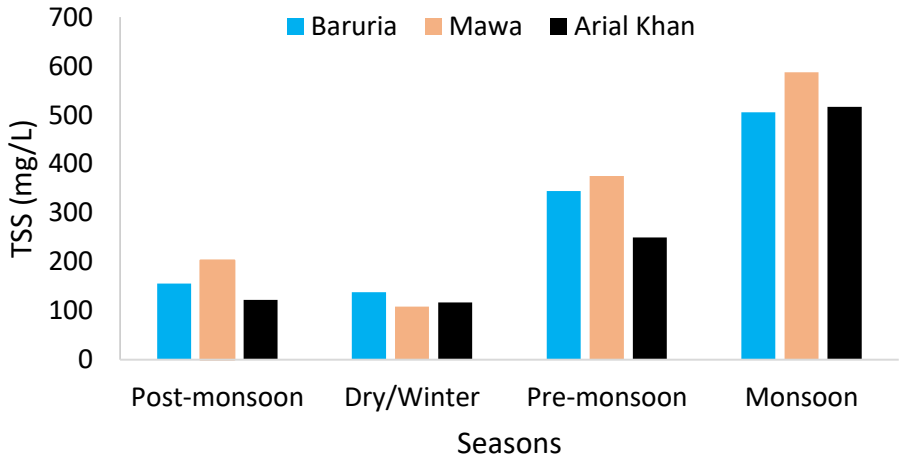

Appendix 6. Seasonal variation of PD (phytoplankton density) in the study area of the Padma River, Bangladesh

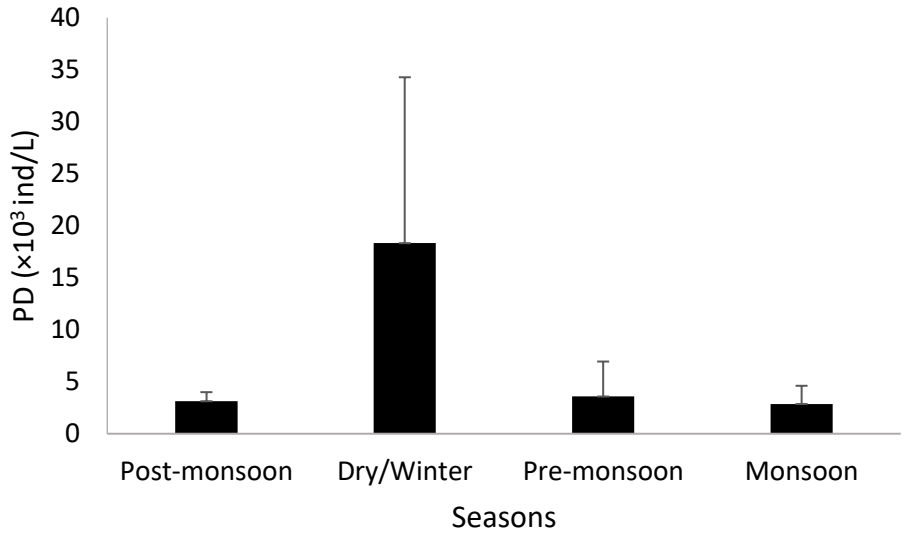

Appendix 7. The surface area (Km2) of submerged GUs in the study area of Padma River calculated from Gani et al. (2022).

Season	Always submerged	EA	EC	ED	EK	VI	WD	Total
Monsoon	249.64	13.29	37.65	0.1	0.57	71.67	10.34	372.92
Post-monsoon	217.97	12.6	28.18	0	0	60.3	3.48	318.48
Dry/Winter	253.08	0	0	0	0	0	2.2	253.08
Pre-monsoon	215.56	0	17.33	0	0	43.6	0.98	275.73

Appendix 8. Boxplot showing mean values of PDR in submerged GUs in the study area of the Padma River, Bangladesh

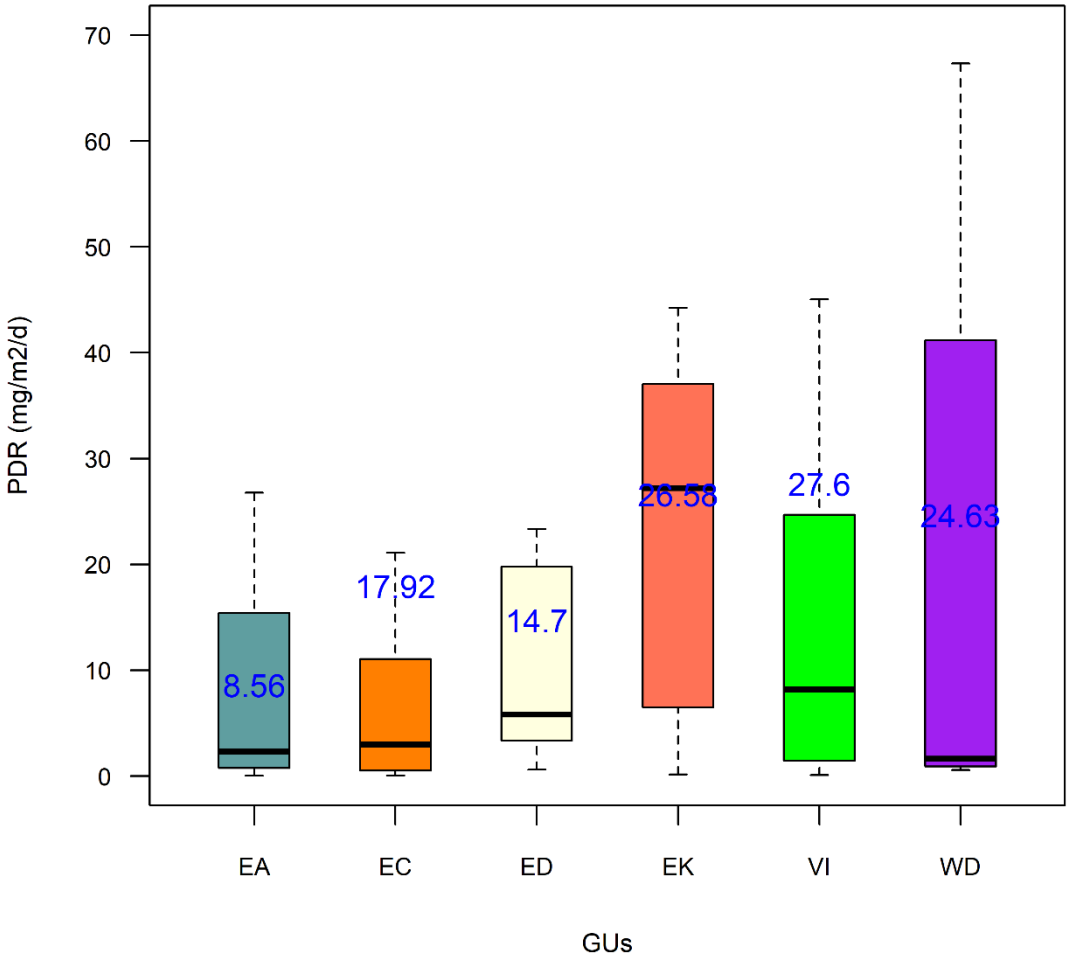

Appendix 9. Monthly variation of rainfall in the study area of the Padma River, Bangladesh.

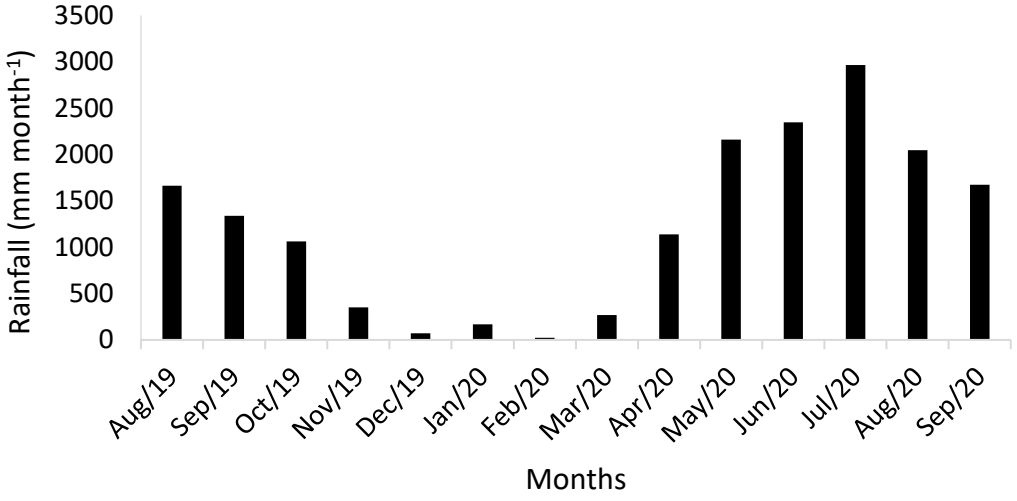

Appendix 10. Seasonal and annual nitrogen retention and retention processes in the study area of Padma River, Bangladesh

	Post-monsoon	Dry/Winter	Pre-monsoon	Monsoon	Annual
Measured Ret (t)	12928	1946	2493	104347	121715
% Retention	10.6	1.6	2	85.7	100
Estimated Ret (t)	12500	2380	2904	101629	119412
Net PDR in WC (t)	322	170	186	1473	2152
PDR in submerged GUs (t)	472	572	630	1121	2795
NLWR (t)	9019	1286	1578	80407	92289
Sedimentation (t)	2688	351	510	18628	22176
% Net PDR in WC to Ret	2.5	8.7	7.5	1.4	1.8
% PDR in submerged GUs to Ret	3.6	29.4	25.3	1.1	2.3
% NLWR to Ret	69.8	66.1	63.3	77.1	77.3
% Sedimentation to Ret	20.8	18.1	20.4	17.9	18.2
Estimated vs Measured Ret (%)	97	122	116	97	98

*Annual time scale was considered from October 2019 to September 2020; Ret= Retention.

Appendix 11. Calculated PDR in the exposed GUs, submerged GUs, and water column in the study area of the Padma River, Bangladesh

	Monsoon	Post-monsoon	Dry/Winter	Pre-monsoon
Exposed GUs	0	11651	98917	89424
Submerged GUs	1120933	471686	572167	630015
Water column	1304896	326830	172549	188780
Total PDR	2425829	810167	843633	908219
Total PDR in GUs	1120933	483337	671084	719439
% of PDR in GUs	0.46	0.60	0.80	0.80

LIST OF ACRONYMS

GUs	Geomorphic units
GMB	Ganges-Brahmaputra-Meghna
NREGUs	Nutrient retention-/export-relevant geomorphic units
NDVI	Normalised difference vegetation index
LULC	Land use and land cover
NDWI	Normalised difference water index
EVI	Enhanced vegetation index
BWDB	Bangladesh Water Development Board
SCP	Semi-automatic classification plugin
C & S	Primary and secondary channels
L	Longitudinal bar
T	Transverse bar
SB	Side bar
EK	Unvegetated bank
ED	Dry channel
VI	Vegetated island
WD	Water depression
P/A	Perimeter area ratio
PDR	Potential denitrification rate
LMMs	Linear mixed models
SWIR	Shortwave infrared
VNIR	Visible and near-infrared
CL	Cropland
NV	Natural vegetation
LW	Land with water
DBL	Dry bare land
WB	Water bodies
DEA	Denitrification enzyme activity
ECD	Electron capture detector
AIC	Akaike Information Criterion
logLik	log-likelihood
REML	Restricted maximum likelihood method
VC	Vegetation cover
SM	Soil moisture
NLWR	Nitrogen loss due to water retention
NFR	Nitrogen fixation rate
TN	Total nitrogen
TDN	Total dissolved nitrogen
TSS	Total suspended solids
PN	Particulate nitrogen
BDP	Bangladesh Delta Plan

NWP	National Water Policy
BWA	Bangladesh Water Act
JRC	Joint Rivers Commission
RRI	River Research Institute
	Water Resources Planning Organization

LIST OF FIGURES

LIST OF TABLES

ABOUT THE AUTHOR

Md Ataul Gani is an Associate professor in the Department of Botany, Jagannath University, Dhaka, specialising in Limnology and Hydrobiology. He has working experience in different projects that mainly dealt with river and coastal ecosystems of Bangladesh, funded by the Royal Netherlands Academy of Arts and Sciences (KNAW), the Ministry of Science and Technology and The University Grants Commission of Bangladesh.

Mr. Gani obtained his Bachelor's and Master's degrees from the Department of Botany, University of Dhaka, Bangladesh. In addition, he completed another interdisciplinary postgraduate degree (MSc) in "Ecological water quality and management at a basin level" at the Aristotle University of Thessaloniki, Greece, through the Erasmus Mundus Scholarship. As a part of the study, he worked on the ecological water quality of the Gallikos River basin in Northern Greece and completed a thesis on ecological water quality assessment of the coastal area of Thermaikos Gulf, Greece. Currently, he is working with modelling and estimating nitrogen retention processes like denitrification and sedimentation in a large lowland river system and trying to show the impact of river engineering programs on the river ecosystem as it can transport nutrient to sea, enhancing nutrient pollution, eutrophication, coastal hypoxia and long-term effect on human health. His other work experiences include:

- Ecological water quality
- Phytoplankton taxonomy and ecology
- River morphology and typology using remote sensing data
- Catchment delineation and monitoring inland waters using QGIS
- Biogeochemical process modelling using LMMs
- Multivariate analysis using R, Canoco, Primer etc.

Journal Articles

1) Hasan M. M., **Gani M. A.**, Alfasane M. A., Ayesha M., Nahar K. (2023). Benthic diatom communities and a comparative seasonal-based ecological quality assessment of a transboundary river in Bangladesh. PLoS One, 18(10), e0291751. https://doi: 10.1371/journal.pone.0291751
2) **Gani M. A.**, Sajib, A.M., Siddik, M., Moniruzzaman M. (2023). Assessing the impact of land use and land cover on river water quality using water quality index and remote sensing techniques. Environ. Monit. Assess., 195, 449. https://doi.org/10.1007/s10661-023-10989-1
3) **Gani M. A.**, van der Kwast J., McClain M. E., Gettel G., Irvine K. (2022). Classification of Geomorphic Units and Their Relevance for Nutrient Retention or Export of a Large Lowland Padma River, Bangladesh: A NDVI Based Approach. Remote Sens., 14, 1481. https://doi.org/10.3390/rs14061481

Conference Presentation

1) Prediction of denitrification rate in the classified geomorphic units of a large lowland river: Linear mixed models using Sentinel-2 data. The **F**luvial **A**eolian **I**nte**R**actions on **PLA**netar**Y** surfaces workshop (FAIRPLAY). Noordwijk, The Netherlands, 1-3 November, 2023.

2) Changes in geomorphic units alter nitrogen fixation in a large lowland tropical river. 18th International Conference on Environmental Science and Technology Athens, Greece, 30 August to 2 September 2023.

3) Nitrogen retention of a large lowland tropical river: a mass balance approach. 5th International Conference on the status and future of the World's Large Rivers. Vienna, Austria, 21-25 August, 2023.

4) Seasonal dynamics of geomorphic units and denitrification rate in a large lowland tropical river. EGU General Assembly, Vienna, Austria, 23-28 April 2023.

5) Changes in geomorphic units alter the nitrogen retention process in large lowland rivers: A case study on Padma River, Bangladesh. International Conference on Environmental Protection for Sustainable Development (ICEPSD 2022), Dhaka, 2-4 September 2022.

6) Geomorphic mapping relevant to nutrient retention of a large lowland river. 14th IHE Delft PhD symposium, Delft, Netherlands, 7-8 October 2020.

7) Temporal dynamics of different nutrient retention relevant geomorphic units in Padma River, Bangladesh. IHE PhD symposium, Netherlands 10-11 October 2019.

8) Nutrient retention in different geomorphic units of a large lowland river, IHE PhD symposium, Netherlands, 1-2 October, 2018.

Netherlands Research School for the
Socio-Economic and Natural Sciences of the Environment

D I P L O M A

for specialised PhD training

The Netherlands research school for the
Socio-Economic and Natural Sciences of the Environment
(SENSE) declares that

Md Ataul Gani

born on 7th of November 1986 in Cumilla, Bangladesh

has successfully fulfilled all requirements of the
educational PhD programme of SENSE.

Delft, 7th of October 2024

Chair of the SENSE board

Prof. dr. Martin Wassen

The SENSE Director

Prof. Philipp Pattberg

The SENSE Research School has been accredited by the Royal Netherlands Academy of Arts and Sciences (KNAW)

KONINKLIJKE NEDERLANDSE
AKADEMIE VAN WETENSCHAPPEN

The SENSE Research School declares that **Md Ataul Gani** has successfully fulfilled all requirements of the educational PhD programme of SENSE with a work load of 37.0 EC, including the following activities:

SENSE PhD Courses

- Environmental research in context (2018)
- Research in context activity: Working in PhD iTeam in IHE Delft (2019)

Other PhD and Advanced MSc Courses

- Model Training for Scenario analysis: River export of nutrients from land to sea, Wageningen University (2018)
- Data Analysis and Modelling for Aquatic Ecosystems, IHE Delft (2018)
- Summer School: Resilience of living systems-from fundamental concepts to interdisciplinary applications, Wageningen University (2018)
- International Summer School on Applications with the Newest Multi Spectral Environmental Satellites, CIMSS, EUMETSAT, Italy (2018)
- Using the Copernicus Marine Data Stream for Ocean Applications, Copernicus and EUMETSAT Latvia (2018)
- Data Acquisition, Preprocessing and Modelling using the PCRaster Python Framework, IHE Delft (2019)
- Agent based Modelling with NetLogo, University of Göttingen, Germany (2022)

Oral Presentations

- *Geomorphic mapping relevant to nutrient retention of a large lowland river*. 14th IHE Delft PhD symposium 7-8 October 2020, Delft, Netherlands
- *Changes in geomorphic units alter the nitrogen retention process in large lowland rivers: A case study on Padma River, Bangladesh.* International conference on environmental protection for sustainable development (ICEPSD 2022), 2-4 September 2022, Dhaka, Bangladesh
- *Seasonal dynamics of geomorphic units and denitrification rate in a large lowland tropical river.* EGU General Assembly, 23-28 April 2023, Vienna Austria

SENSE coordinator PhD education

Dr. ir. Peter Vermeulen

IHE DELFT
Institute for Water Education
under the auspices of UNESCO

WAGENINGEN
UNIVERSITY & RESEARCH

Large lowland rivers are geomorphologically diverse, with variations in flow that influence nitrogen retention. Nitrogen retention is a valuable ecosystem service protecting the downstream aquatic ecosystem from eutrophication. The research focuses on nitrogen retention in distinct geomorphic units of the large lowland Padma River in Bangladesh. Sentinel-2 imagery (2019-2020) was processed using NDVI values to classify geomorphic units (GUs) and map nutrient-retention/export-relevant geomorphic units (NREGUs) of the study area, which showed seasonal discharge variations were responsible for changes in the surface area and a number of GUs. The field measurements of potential denitrification rate (PDR) were performed to show the spatiotemporal distribution of PDR using different linear mixed models (LMMs), including Sentinel-2 band 11 and NDVI, and the application of the best-performed LMM showed that the number and surface area of GUs were responsible for the alteration of PDR in the study reach. Monthly field investigations employing the mass balance approach provide an integrated value of nitrogen retention of the study reach. This enables comparison with the retention processes in the reach, such as nitrogen loss due to water retention, sedimentation and net PDR. The present study showed that the alteration of GUs can regulate these retention processes, thus revealing the effect of river management programmes on river health and ecology.

This book is printed on paper from sustainably managed forests and controlled sources

9 789073 445659